Synthesis, Characterisation and Catalytic Applications of Copper Complexes Encapsulated in Molecular Sieves

A thesis submitted to the

UNIVERSITY OF PUNE

for the degree of

DOCTOR OF PHILOSOPHY

(in Chemistry)

BY

ROBERT RAJA

CATALYSIS DIVISION
NATIONAL CHEMICAL LABORATORY
PUNE 411 008
INDIA

FEBRUARY, 1997

CERTIFICATE

Certified that the work incorporated in the thesis entitled ***"Synthesis, Characterisation and Catalytic Applications of Copper Complexes Encapsulated in Molecular Sieves",*** *submitted by* ***Robert Raja*** *to the University of Pune, was carried out by the candidate under my supervision and guidance. Materials obtained from other sources has been duly acknowledged in the thesis.*

Research Guide

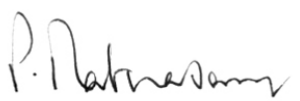

Dr. P. Ratnasamy

Acknowledgments

I would like to express my deep sense of gratitude to my research advisor, Dr. P. Ratnasamy, for his creativity, guidance and for providing me a unique educational experience I shall always treasure.

I would also like to express my sincere appreciation to all members of the Inorganic, Catalysis and Biochemistry divisions for their friendship, technical advise and professional assistance during my tenure at the National Chemical Laboratory.

I am grateful to the Council of Scientific and Industrial Research (CSIR), New Delhi for a Senior Research Fellowship and to the Director, National Chemical Laboratory, Pune for permitting me to submit my work in the form of a thesis.

Last, but not the least, I thank all my friends, my Uncle, Aunt and my cousins for making my stay in Pune a very memorable one.

"Chemistry is not limited to systems similar to those found in Biology, but is free to create unknown species and to invent novel processes..... Supramolecular reagents are abiotic reagents that may perform the same overall processes as enzymes without following the same mechanistic pathways. They present protoenzymatic and biomimetic features."

Jean-Marie Lehn

Nobel laureate, Rajiv Gandhi S & T lecture

Hyderbad, India 22-12-1995

Table of Contents

CHAPTER-1 GENERAL INTRODUCTION

CHAPTER-2 EXPERIMENTAL

CHAPTER-3 CATALYST CHARACTERIZATION

CHAPTER-7 OXHALOGENATION OF AROMATIC COMPOUNDS

CHAPTER-8 GENERAL DISCUSSION

CHAPTER-9 SUMMARY AND CONCLUSIONS

ABSTRACT

Compared to the wealth of information available on iron complexes encapsulated in zeolites, the chemistry of similar copper compounds is known in less detail. This is surprising in view of the major role of copper in catalysing a large number of redox reactions in the biosphere. The synthesis, characterization and catalytic applications of copper acetate and phthalocyanine complexes encapsulated in molecular sieves are described in this thesis. Dimeric copper-acetate complexes were incorporated in zeolites, Na-Y, MCM-22 and VPI-5. The structural and compositional integrity of the incorporated copper-acetate complexes were verified by XRD, IR and UV-Vis spectroscopic techniques. ESR was used to prove the dinuclearity of the incorporated copper acetate. These solid catalysts have been used for the activation of dioxygen at ambient conditions and were effective catalysts in the oxidation of L-tyrosine, phenol and cresols to the corresponding diphenols. The high substrate specificity and regioselectivity of the above catalysts indicate that copper acetate dimers encapsulated in molecular sieves, mimic, in a restricted sense, the catalytic function (both monophenolase and diphenolase activity) of the monooxygenase enzyme, tyrosinase.

Copper phthalocyanine, copper hexadeca chloro phthalocyanine and copper tetra nitro phthalocyanine complexes were synthesized and have been encapsulated in zeolites X, Y, ZSM-5 and K-L by synthesizing the zeolites around the metal complexes. Substitution of the hydrogen atoms in the aromatic nuclei of the phthalocyanine molecule by electron withdrawing groups increases the reactivity of these copper catalysts. The structural integrity of the above complexes in the molecular sieves was confirmed by a wide variety of physicochemical techniques such as XRD, UV-Vis, ESCA, ESR, SEM, TGA/DTA and N_2 sorption. Computer modeling and molecular strain energy minimization calculations indicate that the geometry around the copper atom is distorted tetragonally from the square planar symmetry (of the free complex) when encapsulated inside the supercages of the faujasite. This distortion leads to a *hydrophobic* environment around the copper atom These catalysts have been used in the oxidation of alkanes, aromatics, phenols and oxyhalogenation of aromatic compounds.

CHAPTER-1

GENERAL INTRODUCTION

1. INTRODUCTION

1.1 Introduction

The ease with which nature performs many difficult chemical transformations essential to life processes has long been admired by synthetic chemists. By a judicious choice of catalysts (metal-ion complexes) and supports (proteins) nature has built an impressive array of enzymes that perform complex tasks such as reversible oxygen binding (hemoglobin, myoglobin, tyrosinase)[1,2] , selective partial oxidation of unactivated hydrocarbons (Cytochrome P-450, ω-hydroxylase)[3-5], and electron transport (ferridoxins)[6]. There have been intense efforts to model and mimic the catalytic activities of all these

enzymes- efforts driven by a desire to both understand and exploit the chemistry of these enzymes.

Metalloenzymes having a metal active site, owe their high selectivities in chemical reactions primarily to the protein tertiary structure which wraps around the active site performing several crucial functions : (a). Protecting the active site from deleterious reactions such as self destruction via bimolecular pathways (b). Sieving the substrate molecules so that only those capable of passing through the protein channels can gain access to the embedded prosthetic group, giving the enzyme high substrate/shape selectivity and (c). Providing a very stereochemically demanding void space in the vicinity of the active site where the substrate resides during the reaction.

Zeolites[7] have crystalline open framework structures constructed of SiO_4 and AlO_4 tetrahedra linked through oxygen bridges. The open framework has pores and cavities of molecular dimensions (3-13 Å) that selects only those molecules with proper size and shape to pass through - hence their common name *molecular sieves.* They also orient those molecules (based on their physical dimensions) as they gain access to the internal voids of the crystallite. The cation exchange sites within the internal void space of the crystallites allow the introduction of the active metal ions for catalysis. To some extent, zeolites have a number of striking structural similarities to the protein mantle of natural enzymes. By taking advantage of these similarities new catalysts that combine the features of the robust, chemically inert zeolite with the high selectivity and activity of natural enzymes can be developed.

Even though the oxidation and hydroxylation of organic compounds using molecular dioxygen is of widespread occurrence in nature, such processes are not in common practice either in the laboratory or in the industry. Some of the extensively

studied systems for the oxidation and hydroxylation of aromatic compounds are the Fenton's reagent (Fe^{2+}-H_2O_2)[8], peracids (R-COOOH $\rightarrow$ RCO_2^- + OH^+, trifluoroacetic acid, for example)[9], the Hamilton-Friedman reagent (Fe^{3+}-H_2O_2-Catechol)[10], the Udenfriend reagent (Fe^{2+}-EDTA-ascorbbic acid-O_2)[11] and the Cu^{2+}-O_2-morpholine system[12]. All these systems are homogeneous in nature.

The *heterogenizing* of homogeneous catalysts is an active area of research[13-15]. The term heterogenising[13] refers to a process whereby a homogeneous transition metal complex is immobilized, anchored, incorporated or *encapsulated* in an inert polymer or inorganic support[16]. These heterogeneous catalysts have a lot of advantages over their homogeneous analogues in (i). fixed-bed and continuous flow through operations (ii). in complete separation of the reaction mixture (products and reactants) from the catalyst (iii). commercial utility on a large scale owing to the economic debits of batch type operation and/or expense of catalyst recovery and recycle (iv). in maintaining high selectivities of their homogeneous counterparts for many reactions and (v). in preventing dimerization and aggregate formation of the catalyst complex which normally occurs in solution.

Workers from DuPont were among the early pioneers to exploit the chemistry of natural enzymes[17], adopt strategies and apply them to the rational design of zeolite based catalysts as both mimics of natural enzymes and for processes of industrial interest[18]. In an attempt to prepare analogs of hemoglobin and myoglobin[19-20] which reversibly bind O_2, cobalt salen complexes were encapsulated in the supercages of zeolite-Y[21]. Such encapsulated complexes formed adducts with dioxygen which were more stable than those formed by the same complexes in free solution[17]. Apparently, the isolation of these complexes in the zeolite cavities suppresses the dimerization reactions leading to the inactive μ-oxo and peroxo complexes of cobalt. Dimerization reactions occur to a

significant extent in the case of homogeneous complexes. In a similar attempt to prepare analogs of Cytochrome-P-450, Fe(II)-Pd(0) particles encapsulated in zeolite A exhibited remarkable substrate and regioselectivity in the oxidation of unactivated alkanes with molecular oxygen[22-23]. Recently[24], Jacobs et al, have reported a composite catalytic system that achieves realistic mimicry of Cytochrome P-450, by incorporating iron phthalocyanine complexes in crystals of zeolite Y, which are in turn embedded in a polydimethyl siloxane membrane. This system oxidizes cyclohexane at room temperature at rates comparable to those of the enzyme.

Selective oxidation of aromatic substrates using solid catalysts, preferably at near ambient conditions and using clean oxidants like O_2 or H_2O_2 is a research area of growing importance in recent years. However, extensive studies have been reported on selective oxidation of organic compounds using singlet oxygen sources such as H_2O_2, t-butyl hydroperoxide or iodoso benzene as the oxidants[25-27]. Since the early work of the DuPont workers[17], only a few studies have been reported on the activation of molecular oxygen by metal complexes[28-30] (mostly of Fe with ligands such as porphyrins, phthalocyanines and salens) encapsulated in molecular sieves.[31-34]

The environment around the metal centre and the conformational flexibility of the protein mantle are the key factors for a metalloprotein to carry out a specific physiological function, for example, dioxygen binding by hemoglobin and myoglobin, oxygen utilization by Cytochrome P-450 and Cytochrome c-oxidase, etc. Fine tuning of the electronic structure, by replacement of the easily oxidizable hydrogen atoms by electron withdrawing or donating substituents in the phthalocyanine,[29] porphyrin[35] or salen[36] ligands, enhances the oxidizable stability and improves the catalytic activity of the complexes. Flexibility of

the ligand, as observed in the case of several transition-metal complexes with bidentate ligands,[37-40] is responsible for these complexes to mimic the biological activity of proteins.

1.2 The chemistry of Copper

Even though transition metal complexes (such as copper acatete) were used as oxidizing agents for organic compounds during the era of alchemists,[41] their use as selective oxidation catalysts is of more recent vintage. Copper is known to exist in the 0, 1+, 2+ and 3+ oxidation states. Of these, Copper (III) is the least encountered because of its very large oxidation potential. Copper (II) is the most common valence state and exhibits a coordination number of 4 or 6. In most cases, it possesses either a square planar or octahedral bond orientation. Octahedral Copper (II) complexes usually exhibit a Jahn-Teller distortion owing to its d^9 electronic configuration. All mononuclear Copper (II) complexes are paramagnetic. Copper (I) is always diamagnetic as a result of its d^{10} electronic structure. The nature of the donor atom affects the stability of the metal complex. Copper (II) belongs to the group of metal ions which exhibit the ligand stability orders N>O>S and $F^- >> Cl^- > Br^- > I^-$, while Copper(I) exhibits the order N>S>O and $I^- > Br^- > Cl^- >> F^-$. Chelation generally results in a dramatic increase in the stability of the complex.[42] In the case of Copper (II), however, carbonate and carboxylate anions function as bridging units between the two metal ions to form dimeric complexes. The dimeric structure of cupric acetate remains intact when dissolved in aprotic solvents or glacial acetic acid.[43-45] In the presence of water or nitrogen-containing ligands (e.g. pyridine) the dimer dissociates and is predominantly monomeric.[46] In addition to the entropy effect, Copper (II) chelates are additionally stabilized by means of a benzenoid resonance with

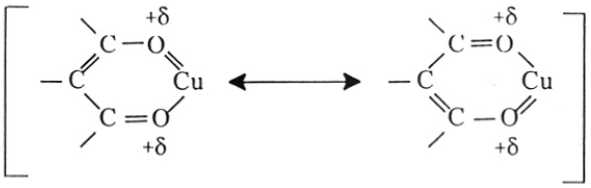

certain ligands. The stability of the copper (II) chelates decreases with decrease in double-bond character within the chelate ring. A similar resonance stabilization is probably responsible, in part, for the extreme stability of the copper (II) phthalocyanine. As a result of the rigid structural requirements of chelate compounds, substitution within polydentate ligands or the entrapment of these complexes within inert environments, may produce very large steric effects. Since this steric hindrance is minimized in the tetrahedral structure of this complex, there is a strong driving force for the conversion of the copper (II) complex to the corresponding copper (I) species, as can be seen from the large oxidation potential for this system.[47]

Copper-containing enzymes play a significant catalytic role in the biosphere. It has been known for some time that the copper containing oxygenase enzyme, tyrosinase (monophenol; dihydroxy-L-phenylalanine; oxygen reductase; EC 1.14.18.1) is responsible for melanization in mammals and browning in fruits.[48] The enzyme catalyses the oxidation of L-tyrosine to L-DOPA and o-quinones.[49] It reversibly binds oxygen and catalyses two different reactions,[50] the hydroxylation of monophenols to o-diphenols (monophenolase activity) and oxidation of the o-diphenols to o-quinones (catecholase activity) using molecular oxygen as the oxidant.[51] Chemical and spectroscopic studies indicate that the coupled binuclear copper active site in tyrosinase is very similar to that found in hemocyanins.[52] The active site consists of a pair of antiferromagnetically-coupled copper ions.[53] The oxygenated form (oxytyrosinase, E_{oxy}) consists of two tetragonal Cu (II) atoms

each coordinated by two strong equatorial and one weaker axial N_{His} ligand.[54] The exogenous oxygen molecule is bound as a peroxide {with a side-on (μ-η^2-η^2) rather than an end-on (cis-μ-1,2) geometry} and bridges the two Cu centres.[55] The latter peroxide bridging mode has been shown to be present in oxyhemocyanin with the peroxide occupying two equatorial positions on each Cu.[56] This electronic side-on approach appears to make a significant contribution to the biological function of oxytyrosinase. Mettyrosinase (E_{met}), like the oxy form, contains two tetragonal Copper (II) ions antiferromagnetically coupled through an endogenous bridge.[57] EPR and optical spectral features of this form reflect electron delocalisation between the two copper atoms. Deoxytyrosinase (E_{deoxy}) has a bicuprous structure [Cu^I-Cu^I]. During hydroxylation, the phenols coordinate directly to the copper, leading to a transfer of electron density from the Cu ions and weakening of both the O-O and Cu-O bonds. Oxygen transfer to the ortho position in the phenol occurs. The resultant coordinated catecholate transfers two electrons to the binuclear cupric site, leading to the dissociative elimination of the o-quinone product and the formation of the deoxy site for further turnover. The monophenolase activity of tyrosinase is generally defined as the first step in the melanization pathway and consists of o-hydroxylation of the monophenol to o-diphenol.[58] Since this is always in conjunction with the oxidation of the o-diphenol to its o-quinones it is also defined as the complete conversion of monophenol to o-quinone. This activity distinguishes tyrosinase from other phenol-oxidizing enzymes such as laccase and peroxidase and is characteristic of the enzyme. There is a lag period which is interpreted as a dynamic equilibrium between the enzymatic and the chemical steps to obtain steady-state diphenol concentration.

1.3 Reversible cleavage and formation of dioxygen bond

Dioxygen O-O bond forming and cleavage reactions occur in the presence of molecular O_2 at transition metal centres in a number of enzymes like Cytochrome-P-450 and methane monooxygenase,[59-61] which hydroxylate alkanes to key metabolites. Similar reactions are witnessed in the case of tyrosinase. Recent studies[62] have shown that in synthetic copper complexes the existence of an equilibrium between a dicopper-dioxygen adduct and its isomer having two oxo-bridges and lacking the O-O bond. This is the type of equilibrium which normally exists in biological systems. The reverse reaction, the oxidative coupling of water molecules to form O_2 during photosynthesis, involves formation of the O-O bond which is reported in the case of tetranuclear Mn clusters.[63] Tolman and his co-workers[64] have characterized the adduct of a copper (I) complex in CH_2Cl_2 and O_2, and suggest that it contains a peroxo dicopper (II) core in which the O-O bond remains intact and cleaves in the presence of tetrahydrofuran. Both species were formed at identical rates. Both activation of O_2 through O-O bond splitting and evolution of O_2 involving O-O bond formation can be envisioned to proceed through $[M_2(\mu\text{-}\eta^2 : \eta^2\text{-}O_2)]^{n+}$ (A) $\leftrightarrow$ $[M_2(\mu\text{-}O_2)]^{n+}$ (B) isomerisation. The existence of isomeric $[M_2(\mu\text{-}\eta^2 : \eta^2\text{-}O_2)]$ core structure (A) : has been established for oxyhemocyanin and its analogs. The compositional similarity between the above two structures suggests that the key step in O_2 activation at a dimetal centre is the transformation of A $\rightarrow$ B, and the pivotal step in O_2 evolution may be the reverse.[65] Since the copper complex[66] does not seem to have a

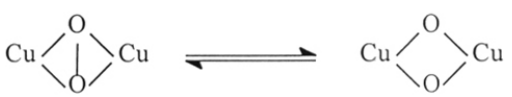

A B

classical electron distribution, the electrons are delocalised over the dioxygen and two copper units.

1.4. Transition metal complexes encapsulated in zeolites

Romanovsky et al first reported the synthesis of metallophthalocyanines inside the supercages of zeolite Na-Y in 1977.[67-68] Because of the similarity in structure and chemical properties between metalloporphyrin and metallophthalocyanine complexes, the latter have often been used as substitutes for active sites in Cytochrome P-450. Several groups have studied the encapsulation and reactivity of metallophthalocyanine complexes,[69-74] related porphyrin complexes[28-29, 75-77] as well as salen[21,78-84] (N,N'- bis (salicylidene) ethylene diamine) complexes encapsulated in molecular sieves. Parallel studies on intrazeolite organometallics and coordination complexes,[85-86] as well as metal oxides[87] have been reported. There are two main approaches followed to create new redox active molecular sieves. In the first approach, the redox active transition metal ions have been incorporated by isomorphous substitution or ion exchange in the lattice of zeolites or aluminophosphate molecular sieves. In this way, heterogeneous Ti and V catalysts have been developed.[88-89] The second approach in creating new redox active molecular sieves involves heterogenisation of transition metal complexes with potential catalytic activity in zeolites or molecular sieves. Klier first formulated the interaction of transition metal cations and small ligands as intrazeolite metal complex formation in zeolites[90] and considerable progress has been made, since then.[25,85,91-94]

Owing to their large size, (10-14 Å), metal-Schiff-base, -porphyrin and -phthalocyanine complexes cannot be encapsulated in zeolites by anion exchange process in conventional zeolites with channel dimensions between 4-8 Å. The encapsulation methods involved, are limited by the ability of the complex to diffuse into the pores of the

crystalline molecular sieve. But if the zeolite is synthesized around the metal complex, then only the cage dimensions are important as far as ligand size is concerned. However, the stability of the metal complex during the zeolite synthesis is a major requirement. The complex in this case, functions as a template. Several routes have been adopted to heterogenise transition metal complexes in zeolites. Apart from the above, another method is the anchoring on the zeolite surface of precursors of the desired complex through formation of new bonds.[95]

Encapsulation methods

1.4.1. Intrazeolite metal carbonyl cluster synthesis

Metal carbonyl clusters with nuclearity greater than three could potentially be encapsulated in FAU type zeolites. In this method, the reaction of CO/H_2 or CO/H_2O with metal ion exchanged Y type zeolite has led to the encapsulation of the metal carbonyl cluster. The presence of H_2 or H_2O is necessary for the formation of the clusters by the reductive carboxylation of the intrazeolite metal ions. Anionic complexes could be easily encapsulated within the supercages of FAU type zeolites. Table 1 lists the different types of carbonyl complexes encapsulated in zeolites by this method.

Table-1

Zeolite encapsulated metal carbonyl clusters

Cluster	Zeolite	Type	Reference
$Rh_6(CO)_{16}$	Na-Y	Carbonyl	96-98
$Rh_4(CO)_{12}$	Na-Y	Carbonyl	99
$[Rh_4Fe_2(CO)_{16}]^{2-}$	Na-Y	Bimetallic carbonyl	100,101
$Ir_4(CO)_{12}$	Na-Y	Carbonyl	99

Rh_{6-x} Ir_x $(CO)_{16}$ (x = 0-6)	Na-Y	Bimetallic Carbonyl	100,101
$[HFe_3 (CO)_{11}]^-$	Na-Y	Anionic carbonyl	100,102
$[HOS_3 (CO)_{11}]^-$	Na-Y	Anionic carbonyl	103
$[Ir_6 (CO)_{15}]^{2-}$	Na-Y	Anionic carbonyl	104,105
$[Co_6 (CO)_{15}]^{2-}$	Na-Y	Bimetallic carbonyl	103
$[Pt_3 (CO)_3 (\mu_2\text{-}CO)_3]_n^{2-}$ (n= 3,4,5)	Na-Y	Chini Type	104,105
$Pd_{13} (CO)_x$	Na-Y	Chini Type	106

1.4.2 Ligand synthesis method

This approach which has been successful only for phthalocyanines is also known as template synthesis method. The ligands can be synthesized out of four identical or substituted dicyano benzene molecules which assemble around an intrazeolite metal ion that acts as a template. The synthesis involves heating zeolites X, Y, aluminophosphates or VPI-5 modified with metal ions, metallocenes (Cp_2 Ni, Cp_2 Fe or Cp Mn $(CO)_3$, etc.) and metal carbonyl complexes (Ni $(CO)_4$, Os_3 $(CO)_{12}$, etc.) with excess dicyanobenzene (DCB) in a bomb reactor between 150-350 °C or 180 °C, in the presence of a solvent.[71] The condensation of the four DCB molecules around a metal ion to form a phthalocyanine requires two reducing equivalents which may probably originate from H_2O or metal ions in the case of organometallic precursors. The synthesis of zeolite encapsulated phthalocyanine complexes of Cu,[79,107-108] Co,[34,67,70,109-110] Ni,[67,111] Fe,[25,69,109-110] Mn,[75] Ru,[75,108,112-113] Rh,[113] Os,[109-110] Ti,[25] Li_2Pc and H_2Pc,[25] perhalogenated phthalocyanines[114-115] t-butyl phthalocyanines,[74] nitrophthalocyanines,[25] Cobalt porphyrins,[28] Fe and Mn tetramethyl porphyrins[25,77] as well as tetraphenyl porphyrin complexes[75] by the above

method have been reported. One disadvantage of the above method is the formation of aggregates during the synthesis, which hinders or limits encapsulation. Even though there are reports on the encapsulation of Fe and Mn tetramethyl and tetraphenyl porphyrins in zeolite Y by the above method, no convincing data on the intrazeolite formation of the phthalocyanine complexes have been reported.

1.4.3 Flexible ligand method

The flexible ligand method involves the diffusion of the ligands with one to five coordinating atoms into the zeolite pores, where, upon complexation with the metal ion, the resulting complex becomes too large to exit. This approach is especially well suited for the encapsulation of metal-Schiff-base complexes (e.g. SALEN), since this ligand offers the desired flexibility. The ligand should have a sufficiently low melting or sublimation point and should be small enough to enter the zeolite cavities. The void volume in the zeolite is filled homogeneously with the ligand molecules and these form a complex with the cation on heating and are sterically constrained in the supercage. The ligand may bind in a bidentate or tetradentate fashion depending on the nature of the metal ion. The disadvantage of this method is that it is difficult to control metal speciation; the zeolite often remains in the primary coordination sphere of the transition metal ion. A wide variety of cobalt,[21,82-83] iron,[84] rhodium,[79] ruthenium,[116] manganese,[78,84] and palladium[80-81] complexes have been prepared according to this method within the supercages of faujasites.

1.4.4 Zeolite synthesis method

This method offers the advantage of encapsulating a well defined metal complex without contamination by uncomplexed or partially complexed metal ions as well as free ligands. These problems are encountered using the template and flexible ligand

approaches. In this approach, the well defined metal complex is added to the silica prior to the gel formation. When a homogeneous dispersion results, the aluminate solution is added and the gel is aged prior to crystallization. However, if the metal complex is added to the aluminate solution or aluminophosphate gel, a heterogeneous mixture results and there is virtually no encapsulation in the zeolites. Metal phthalocyanines[117-118] and perfluorophthalocyanines[114-115] were encapsulated in NaX during zeolite crystallization. In a similar way, metal complexes were also incorporated in ZSM-5 and mordenite.[119-120] The metal complex, possibly, plays the role of a template in directing the synthesis. The aggregation of the metal complexes in the aqueous synthesis medium can be overcome by careful design of the zeolite synthesis procedure. The disadvantages involved in the above method are that the complex should be stable during all stages of the zeolite synthesis and crystallization. Further in the case of zeolites requiring a supplementary template molecule, removal of this template may necessitate calcination, which may also damage the complex during the process.

1.4.5 Cationic exchange of complexes

If the complex is cationic and if the zeolite has sufficient cation exchange capacity, the complex can be directly exchanged from the aqueous solution; provided the complex is small enough to pass through the pores of the zeolite.[121]

1.4.6 Ligand adsorption on metal ion exchanged zeolites

Adsorption of amines from aqueous solutions on transition metal containing zeolites is a typical example.[122] The only controlling parameter in such synthesis procedures is the pH. A low pH results in protonation of the ligand, while a high pH may damage the zeolite structure. Impregnation of transition metal containing zeolites with

NaCN solution results in entrapment of anionic $[M^{n+} (CN)^{-}_{m}]^{n-m}$ chelates in anionic zeolites [e.g. $Co^{n+} (CN)^{-}_{m}]^{n-m}$ -Na-Y.[123]

1.5 Catalysis with zeozymes

1.5.1 Molecular O_2 binding

Zeolite-based enzyme mimics are called zeozymes. Zeolite-based synthetic mimics with Fe (II) and Co (II) as central metal atoms of chelates exhibited remarkable ability for reversible binding with dioxygen.[18] In hemoglobin, which is a four subunit enzyme, with Fe=O as active site, the four subunits interact, so that the binding of dioxygen to the first site facilitates its binding to the other two sites. Co (salen)-Y contains a square planar complex which forms an adduct with dioxygen, as can be seen from its EPR signal.[18,82-82] Peroxo-dimerisation cannot occur due to site isolation of the individual complex in the supercages of the faujasite. Diegruber et al[34] reported the selective oxidation of propene to formaldehyde and acetone with dioxygen using Co $(dmg)_2$-X and Co (py)-X as catalysts. These zeolite-encaged adducts display interesting features as compared to the free complex. The initial fixing of the oxygen molecule makes it more difficult for the subsequent oxygen to bind to the subsequent sites. Oxygen binding may become more difficult on moving from the outer to the inner layers of the zeolite crystals,[34] thus explaining the negative cooperative effect.

1.5.2 Biomimetic Oxidations

Herron et al[124-125] reported the first example of zeolite encapsulated FePc catalysts in hydrocarbon oxidations using iodosyl benzene as the oxidizing agent. Iodoxy benzene is formed in the zeolite pores[69] by the disproportionation reaction of the oxidant :

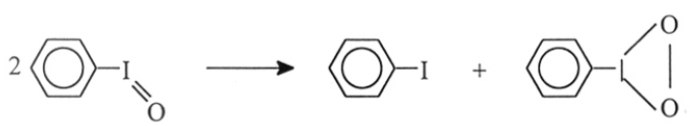

The use of tertiary butyl hydroperoxide as the oxidant and the ferrocene route for the synthesis of FePc-Y results in increased turnover numbers, TON. These zeolite entrapped chelates show high resistance towards oxidation and can even be used at higher temperature. The stability of the complex improved significantly on encapsulation. As suggested by Herron,[125] the encapsulation of the phthalocyanine complex within the zeolite cavities effects spatial isolation of the monomer species, so that bimolecular mechanisms leading to the formation of peroxo dimers, which are commonly involved in auto-oxidative degradation of many synthetic models of enzymes and free coordination complexes of transition metals is strongly inhibited. This prevents catalyst deactivation and destruction.[126-127] The improved stability towards oxidative destruction could permit one to perform catalytic oxidations using heterogenised metal complexes under more severe process conditions in comparison to the free analogs. Table 2 illustrates some examples of alkane oxidation catalyzed by metal complexes and zeolite encapsulated metal complexes.

Table-2

Alkane oxidation catalyzed by metal complexes

and zeolite encapsulated metal complexes

Substrate	Catalyst	Oxidt	Products	Ref
Methane	RuPc-Y	O_2	Methanol, CO_2	75
	Co-TPP-Y	O_2	CO_2, H_2O, Methanol	128
	Mn-TPP-Y	O_2	CO_2, H_2O, Methanol	128
Propane	Fe ($TPPF_2OBr_8$)Cl	O_2 (Air)	Isopropyl alcohol, acetone	28
	Fe ($FPc)N_3$			
	Fe ($TPP)N_3$			
	Cr ($TPP)N_3$			
	Mn ($TPP)N_3$			

	Fe ($TPPF_{20}$)N_3	O_2		28
Isobutane	Fe ($TPPF_{20}$)OH Fe ($TPPF_{20}$-β-Br_8)ClO_2 Fe ($TPPF_{20}$)Cl	O_2 , (AIR)	t-butyl alcohol, acetone t-butyl alcohol, acetone, CO, CO_2 t-butyl alcohol, acetone	28
n-butane	Fe ($TPPF_{20}$-β-Cl_{18})Cl Cr ($TPPF_{20}$-β-Cl_{18})Cl Cr ($TPPF_{20}$-β-Cl_{18})N_3	O_2 (Air)	s-butyl alcohol, methyl-ethyl ketone, acetaldehyde, acetic acid	28
2 methyl butane	Fe ($TPPF_{20}$)OH Fe ($TPPF_{20}$-β-Br_8)ClO_2 Fe ($TPPF_{20}$)Cl	O_2 (Air)	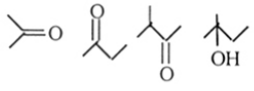	28
2,3 dimethyl butane	Fe ($TPPF_{20}$-β-Br_8)ClO_2	O_2 (Air)	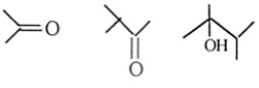	28
2,2,3 trimethyl butane	Fe ($TPPF_{20}$)OH Fe ($TPPF_{20}$-β-Cl_{18})OH	O_2 (Air)	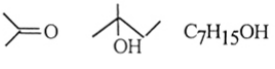	28
3 methyl pentane	Fe ($TPPF_{20}$-β-Br_8)ClO_2	O_2 (Air)	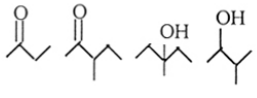	28
n-hexane	FePc-Y	TBHP	C_2, C_3, alcohols/ketones	74
	Fe-TTPP	PhIO	1, 2, 3, alcohols	129
	Fe/Pd/Zeolite	O_2	1, 2, alcohol	18
		H_2O_2	1, 2, alcohol	22
	Fe/ZSM-5	H_2O_2	1, 2, alcohol	22
	FePc-Na-Y	PhIO	2, 3, alcohol	130
n-heptane	FePc-Y	TBHP	C_2-C_4 alcohols/ketones	17
n-octane	FePc-Y	TBHP	C_2-C_4 alcohols/ketones	17
n-nonane	FePc-Y	TBHP	C_2-C_5 alcohols/ketones	17
n-decane	FePc-Y	TBHP	C_2-C_5 alcohols/ketones	17
Cyclohexane	FePc-Y-PDMS	TBHP	adipic acid	24

	Fe $(pic)_2$-Y	TBHP		
	Fe (bpch)-Y	H_2O_2		
	Fe (bpb)-Y	H_2O_2	cyclohexanol,	
	Fe (bpen)-Y	H_2O_2	cyclohexanone,	131
	Fe (bppn*)-Y	H_2O_2	cyclohexyl hydroperoxide	
	Fe $(NO_2)_4$Pc-Y	TBHP		
	Fe(III) (HPTTP) (Cl)-PS	O_2	cyclohexan-ol / one	132
	Fe(III) (THPP) (Cl)-PS	O_2	cyclohexanol,	133
	Fe(III) (THMPP) (Cl)-PS	O_2	cyclohexanone	
	FePc-VPI-5	TBHP		133
	RuF_{16}Pc-Na-X	TBHP	cyclohexan-ol / one	132
	Mn $(bipy)_3$-Na-Y	H_2O_2	cyclohexanone	134,135
			adipic acid, 1,2 diol/dione	135
Methyl	FePc-X	PhIO	Me-cyclohexan- ol/one	69
cyclohexane	FePc-Na-Y	PhIO	cis, trans, 4-ols	124
Cyclododecane	FePc-VPI-5	TBHP	cyclododecan- ol/one	134

The following generalizations can be made :

(i). TON increases on encapsulation of the metal complex as compared to the free analogues.

(ii). TON decreases with increasing loading of the metal complex, possibly due to pore blockage of the zeolite system with reaction products, thereby preventing further access of reagents and substrate to the active site.

(iii). The dimension and shape of the active site environment control shape selectivity and regioselectivity (Tables 3 and 4).

(iv). High yields of oxygenated products are obtained when the metal complex is encapsulated and not merely impregnated on the zeolite surface, indicating that the residual

free metal mainly catalyses the peroxide decomposition rather than the incorporation of the O atoms in the substrate molecules.

Table-3

Regioselectivity in n-alkane oxidation of encapsulated FePc [130]

Position of oxidation	C_6H_{14}	C_7H_{16}	C_8H_{18}	$C_{10}H_{22}$
C 2	48	39	43	49
C 3	52	35	33	32
C 4	-	26	22	18

Table-4

Regioselectivity (%) in n-octane oxidation over FePc in Y and VPI-5 zeolites[128]

Position of	Regioselectivity (%)	
Oxidation	Y	VPI-5
C 2	43	38
C 3	34	31
C 4	22	29

Some olefin oxidations catalyzed by metal complexes encapsulated in zeolites are shown in Table-5

Table-5

Olefin oxidations catalyzed by zeolite encapsulated metal complexes

Substrate	Catalyst	Oxidt	Products	Ref
Propene	Co $(dmg)_2$-X	O_2	CH_3CHO, HCHO	34
	Co (Py)-X		acetone	
	CoPc-X/Y		CH_3CHO, HCHO	
1-hexene	CoPc-Na-Y	PhIO	1-hexene-oxide	138
		TBHP	1-hexene-oxide, t-butyl hexene-peroxide	138
	Mn $(bpy)_2$- X/Y	H_2O_2	hexene-oxide, hexenediol	26
1-octene	FePc-Y	O_2	2-octanone	74
	Co-salophen-Na-Y	O_2	2-octanone	139
2-octene	MnPc-Na-Y	PhIO	2-octene-oxide	140
1-decene	FePc-Y / Pd $(OAc)_2$	O_2	2-decanone	31
1-dodecene	Mn $(bpy)_2$- X/Y	H_2O_2	epoxide, diol	26
Indene	Mn(III)-salen-EDGMA	PhIO	epoxide	141
1-indecene	MnPc-Na-Y	PhIO	1-indecene-oxide	140
trans-stilbene	Mn-salen-Y	PhIO	trans stilbene oxide	78
	Mn(III)-salen-EDGMA	PhIO	epoxide	141
cis-stilbene	Mn-salen-Y	PhIO	cis stilbene oxide	78
DHNP	Mn(III)-salen-EDGMA	PhIO	epoxide	141
Cyclohexene	Mn-salen-Y	PhIO	cyclohexeneoxide cyclohexeneol	78
	CoPc-Na-Y	PhIO	cyclohexeneoxide 2-cyclohexen-1-one	138
		TBHP	cyclohexene oxide t-butylcyclohexene peroxide	138
	Mn(TMTACN)-Na-Y	O_2	cyclohexene oxide trans 1,2 cyclohexane diol	142
	Mn $(bpy)_2$- X/Y	H_2O_2	oxide, diol, diacid	26
	Co-salophen-Y	O_2	3-acetoxycyclohexene	139

	FePc-Y / Pd $(OAc)_2$	O_2	1-acetoxy 2-cyclohexene	31
cyclododecene	Mn $(bpy)_2$- X/Y	H_2O_2	oxide, diol, diacid	26
Styrene	Mn-salen-Y	PhIO	styrene oxide, phenylacetaldehyde	78
	MnPc-Na-Y	PhIO	styrene oxide	140
	Mn(TMTACN)-Na-Y	O_2	benzene, styrene oxide	142
	Mn(III)-salen-EDGMA	PhIO	epoxide (enantioselective)	141

1.5.3 Reactivity of Zeolite Encapsulated Copper (II) Amino Acid (AA) Complexes :

Cu $(AA)_n$ complexes have been shown to mimic copper-containing enzymes, which are active in selective oxidation reactions.[143-144] These complexes are immobilized in a zeolite matrix, which performs the function similar to the protein mantle of enzymes. This heterogeneous system is more stable and has a larger operational domain (compared to the free complexes) as far as temperature and solvent are concerned. The Cu $(AA)_n^{m+}$ (AA = amino acid, glycine, lysine, histidine, alanine serine, proline, tyrosine, phenylalanine, glutamine, glutamic acid, cysteine, tryptophan, leucine and arginine) were immobilized into zeolite Y by a simple cation-exchange procedure with aqueous solutions of preformed Cu $(AA)_n^{m+}$ complexes. The type of binding between an amino acid and Cu^{2+} is the same for all α amino acids with the exception of histidine.[145] The general coordination for a Cu complex with two α amino acids is the binding of both the AA by an amino nitrogen and a carboxyl oxygen, i.e. a NNOO coordination or a glycine-like bonding. For example, in the case of Cu $(histidine)_2$ complexes, the two histidine ligands are coordinated to Cu^{2+} in the coordination plane by the amino N and the imidazole N, while the carboxylate group coordinates in an apical plane. However, an equilibrium exists between the NNNN and NNNO bonding in the coordination plane of the bis-(histidine) complexes, as the carboxylate oxygen of one of the histidine ligands can replace

partially one of the imidazole nitrogens. NNNN coordinations are referred to as histamine-like coordinations while in NNNO coordinations one histidine is bound histamine-like and the other glycine-like. The catalytic performance of these zeolite encapsulated Cu $(AA)_n^{m+}$ complexes are tabulated in Table-6.

Table-6

Zeolite-encapsulated Cu $(AA)_n^{m+}$ complex catalysts[146]

Substrate	Catalyst	Oxidant	Products
Cyclohexane	Cu[(histidine)$_2$]-Y	TBHP	cyclohexanol, cyclohexanone
Benzyl alcohol	Cu[(histidine)$_2$]-Y	TBHP	benzoic acid, benzaldehyde
1-pentanol	Cu[(histidine)$_2$]-Y	TBHP	pentanoic acid
cyclohexene	Cu[(histidine)$_2$]-Y Cu[(lysine)$_2$]$^{2-}$-Y Cu[(arginine)$_2$]$^{2-}$-Y	TBHP	cyclohexene oxide 1,2 cyclohexene diol cyclohex-2-en-1- ol/one
benzene	Cu$(CH_3COO)_2$-Y/AA	O_2	Phenol

1.5.4 Hydrogenation of hydrocarbons

Though the majority of the work done on enzyme mimics were carried out using oxidation as a test reaction, some work has also been done for hydrogenation processes over transition metal complexes encapsulated in zeolite matrices Table-7.

Table-7

Hydrogenation reactions over zeolite encapsulated metal complexes

Substrate	Catalyst	Products	Ref
Butadiene	$(Na^+)_4$ $FePc^{4-}$-Y	butane, but 1-ene, t-but-2-ene, c-but-2-ene	147

Cyclohexene	Pd $^{(II)}$ salen-Y	cyclohexane	80
1-hexene	Pd $^{(II)}$ salen-Y	n-hexane	80
Toluene	Fe (II) Pc-Na-Y	Methyl cyclohexane	148

1.6 Oxyhalogenation of aromatic compounds

Dinesh et al,[149] have recently shown that ammonium metavanadate efficiently catalyses the oxyhalogenation of a variety of organic substrates in moderate to good yields, using dilute hydrogen peroxide (30 %) as an oxidizing agent, exhibiting remarkable ortho selectivity with electron-rich aromatics. Similar results had been reported earlier by Conte et al[150] and Rosa et al.[151] In the above studies the authors' main goal was the development of functional mimics of the haloperoxidase marine enzymes. These enzymes oxyhalogenate aromatic substrates using H_2O_2 and halide ions present in the marine environment. Very recently, a two-stage vapour phase process for the conversion of HCl to Cl_2 using solid catalysts has been reported.[152]

1.7 Objective of the Thesis

Compared to the wealth of information available on iron complexes encapsulated in zeolites, the chemistry of similar copper compounds is known in less detail. This is surprising in view of the major role of copper in catalyzing a large number of redox reactions in the biosphere. **The main objective of this thesis** is to study the *Synthesis, Characterization and Catalytic Applications of Copper Complexes Encapsulated in Molecular Sieves.* In the present work, catalysts that combine the features of the zeolites with the tremendous selectivity and activity of homogeneous copper complexes were synthesized and characterized by a wide variety of physico-chemical techniques. The catalytic properties of these copper complexes encapsulated in zeolites in the selective

oxidation of paraffins, aromatics, phenols and in the oxyhalogenation of aromatics using both H_2O_2 and O_2 as oxidants were investigated in systematic detail and are reported in this thesis.

1.8 Plan of the thesis

CHAPTER-1 : **Introduction**

The chemistry of copper complexes in oxidation reactions has been discussed with special reference to the copper containing monooxygenase enzyme, tyrosinase (E.C. 1.14.18.1). A general overview with a detailed literature survey on the different methods of synthesis and catalytic reactions over zeolite encapsulated metal complexes is reported in this chapter. The objective of the thesis as well as the plan and strategy of the work are outlined.

Chapter-2 **Experimental**

The experimental techniques and procedures adopted in the synthesis of copper-acetate, copper phthalocyanine (CuPc), copper hexadeca chloro phthalocyanine ($CuCl_{16}Pc$), copper tetra nitro phthalocyanine ($Cu(NO_2)_4Pc$) and iron hexadeca chloro phthalocyanine ($FeCl_{16}Pc$), complexes and their encapsulation in molecular sieves, (X, Y, MCM-22, VPI-5, ZSM-5 and K-L) is described in detail. Detailed procedures of the catalytic reaction and product analysis of the oxidation and oxyhalogenation reactions is also given.

Chapter-3 **Catalyst Characterization**

The physicochemical characteristics of the catalysts are described in this chapter. Various techniques have been used in tandem to characterize the encapsulated metal complexes and the support used for encapsulation. The bulk characteristics, electronic

and vibrational properties, surface features, nuclearity, electrochemical nature, distortions and integrity of the metal complexes in the neat as well as in the encapsulated state are described in detail.

Chapter-4 **Oxidation of alkanes**

In chapters 4-7, the oxidation and oxyhalogenation activity of the encapsulated copper complexes in various reactions is described. In chapter-4, the selective oxidation of n-hexane (to hexanol + hexanone), cyclohexane (to cyclohexanol, cyclohexanone and adipic acid) and methane (to methanol and formaldehyde) over the phthalocyanine complexes of copper, cobalt and iron, in the neat as well as in the zeolite encapsulated state are described and discussed .

Chapter-5 **Oxidation of Aromatics**

This chapter describes and discusses the selective oxidation and hydroxylation of aromatic substrates (like benzene, toluene, ethylbenzene and naphthalene) at ambient conditions, using *clean* oxidants like O_2 or H_2O_2 over copper tetradeca chlorophthalocyanine and copper tetranitrophthalocyanine encapsulated in zeolites Na-X and Na-Y.

Chapter-6 **Oxidation of phenols**

This chapter reports a novel catalytic system consisting of dimeric complexes of copper acetate monohydrate encapsulated in molecular sieves, Y, MCM-22 and VPI-5 which utilizes O_2 in the ortho hydroxylation of phenols (in L-tyrosine, phenol and cresols), thereby mimicking the catalytic properties of the enzyme, tyrosinase. The catalytic properties of the copper phthalocyanine system in the selective oxidation of phenol to both catechol and hydroquinone using H_2O_2 as the oxidant is also described.

Chapter-7 **Oxyhalogenation of Aromatics**

The oxychlorination and oxybromination, at near-ambient conditions, of benzene, toluene, phenol, aniline, anisole and resorcinol using as catalysts, the phthalocyanines of Cu, Co and Fe encapsulated in zeolites X, Y and L are reported in this chapter. H_2O_2 and O_2 have been used as the oxidants while HCl and alkali chlorides/bromides have been used as the sources of halogens. Oxyhalogenation of both the aromatic nucleus and the alkyl side-chain occur. The performance of these novel catalytic systems holds promise in the organic and fine chemicals industry for the manufacture of halogenated aromatics in an environmentally *clean* manner.

Chapter-8 **General Discussion**

In this chapter, the results of the selective oxidation and oxyhalogenation described in chapters 4-7 have been discussed with a view to understanding the *mechanism* of catalytic action over the copper acetate as well as the copper phthalocyanine catalyst systems.

Chapter-9 **Summary and Conclusions**

This chapter summarizes the major findings of chapters 3-8 and draws the conclusions needed for further progress in this area.

1.9 References

1. D.A. Robb, in R. Lontie (Ed); "*Copper proteins and copper enzymes*" CRC Press, Boca Raton, Florida, (1984) 207.

2. E.T. Adman, in C.B. Anfinsen, J.T. Edsall, F.M. Richards and D.S. Eisenberg (Eds); *"Advances in protein chemistry*, Vol. 42, Academic Press, New York, (1991) 145.

3. R.E. White and M.J. Coon, *Ann. Rev. Biochem.*, **49** (1980) 315.

4. I.C. Gunsalus and S.C. Sligar, *Adv. Enzymol. Relat. Areas. Mol. Biol.*, **47** (1978) 1.

5. M. Hamburg, B. Samuelsson, I. Bjorkhem and H. Danielsson, in O. Hayaishi (Ed); *"Molecular mechanisms of oxygen activation"* Academic Press, New York, (1974) 29.

6. J.C.M. Tsibris and R.D. Woody, *Coord. Chem. Revs.*, **5** (1970) 417.

7. D.W. Breck, "*Zeolite Molecular Sieves*" Wiley, New York, (1974).

8. F. Haber and J. Weiss, *Proc. Roy. Soc. (London), A* **147** (1934) 332.

9. R. D. Chambers, P. Goggin and W.K.R. Musgrave, *J. Chem. Soc. Chem. Commun.*, (1959) 1804.

10. G.A. Hamilton and J.P. Friedman, *J.Am. Chem. Soc.*, **85** (1963) 1008.

11. S. Udenfriend. C.T. Clark, J. Axelrod and B.B. Brodie, *J. Biol. Chem.*, **208** (1954) 731.

12. W. Brackman and E. Havinga, *Rec. Trav. Chim.*, **74** (1955) 937.

13. J. Manassen, in F. Basolo and R.E. Burwell Jr., (Eds); *"Catalysis, Progress in Research*" Plenum, New York, (1973) 177.

14. J.C. Bailar Jr., *Catal. Rev. Sci. Eng.*, **10 (1)** (1974) 17.

15. J.P. Candlin and H. Thomas, in D. Forster and J.F. Roth, (Eds); "*Homogeneous Catalysis-II*, American Chemical Society, Washington, D.C., (1974) 212.

16. H.P. Boehm in D.D. Eley, H. Pines, P.B. Weiss and H.P. Boehm (Eds); "*Advances in Catalysis and related subjects*", Academic Press, New York, Vol. 16 (1966) 179.

17. N. Herron and C.A. Tolman, *J. Am. Chem. Soc.*, **109** (1987) 2837.

18. N. Herron, *Chemtech,* Sept. (1989) 542.

19. J.P. Collman, R.R. Gagne, T.R. Halbert, J.C. Marchon and C.A. Reed, *J. Am. Chem. Soc.*, **95** (1973) 7868.

20. R.D. Jones, D.A. Summerville and F. Basolo, *Chem. Rev.*, **79** (1979) 139.

21. N. Herron, *Inorg. Chem.*, **25** (1986) 4717.

22. N. Herron, *New. J. Chem.*, **13** (1989) 761.

23. D.R. Corbin and N. Herron, *J. Mol. Catal.*, **86** (1994) 343.

24. R.F. Parton, I.F.J. Vankelecom, M.J.A. Casselman, C.P. Bezoukhanova, J.B. Uytterhoeven and P.A. Jacobs, *Nature*, **370** (1994) 541.

25. R. Parton, D. De Vos and P.A. Jacobs, in E.G. Derouane, F. Lemos, C. Naccache and R.F. Ribeiro (Eds); "*Zeolite Microporous Solids : Synthesis, Structure and Reactivity*," Khumer Academic Publishers, London (1991) 555.

26. P.P.K. Gerrits, D. De Vos, F.T. Starzyk and P.A. Jacobs, *Nature*, **369** (1994) 543.

27. P.R.H.P. Rao, A.V. Ramaswamy and P.Ratnasamy, *J. Catal.*, **137** (1992) 225.

28. J.E. Lyons, P.E. Ellis, Jr. and H.K. Myers, Jr., *J. Catal.*, **155** (1995) 59.

29. P.E. Ellis, Jr., and J.E. Lyons, *Coord. Chem. Rev.* **105** (1990) 181.

30. S. Ernst, Y. Traa and U. Deeg, *Stud. Surf. Sci. Catal.*, **84** (1994) 925.

31. A. Zsigmond, F. Notheisz, M. Bartok and J.E. Backval, *Stud. Surf. Sci. Catal.*, **78** (1993) 417.

32. R.J. Taylor, R.S. Drago, and J.P. Hage, *Inorg. Chem.*, **31** (1992) 253.

33. E.R. Birnbaum, M.W. Grinstaff, J.A. Labinger, J.E. Bercaw and H.B. Gray, *J. Mol. Catal.*, **104** (1995) L119.

34. H. Diegruber, P.J. Plath, E.G. Schulz-Elkoff and M. Mohl, *J. Mol. Catal.*, **24** (1984) 115.

35. J.E. Lyons and P.E. Ellis, Jr., *Appl. Catal. A.*, **84** (1992) L1 .

36. B.B. Corden, R.S. Drago and R.P. Perito, *J. Am. Chem. Soc.*, **107** (1985) 2903.

37. R.B. Lauffer, R.H. Heistand and L. Que, Jr., *Inorg. Chem.*, **22** (1983) 50.

38. M. Calligaris, G. Manzini, G. Nardin and L. Randaccio, *J. Chem. Soc., Dalton Trans.*, (1972) 5430.

39. S.L. Kessel, R.M. Emberson, P.G. Debrunner and D.N. Hendrickson, *Inorg. Chem.*, **19** (1980) 1170.

40. D. Cummins, E.D. McKenzie and H. Milburn, *J. Chem. Soc., Dalton Trans.*, (1976) 130.

41. E. Vogel, *Schwiegger's Journal*, **13** (1815) 162.

42. L.G. Sillen and A.E. Martell, *Chem. Soc., Spec. Publ.*, **17** (1964).

43. B.N. Figgis and R.L. Martin, *J. Chem. Soc., London* (1956) 3837.

44. M. Kato, H.B. Jonassen and J.C. Fanning, *Chem. Rev.*, **64** (1964) 99.

45. J.K. Kochi and R.V. Subramaniam, *Inorg. Chem.*, **4** (1965) 1527.

46. M. Kondo and M. Kubo, *J. Phys. Chem.*, **62** (1958) 468.

47. W.G. Nigh, *Oxidation in organic chemistry B*, (1973) 8.

48. A.M. Korner and J.M. Pawelek, *Science*, **217** (1982) 1163.

49. K. Lerch, in "*Metal ions in biological systems*", S. Sigel (Ed); Marcel Dekker, New York, Vol 13, (1981) pp. 143.

50. W.H. Vanneste and A. Zuberbühler, in "*Molecular mechanism of oxygen activation*," O. Nayaishi (Eds); Academic Press, New York, (1974) pp. 371.

51. V.J. Hearing and M. Jimenez, *Int. J. Biochem.*, **19** (1987) 1141.

52. R.S. Himmelwright, N.C. Eickman, C.D. LuBien, K. Lerch and E.I. Solomon, *J. Am. Chem. Soc.*, **102** (1980) 7339.

53. A.S. Ferrer, J.N.R. Lopez, F.G. Canovas and F.G. Carmona, *Biochim. Biophys. Acta.*, **1247** (1995) 1.

54. E.I. Solomon and M.D. Lowery, *Science*, **259** (1993) 1575.

55. N.C. Eickman, R.S. Himmelwright and E.I. Solomon, *Proc. Natl. Acad. Sci., USA* **76** (1979) 2094.

56. K. Magnus and H. Ton-That, *J. Inorg. Biochem.*, **47** (1992) 20.

57. E.I. Solomon, in "*Copper Proteins*," T.G. Spiro (eds); Vol III, Wiley-Interscience, New York, (1981) pp. 41.

58. H.S. Mason, *Nature* **177** (1956) 79.

59. A.C. Rosenzweiz, C.A. Frederick, S.J. Lippard and P. Nordlund, *Nature*, **366** (1993) 537.

60. A.L. Feig and S.J. Lippard, *Chem. Rev.*, **94** (1994) 759.

61. L. Que, Jr. and A.E. True, Prog. *Inorg. Chem.*, **38** (1990) 97.

62. J.A. Halfen, S. Mahapatra, E.C. Wilkinson, S. Kaderli, V.G. Young, Jr., L. Que, Jr., A.D. Zuberbühler and W.B. Tolman, *Science,* **271** (1996) 1397.

63. K. Wieghardt, *Angew. Chem. Int. Ed. Engl.*, **28** (1989) 1153.

64. S. Mahapatra, J.A. Halfen, E.C. Wilkinson, L. Que, Jr. and W.B. Tolman, *J. Am. Chem. Soc.*, **116** (1994) 9785.

65. V.L. Pecoraro, M.J. Baldwin and A. Gelasco, *Chem. Rev.*, **94** (1994) 807.

66. Z. Tyeklar and K.D. Karlin, *Stud. Surf. Sci. Catal.*, **66** (1991) 237.

67. V.Y. Zakharov and B.V. Romanovsky, *Sov. Mosc. Univ. Bull.*, **32** (1977) 16.

68. V.Y. Zakharov, O.M. Zakharova, B.V. Romanovsky and R.E. Mardaleishvili, *React. Kinet. Catal. Lett.*, **6** (1977) 133.

69. N. Heron, C.A. Tolman and G.D. Stucky, *J. Chem. Soc., Chem. Commun.*, (1986) 1521.

70. B.V. Romanovsky, in *Proceedings of the 8th International Congress on Catalysis*, Verlag Chemie, Weinheim, (1984) pp. 657.

71. G. Meyer, D. Wohrle, D. Mohl and G. Schultz-Ekloff, *Zeolites*, **4** (1984) 30.

72. A.N. Zakharov and B.V. Romanovsky, *J. Inclus. Phenom.*, **3** (1985) 389.

73. T. Kimura, A. Fukuoka and M. Ichikawa, *Shokubai*, **31** (1988) 357.

74. M. Ichikawa, T. Kimura and A. Fukuoka, *Stud. Surf. Sci. Catal.*, **60** (1991) 335.

75. Y.W. Chan and R.B. Wilson, *Preprint papers - ACS, Div. Fuel. Chem.*, **33** (1988) 453.

76. E. Paez-Mozo, N. Gabriunas, F. Lucaccioni, D.D. Acosta, P. Patrono, A. La Ginestra, P. Ruiz and B. Delmon, *J. Phys. Chem.*, **97** (1993) 12819.

77. M. Nakamura, T. Tatsumi and H. Tominaga, *Bull. Chem. Soc. Jpn.*, **63** (1990) 3334.

78. C. Bowers and P.K. Dutta, *J. Catal.*, **122** (1990) 271.

79. K.J. Balkus, Jr., A.A. Welch and B.E. Gnade, *Zeolites*, **10** (1990) 722.

80. S. Kowalak, R.C. Weiss and K.J. Balkus, Jr., *J. Chem. Soc., Chem. Commun.*, (1991) 57.

81. D.E. De Vos and P.A. Jacobs, in *Proceedings from the 9th International Zeolite Conference*, R. Von Ballmoos, J.B. Higgins and M.M.J. Treacy (Eds); Butterworth-Heinemann, Boston, Vol. 2 (1992) pp. 615.

82. K. Putyera, G. Plesch, L. Benco, J. Dobrovodsky, A.V. Tchuvaev, V.I. Nefedov and M. Zikmund, *Proc. 12th Conf. Coord. Chem.*, (1990) 295.

83. F. Bedioui, E. DeBoysson, J. Devynck and K.J. Balkus, Jr., *J. Chem. Soc., Farad. Trans*, **87** (1991) 3831.

84. L. Gaillon, N. Sajot, F. Bedioui, J. Devynck and K.J. Balkus, Jr., *J. Electroanal. Chem. Interface. Electrochem.*, **345** (1993) 157.

85. G.A. Ozin and C. Gil, *Chem. Rev.*, **89** (1989) 1749.

86. N. Jaeger, P. Plath and G. Schultz-Ekloff, *Acta Phys. Chem.*, **31** (1985) 189.

87. G.A. Ozin, S. Ozkar and R.A. Prokopowicz, *Acc. Chem. Res.*, **25** (1992) 553.

88. P.H. Espeel, M. Tielen and P.A. Jacobs, *J. Chem. Soc., Chem. Commun.*, (1991) 669.

89. D.R.C. Huybrechts, L. De Bruyker and P.A. Jacobs, *Nature*, **345** (1990) 242.

90. K.Klier and M. Ralek, *J. Phys. Chem. Solids*, **29** (1968) 951.

92. W.J. Mortier and R.A. Schoonheydt, *Progr. Solid State Chem.*, **16** (1985) 99.

93. K. Kalyanasundaram, *Coord. Chem. Rev.*, **46** (1982) 159.

94. K. Kalyanasundaram, in "*Photochemistry in Microheterogeneous Systems*", Academic Press, Orlando, Fl., (1987).

95. G.M. Woltermann and V.A. Durante, *Inorg. Chem.*, **22** (1983) 1954.

96. L.F. Rao, A. Fukuoka and M. Ichikawa, *J. Chem. Soc., Chem. Commun.*, (1988) 458.

97. L.F. Rao, A. Fukuoka, N. Kosugi, H. Kuroda and M. Ichikawa, *J. Phys. Chem.*, **94** (1990) 5317.

98. N. Takahashi, A. Mijin, H. Suematsu, S. Shinohara and H. Matsuoka, *J. Catal.*, **177** (1989) 348.

99. P. Gelin, C. Naccache and Y. Ben Taarit, *Pure Appl. Chem.*, **60** (1988) 1315.

100. M. Ichikawa, L.F. Rao, A. Fukuoka, *Catal. Sci. Tech.*, **1** (1991) 111.

101. A. Fukuoka, L.F. Rao, N. Kosugi, H. Kuroda and M. Ichikawa, *Appl. Catal.*, **50** (1989) 295.

102. M. Iwamoto, S.I. Nakamura, H. Kusano and Sh. Kagawa, *J. Phys. Chem.*, **90** (1986) 5244.

103. R. Nakamura, N. Okada, A. Oomura and E. Echigoya, *Chem. Lett.*, **119** (1984) 55.

104. A. De Mallmann and D. Barthomeuf, *Catal. Lett.*, **5** (1990) 293.

105. P.L. Zhou, S.D. Maloney and B.C. Gates, *J. Catal.*, **129** (1991) 315.

106. L.L. Sheu, H. Knozinger and W.M.H. Sachtler, *J. Am. Chem. Soc.*, **111** (1989) 8125.

107. J.P. Ferraris, K.J. Balkus, Jr., and A. Schade, *J. Inclus. Phenom. Molec. Recog. Chem.*, **14** (1992) 163.

108. E.S. Shpiro, G.V. Antoshin, O.P. Tkachenko, S.V. Gudkov, B.V. Romanovsky and Kh. M. Minachev, *Stud. Surf. Sci. Catal.*, **18** (1984) 31.

109. B.V. Romanovsky and A.G. Gabrielov, *Stud. Surf. Sci. Catal.*, **72** (1992) 443.

110. B.V. Romanovsky and A.G. Gabrielov, *J. Mol. Catal.*, **74** (1992) 293.

111. A.G. Gabrielov, A.N. Zakharov and B.V. Romanovsky, *Koord. Khim.*, **14** (1988) 214.

112. A.G. Gabrielov, A.N. Zakharov and B.V. Romanovsky, O.P. Tkachenko, E.S. Shpiro and Kh. M. Minachev, *Koord. Khim.*, **14** (1988) 821.

113. K.J. Balkus, Jr., A.A. Welch and B.E. Gnade, *J. Inclus. Phenom. Molec. Recog. Chem.*, **10** (1991) 141.

114. A.G. Gabrielov, K.J. Balkus, Jr., F. Bedioui and J. Devynck, *Micropor. Mater.*, **2** (1994) 119.

115. K.J. Balkus, Jr., A.G. Gabrielov, F. Bedioui and J. Devynck, *Inorg. Chem.*, **33** (1994) 67.

116. F. Bedioui, L. Roue, L. Gaillon, J. Devynck, S.L. Bell and K.J. Balkus, Jr., *Petrol. Preprints*, **38** (1993) 529.

117. K.J. Balkus, Jr., and S. Kowalak, *U.S. Patent* 5,167,942 (1992).

118. K.J. Balkus, Jr., S. Kowalak, K.T. Ly and C.D. Hargis, *Stud. Surf. Sci.Catal.*, **69** (1991) 93.

119. L.A. Rankel and E.W. Valyocsik, *U.S. Patent* 4,500,503 (1985).

120. L.A. Rankel and E.W. Valyocsik, *U.S. Patent* 4,388, 285 (1983).

121. P. Peigneur, J.H. Lunsford, W. De Wilde and R.A. Schoonheydt, *J.Phys. Chem.*, **81** (1977) 1179.

122. R.A. Schoonheydt, P. Peigneur and J.B. Uytterhoeven, *J. Chem. Soc. Faraday Trans. I*, **74** (1978) 2550.

123. R.J. Taylor, R.S. Drago and J.E. George, *J. Am. Chem. Soc.*, **111** (1989) 6610.

124. N. Herron, *J. Coord. Chem.*, **19** (1988) 25.

125. C.A. Tolman and N. Herron, *Catal. Today.*, **3** (1988) 235.

126. R.F. Parton, D.R.C. Huybrechts and P.A. Jacobs, *Stud. Surf. Sci. Catal.*, **65** (1991).

127. D.R.C. Huybrechts, R.F. Parton P.A. Jacobs, *Stud. Surf. Sci. Catal.*, **60** (1991) 225.

128. Y.W. Chan and R.B. Wilson, *Preprint papers - ACS, Div. Fuel. Chem.*, **3** (1988) 271.

129. B.R. Cook, T.J. Reinert and K.S. Suslick, J. Am. Chem. Soc., **108** (1986) 7281.

130. R.F. Parton, L. Uytterhoeven and P.A. Jacobs, *Stud. Surf. Sci. Catal.*, **59** (1991) 395.

131. P.P. K. Gerrits, M.L. L'abbe, W.H. Leung, A.M. Van Bavel, G. Langouche, I. Bruynseraede and P.A. Jacobs, *Stud. Surf. Sci. Catal.*, **101** (1996) 811.

132. R.F. Parton, C.P. Bezouhanova, J. Grobet, P.J. Grobet and P.A. Jacobs, *Stud. Surf. Sci. Catal.*, **83** (1994) 371.

133. Z.L. Liu, J.W. Huang and L.N. Ji, *J. Mol. Catal. A : Chemical*, **104** (1996) L193.

134. K.J. Balkus, Jr., M. Eissa and R. Lavado, *Stud. Surf. Sci. Catal.*, **94** (1995) 713.

135. K.J. Balkus, Jr., M. Eissa and R. Lavado, *J. Am. Chem. Soc.*, **117** (1995) 10753.

136. P.P. K. Gerrits, F.T. Starzyk and P.A. Jacobs, *Stud. Surf. Sci. Catal.*, **84** (1994) 1411.

137. R.F. Parton, C.P. Bezouhanova, F.T. Starzyk, R.A. Reynders, P.J. Grobet and P.A. Jacobs, *Stud. Surf. Sci. Catal.*, **84** (1994) 813.

138. E. Paez-Mozo, N. Gabriunas, R. Maggi, D. Acosta, P. Ruiz and B. Delmon, *J. Mol. Catal.*, **91** (1994) 251.

139. A. Zsigmond, F. Notheisz, Z.S. Szegletes and J.E. Backval, *Stud. Surf. Sci. Catal.*, **94** (1995) 728.

140. Z. Jiang and Z. Xi, *J. Mol. Catal. (China)*, **6** (1992) 467.

141. B.B. De, B.B. Lohray, S. Sivaram and P.K. Dhal, *Tetrahedron Asymmetry*, **6 (9)** (1995) 2105.

142. D. E. De Vos, J. Meinershagen and T. Bein, *Stud. Surf. Sci. Catal.*, **101** (1996) 1303.

143. B.P. Murphy, *Coord. Chem Rev.*, **124** (1993) 63.

144. H. Beinert, *Coord. Chem. Rev.*, **23** (1977) 119.

145. H. Sigel and D.B. McCormick, *J. Am. Chem. Soc.*, **93** (1971) 2041.

146. B.M. Weckhuysen, A.A. Verberckmoes, L. Fu and R.A. Schoonheydt, *J. Phys. Chem., Preprint* (1996).

147. T. Kimura, A. Fukuoka and M. Ichikawa, *Catal. Lett.*, **4** (1990) 279.

148. A.N. Zakharov, *Mendeleev Commun.*, (1991) 80.

149. C.U. Dinesh, R. Kumar, B. Pandey, and P. Kumar, *J. Chem. Soc. Chem. Commun.*, (1995) 611.

150. V. Conte, F.D. Furia, and S. Moro, *Tetr. Lett.*, **35 (40),** 7429 (1994).

151. R.I. de la Rosa, M.J. Clague, and A. Butler, *J. Am. Chem. Soc.*, **114,** 760 (1992).

152. R. Westervelt, in *Chemical Week*, p. 26, Aug. 14 (1996).

CHAPTER-2

EXPERIMENTAL

2. EXPERIMENTAL

2.1. Copper-Acetate System

2.1.1 Zeolite-encapsulated copper acetate catalysts

In addition to neat copper acetate monohydrate (CuAc), four more solid catalysts containing encapsulated copper acetate were prepared. The solid matrices were (1).

zeolite Na-Y (Si/Al = 2.5; 0.08% wt. Cu; designated as Cu-Na-Y) (2) zeolite H-Y (Si/Al = 2.5; 0.12 % wt. Cu; designated as Cu-H-Y) (3) zeolite H-MCM-22 (SiO_2/Al_2O_3 = 30; 0.05% wt. Cu; designated as Cu-MCM-22) and (4) the aluminophosphate molecular sieve VPI-5 (0.06% wt. Cu; designated as Cu-VPI-5). Cu-Na-Y was prepared by stirring 3.5 g of copper acetate and 7 g of Na-Y (PQ Corporation, USA) in 17 ml of glacial acetic acid for 8 hrs., filtering and washing with distilled water till the washings are free of copper. The above procedure was again repeated with 3.5 g of copper acetate monohydrate. The catalyst was later evacuated (10^{-3} Torr.) and dried at 383 K for 24 hrs. Cu-H-Y was prepared by first exchanging the Na-Y (twice) with 1 M. ammonium acetate for 8 hours. The ammonium form was calcined at 753 K for 24 hrs. to obtain H-Y. Cu-H-Y was prepared by the same procedure described earlier for Cu-Na-Y. Cu-MCM-22 was prepared by stirring 5.0 g of copper acetate and 9.0 g of H-MCM-22 in 25 ml of glacial acetic acid, for 8 hrs., filtering, washing with distilled water till the filtrate is free from copper, evacuation (10^{-3} Torr.) and drying at 383 K for 24 hrs. MCM-22[1-3] with SiO_2/Al_2O_3 = 30 was synthesized as described in reference 3. 43.58 g of sodium silicate (Lona Industries, Bombay) was mixed with 20 g of distilled water and stirred for 5 mins in a polypropylene bottle. 8.81 g of hexamethyleneimine (Aldrich) was added over a period of 30 mins and the pale yellow mixture was aged for about 30 mins. A solution of aluminium sulfate (4.33 g in 100 g of distilled water) and concentrated sulfuric acid (3.52 g) was added dropwise with continuous stirring to the silicate solution and the mixture was aged for 24 h. The final pale yellow mixture had a pH of 11.4 and its composition in terms of oxide mole ratio was 9.83 Na_2O : 29.78 SiO_2 : Al_2O_3 : 1367.9 H_2O. The mixture was autoclaved and crystallized at 423 K for 80 h. The crystalline white powder was filtered and the mother liquor was found to have a pH of 12.4. The as-synthesized samples were

thoroughly washed with distilled water and dried at 393 K for 6 h. The as-synthesized materials were calcined at 823 K for 24 h to remove the template. Cu-VPI-5 was prepared by stirring 4 g of copper acetate and 6.5 g VPI-5 molecular sieve in 15 ml of glacial acetic acid for 8 hrs; filtering and washing with distilled water to remove excess copper acetate. The above procedure was repeated with 4 g of copper acetate. The material was then evacuated and dried at 373 K for 36 hrs. The aluminophosphate molecular sieve, VPI-5, was synthesized by the procedure described by Mark Davis et al.[4-6] Pseudoboehmite alumina (Catapal B, Sigma) and 85 % wt H_3PO_4 were used as the aluminium and phosphorous sources. n-dipropylamine (DPA, Aldrich) was used as the organic additive. 6.9 g of pseudoboehmite was slurried in 20 g of water. The phosphoric acid solution (10 g of water in 11.5 g phosphoric acid) was added to the alumina slurry to form a precursor mixture. The precursor mixture is aged for 2 hrs at ambient conditions with stirring. 5.1 g of dipropylamine (DPA) was added to the precursor mixture and the resulting gel was aged with constant stirring for 2 hrs at ambient conditions. The reaction mixture was heated at 142 °C for 24 hrs. The gel composition of the final mixture was DPA : Al_2O_3 : P_2O_5 : 40 H_2O. The synthesis was carried out in 100 ml Teflon-lined autoclaves. At the end of the specified time, the autoclaves were quenched in cold water and the product was recovered by slurrying the autoclave contents in water, decanting the supernatent liquid, filtering the white solid and drying the crystals in ambient air. After incorporation of the copper acetate, the solids were first dried in vacuum, then in nitrogen at 298 K and stored in a desiccator. The enzyme tyrosinase (from Mushrooms, salt-free, lyophilized) was obtained from Koch Light Labs., England (Lot. No. 5568t).

2.1.2 Procedures

Catalytic Reaction - Oxidation of phenols

In a typical oxidation reaction, the solid copper acetate-containing catalyst (20 to 40 mg.) was added to the substrate in a phosphate buffer (0.05 M, pH = 6.5). {The stock solution of phosphate buffer was prepared as described below : (A). 0.2 M solution of monobasic sodium phosphate (27.8 g in 1000 ml of water). (B). 0.2 M solution of dibasic sodium phosphate (53.65 g of $NaH_2PO_4.7H_2O$ in 1000 ml of water). 68.5 g of A was mixed with 31.5 g of B and this resulting solution was diluted to a total of 200 ml to give phosphate buffer of pH 6.5}. The contents were stirred at 298 K in the presence of molecular oxygen (from air). Periodically, samples were removed and centrifuged to remove the solid catalyst. Copper was not detected (by atomic absorption spectroscopy, Hitachi Model Z-8000) in the colourless filtrate when using copper acetate, Cu-Na-Y, Cu-H-Y, Cu-MCM-22 or Cu-VPI-5. The substrates chosen were monohydroxy aromatic compounds like L-tyrosine (Aldrich, USA, 2 dM), phenol (S.D. Fine Chemicals, 8 % wt), meta and ortho cresols (B.D.H., 15 % wt) in phosphate buffer. In experiments involving the enzyme, 30 μg of tyrosinase (Koch Light Labs, England) in 30 μl of 0.05 M phosphate buffer was added to a 1 ml solution of 2 mM tyrosine in 0.05 M phosphate buffer.

Product Analysis

The progress of the oxidation was monitored by HPLC (for reactions of tyrosine), gas chromatography (for phenol and cresols) and UV spectroscopic techniques for all the substrates. In the oxidation of L-tyrosine, after removal of the solid catalyst, by centrifugation, the filtrate containing the reactants and products was analyzed by HPLC (Shimadzu Model LC-9A), G.C. (Hewlett Packard, Model 5880) and UV spectroscopy

(Shimadzu Model UV-2101PC). The range 190 - 350 nm was scanned by UV spectrophotometry. For the quantitative assay of L-tyrosine and L-DOPA, absorption at 280 nm by the UV detector (Shimadzu Model SPD-6AV) in the HPLC was utilized. The HPLC chromatograms were calibrated using known quantities of L-tyrosine and L-DOPA (Aldrich). The HPLC column was an ODS-C_{18} column. The carrier was a 20:80 (v/v) mixture of methanol and 1% phosphate buffer solutions. The flow rate was 1 ml/min. The L-tyrosine and L-DOPA standards were prepared as 2 mM solutions in 30 ml of phosphate buffer of pH = 6.5 (prepared from 0.05 M solution of Na_2HPO_4 and NaH_2PO_4). 15 µl of sample was injected in all cases. The retention time of L-tyrosine and L-DOPA under these conditions were 3.4 and 2.6 min, respectively. The reactants and products of the phenol, o-cresol and m-cresol reactions were analyzed by gas chromatography employing a FID detector and HP1 capillary column crosslinked with methyl silicone gum (50 m x .25 mm). The identity of L- and D-DOPA in the products was also confirmed by ^1H NMR spectroscopy (Bruker MSL-300) of the products. The samples were lyophilized twice in D_2O medium to exchange the protons for deuterium.

2.2 The Phthalocyanine system

2.2.1 Materials

Synthesis of copper (II) perchlorophthalocyanines ($CuCl_{16}Pc$)

The *neat* $CuCl_{16}$ Pc (where Pc stands for phthalocyanine) complexes were synthesized according to the procedure reported by Birchall et al[7]. 2.8 mmol of $Cu(CH_3CO_2)_2$ (0.56 g, BDH) was mixed with 14.0 mmol (2.8 g, Aldrich) of tetrachlorophthalonitrile in 40 ml of 1-chloronaphthalene (Aldrich) in a Parr reactor under nitrogen (500 psi.) The mixture was heated for 24 h, cooled to room temperature and centrifuged. Then 200 ml of petroleum ether was added to the greenish blue filtrate that

was then submerged in an ice bath. The dark green precipitate was recovered by centrifugation. The $CuCl_{16}Pc$ complex was recrystallized from sulfuric acid and isolated in 50.2 % yield.

Synthesis of iron (II) perchlorophthalocyanines ($FeCl_{16}Pc$)

Iron (II) acetate (Aldrich, 0.15 g) was mixed with 0.60 g of tetrachlorophthalonitrile (Aldrich) in 55 ml of 1-chloronaphthalene (Aldrich) in a Parr reactor under nitrogen (500 psi.) The mixture was heated for 24 h, cooled to room temperature and centrifuged. Then 200 ml of petroleum ether was added to the brownish blue filtrate that was then submerged in an ice bath. The dark brown precipitate was recovered by centrifugation. The $FeCl_{16}Pc$ complex was recrystallized from sulfuric acid and isolated in 38.5 % yield.

Synthesis of copper (II) tetra nitro phthalocyanines ($Cu(NO_2)_4Pc$)

0.63 g copper (II) acetate (BDH) was mixed with 3.75 g of 4-nitro phthalonitrile (Aldrich) and 14.2 g of 1-nitronaphthalene (Aldrich) in 40 ml of 1-chloronaphthalene (Aldrich) in a Parr reactor under nitrogen (500 psi.) with constant stirring (300 rpm). The mixture was heated for 24 h, cooled to room temperature and centrifuged. Then 200 ml of petroleum ether was added to the bluish grey filtrate that was then submerged in an ice bath. The dark blue precipitate was recovered by centrifugation. The $Cu(NO_2)_4Pc$ complex was recrystallized from sulfuric acid and isolated in 45 % yield.

Synthesis of Na-X zeolite around the metal complexes

The synthesis of $CuCl_{14}Pc$, $CuCl_{16}Pc$ $Cu(NO_2)_4Pc$, $FeCl_{16}Pc$ or $CoCl_{14}Pc$ complexes encapsulated in zeolite NaX is described below : Aluminium isopropoxide and NaOH (Aldrich) were used without further purification. The silicate gel was prepared from 4.0g of fumed silica (Sigma), 3.2 g NaOH, 0.30 g of $CuCl_{16}Pc$, $CuCl_{14}$ Pc, $Cu(NO_2)_4$ Pc,

$FeCl_{16}Pc$ or $CoCl_{14}Pc$ and 8.0 ml of H_2O. Addition of the aluminate solution (9.0 g of Al $(iOPr)_3$, 3.2 g NaOH, 6.0 ml H_2O) resulted in a slurry with an intense greenish/blue colour. An additional 36 ml of deionized water was added. The gel was then transferred to a polypropylene bottle. The mixture with a molar composition of SiO_2 : Al_2O_3 : Na_2O : H_2O : $CuCl_{14}Pc$ = 3 : 1 : 3.6 : 141 : 0.015 was aged at room temperature with stirring for 24 hrs and then heated at 363K for 15 hrs. It was then allowed to cool to room temperature and was diluted with copious amounts of deionized water. The solid crystals were isolated by centrifugation at 8000 rpm for 2 hrs. The light, greenish/blue solid was dried at 363K for 24 hrs in air and extracted (soxhlet) first with acetone, then with pyridine, acetonitrile and finally again with acetone for 72 hrs. It was finally dried at 363 K under vacuum (10^{-3} Torr) for 15 h. The X-ray diffraction pattern of the material confirmed it to be the zeolite, Na-X. NaX with varying loadings of $CuCl_{14}Pc$, $CuCl_{16}Pc$ $Cu(NO_2)_4Pc$, $FeCl_{16}Pc$ or $CoCl_{14}Pc$ were prepared similarly.

Synthesis of Na-Y zeolite around the metal complexes

The synthesis of $CuCl_{16}Pc$, $CuCl_{14}$ Pc, $FeCl_{16}Pc$, $CoCl_{14}Pc$ or $Cu(NO_2)_4Pc$ encapsulated in Na-Y was also similar to the synthesis procedure described above for Na-X. The silica source was sodium silicate (Lona). A mixture of sodium aluminate and aluminium sulfate (Aldrich) was used as the alumina source. The hydrothermal synthesis of the faujasites was carried out at 373 K in polypropylene bottles under non stirring static conditions. The faujasites were synthesized using seeds of an alumino-silicate gel. 12 g of homogeneous seed slurry (aged for 24 h at room temperature) was added to a mixture containing 21.7 g of sodium silicate. 0.30 g of the metal complex ($CuCl_{16}Pc$, $CuCl_{14}Pc$, $FeCl_{16}Pc$, $CoCl_{14}Pc$ or $Cu(NO_2)_4Pc$) was homogeneously blended with the silicate solution. The aluminate solution (1.4 g of sodium aluminate and 2.1 g of aluminium

sulphate) was added dropwise to the silicate solution and this resulted in a slurry with an intense green colour. The gel was aged at room temperature with stirring for 24 hrs and then heated at 373K for 12 hrs. It was then allowed to cool to room temperature and was diluted with copious amounts of deionized water. The solid crystals were isolated by centrifugation at 8000 rpm for 2 hrs. The light, green/brown solid was dried at 373K for 24 hrs in air and extracted (soxhlet) first with acetone, then with pyridine, acetonitrile and finally again with acetone for 72 hrs. It was finally dried at 373 K under vacuum (10^{-3} Torr) for 15 h. The X-ray diffraction pattern of the material confirmed it to be the zeolite, Na-Y. NaY with varying loadings of $CuCl_{14}Pc$, $CuCl_{16}Pc$ $Cu(NO_2)_4Pc$, $FeCl_{16}Pc$ or $CoCl_{14}Pc$ were prepared similarly.

Synthesis of K-L zeolite around the metal complexes

$CuCl_{16}Pc$, $CuCl_{14}Pc$, $FeCl_{16}Pc$, $CoCl_{14}Pc$ or $Cu(NO_2)_4Pc$ were encapsulated in K-L by the following procedure : 12.44 g of fumed silica (Aldrich) was stirred in 17 ml of distilled, deionised water for 30 mins. 0.15 g of $CuCl_{16}Pc$, $CuCl_{14}Pc$, $FeCl_{16}Pc$, $CoCl_{14}Pc$ or $Cu(NO_2)_4Pc$ were added to the silica-sol and the mixture was stirred for another 30 min at 333 K. In a separate polypropylene beaker 8.96 g of KOH (A.R. Grade, S.D. Fine Chemicals), 1.55 g of hydrated alumina (Catapal B, Sigma) and 17 ml of distilled, deionised water were stirred for 60 min. at 333 K. The silica solution containing the metal complex was gradually added to the alumina solution over a period of 45 min. An additional 10 ml of distilled deionised water was added to get an uniform gel. The contents were stirred for a further 60 min. and then transferred to an autoclave reactor (Parr). The autoclave was maintained at 414 K, for 4.5 days under stirring (rpm = 300). The SiO_2/Al_2O_3 ratio of the final zeolite L was 6.8. The dark/greenish brown solid was dried at 383K for 24 hrs in air and extracted (soxhlet) first with acetone, then with

pyridine, acetonitrile and finally again with acetone for 72 hrs. It was finally dried at 383 K under vacuum (10^{-3} Torr) for 15 h. The X-ray diffraction pattern of the material confirmed it to be the zeolite, K-L. The catalysts are designated by the following notation [(Complex) - (Zeolite) (metal content in the zeolite, % wt)]. Thus $CuCl_{14}Pc$-Na-X (0.27) designates a Na-X zeolite containing 0.27% wt copper in the form of a tetradeca chloro copper phthalocyanine complex encapsulated, most probably, in the supercages of the faujasite structure, X.

Synthesis of ZSM-5 around the metal complexes

$CuCl_{16}Pc$, $CuCl_{14}Pc$, $FeCl_{16}Pc$, $CoCl_{14}Pc$ or $Cu(NO_2)_4Pc$ were encapsulated in ZSM-5 by the following procedure: A seeded synthesis involved the use of Na-rich ZSM-5 seed crystals as promoters. In a typical seeded synthesis 100 g of demineralised water was mixed under stirring to 143.8 g sodium silicate (28.1 % SiO_2, 8.8 % Na_2O and 63.1 % H_2O, Allied Ind. India). 0.22 g of the metal complex was dissolved in 7.2 g of H_2SO_4 (98 % B.D.H.) at ambient temperature giving a dark green/brown clear solution and then added very slowly to the previously made sodium silicate solution resulting in a green/brown colour gel which was stirred for about an hour till a fairly homogeneous dispersion results. The aluminum sulphate solution was obtained by dissolving 8.98 g of $Al_2(SO_4)_3.18H_2O$ in 100 g of demineralised water and was added to the above homogenized slurry under stirring resulting in a viscous greenish/brown gel. 1.3 g of crystalline Na-ZSM-5 (Si/Al = 20) seed precursors were dispersed in 60 g of demineralised water and were blended with the above hydrogel where the seed amounts corresponds to 0.3-0.4 % wt. of the total gel. The final pH of the gel ranged between 8.0-9.0, depending on the quantity of the H_2SO_4 used. The gel was homogenized and then aged at room temperature for 24 h in a Parr

reactor (Parr 4561) before crystallization. The gel composition in terms of oxide moles is given below :

15 Na_2O : 0.14 $CuCl_{16}Pc$ or $CuCl_{14}Pc$ or $FeCl_{16}Pc$ or $CoCl_{14}Pc$ or $Cu(NO_2)_4Pc$: 1.0 Al_2O_3 : 50 SiO_2 : 1460 H_2O : 5.75 H_2SO_4

After 24 h, the Parr reactor was heated to 453 K and kept at this temperature for 48 hrs with a constant stirring of 400 rpm. After 48 hrs the Parr reactor was quenched and the product was recovered by centrifugation at 5000 rpm for 2 hrs. The light green/brown solid was dried at 373K for 24 hrs in air and extracted (soxhlet) first with acetone, then with pyridine, n-hexane, acetonitrile and finally again with acetone for 72 hrs. It was finally dried at 373 K under vacuum (10^{-3} Torr) for 15 h. The product yield was 82 % on the basis of SiO_2 input. The Si/Al ratio did not exceed a value of 15 while using the non-seeded system and were often contaminated with dense phase formation. On the other hand, hydrogels of metal phthalocyanines supplemented with seed precursors crystallized over a wider Si/Al ratio (Si/Al = 15-40) and higher incorporations could be obtained. The X-ray diffraction pattern of the material confirmed it to be the zeolite, ZSM-5.

The catalysts used in the oxidation and oxyhalogenation reactions were $CuCl_{14}Pc$-Na-Y(0.11), $CuCl_{16}Pc$-Na-Y(0.17), $CuCl_{14}Pc$-Na-Y(0.26), $CuCl_{16}Pc$-Na-Y(0.27), $CuCl_{14}Pc$-Na-X(0.14), $CuCl_{16}Pc$-Na-X(0.28), $CuCl_{14}Pc$-K-L(0.11), $CuCl_{16}Pc$-ZSM-5(0.10), $CuCl_{16}Pc$-ZSM-5(0.17), $Cu(NO_2)_4Pc$-Na-Y(0.09), $Cu(NO_2)_4Pc$-Na-Y(0.16), $Cu(NO_2)_4Pc$-Na-X(0.11) and $Cu(NO_2)_4Pc$-Na-X(0.14) where the numbers in the parentheses refer to the wt % of copper in the zeolite catalyst.

2.2.2 Procedures

2.2.2.1 Oxidation Reactions

The catalytic runs were carried out in a three necked flask (100 ml capacity) fitted with a condenser (circulating chilled water) and magnetic stirring. The temperature of the reaction vessel was maintained using an oil bath. In a typical oxidation reaction, the solid catalyst (0.2 to 0.75g) was added to the substrate in the specified solvent (acetonitrile, acetone, etc). Aqueous H_2O_2 (25% wt) was added after the desired temperature was attained. In the case of oxidations using O_2 as the oxidant, tertiary butyl hydroperoxide (70% aqueous solution, {Aldrich}) equivalent to 1-3 % by weight of the substrate) was added to the reaction mixture before air was admitted into the Parr autoclave (300 ml capacity). In the case of methane oxidation reactions, the temperature of the reaction vessel was maintained using a Cryostat (Julabo, FT 901). The Parr reactor was cooled to 273 K before admitting methane from a cylinder (Alphagaz). Periodically, samples were removed and centrifuged to remove the solid catalyst. The gas from the Parr reactor was collected in a gas bulb fitted with a three-way valve. Copper, iron or cobalt were not detected (by atomic absorption spectroscopy, Hitachi Model Z-8000) in the colourless reaction product when using any of the solid catalysts used in the present study. The substrates chosen were monohydroxy aromatic compounds like phenol (AR grade, S.D. Fine Chemicals, India), meta and ortho cresols (B.D.H., 15 % wt), n-hexane (AR grade, S.D. Fine Chemicals, India), cyclohexane (Aldrich) benzene (Aldrich), toluene (AR grade, S.D. Fine Chemicals, India), ethyl benzene (B.D.H.) and naphthalene (AR grade, S.D. Fine Chemicals, India).

The products of the oxidation reactions were analyzed by gas chromatography (Hewlett Packard, 5880 A), employing a FID detector and equipped with a capillary

column (50 m x 0.25 mm crosslinked methyl silicone gum). The reactants and products of ethyl benzene, n-hexane and cyclohexane oxidation were analyzed by gas chromatography (Hewlett Packard, 5890) equipped with a FFAP column (30 m x 0.25 mm). The analysis for CO_2 and water were carried out using a Shimadzu GC-15-A equipped with a TCD detector and a porapak N column. The liquid products were extracted with diethyl ether. The acids formed (formic, adipic, succinic, valeric and glutaric acids) were esterified and analyzed as methyl esters by the procedure given below : 300 microliter of the sample was taken in a glass vial. 2 ml of 14 % boron trifluoride (BF_3) in methanol was added to the glass vial which was stoppered with a teflon lined stopper and heated for 1 hr at 353 K. The sample was cooled to room temperature and 2 ml of Milli-Q reagent water was added with mild shaking. 2 ml of HPLC grade dichloromethane (S.D. Fine Chemicals) was added before the GC analysis. The identity of the products was further confirmed by GC-MS (Shimadzu QCMC-QP 2000A).

2.2.2.2 Oxyhalogenation Reactions

In a typical oxyhalogenation reaction, the solid catalyst (0.2 to 0.75g) was added to the substrate in a suitable solvent [for example, a 1:2 volume mixture of water : acetonitrile] where the halide source KX or HX (X = Cl, Br, I) was previously dissolved. In reactions involving molecular Cl_2, as the halogenating agent chlorine gas was admitted at a flow rate of 0.09 mol/h. When HCl was used as the halide source the pH of the mixture was adjusted to 5.0 using phosphate buffer. Aqueous H_2O_2 (25% wt) was added after the desired temperature was attained. The catalytic runs were carried out in a three necked flask (100 ml capacity) fitted with a condenser (circulating chilled water) and magnetic stirring. The temperature of the reaction vessel was maintained using an oil bath. Periodically, samples were removed and centrifuged to remove the solid catalyst. Copper

was not detected (by atomic absorption spectroscopy, Hitachi Model Z-8000) in the colourless reaction product when using any of the solid catalysts for oxyhalogenation. In the case of oxyhalogenation reactions using molecular O_2 as the oxidant, tertiary butyl hydroperoxide (TBHP, 70 % aqueous solution, {Aldrich} equivalent to 1 % by weight of the substrate) was added to the reaction mixture before air was admitted to the Parr autoclave (300 ml). The substrates chosen were toluene, phenol (AR grade, S.D. Fine Chemicals, India), aniline, resorcinol (B.D.H.), anisole and benzene (Aldrich, USA)

The products of the oxyhalogenation reaction were analyzed by gas chromatography (Hewlett Packard, 5880 A), employing a FID detector and equipped with a capillary column (50 m x 0.25 mm crosslinked methyl silicone gum). At the end of the reaction, the halogenated aromatics were extracted with diethyl ether and saturated with sodium hydrogen carbonate prior to analysis. In some cases, the products were isolated by column chromatography, after appropriate work-up to establish yields. The identity of the products was further confirmed by GC-MS (Shimadzu QCMC-QP2000A).

2.3 Catalyst Characterization

2.3.1 Chemical analysis

A known weight of sample was taken in a platinum crucible with lid and ignited at 393 K to get the dry weight of the sample. The sample was weighed after equilibration. The difference in weights gives the loss on ignition. The anhydrous sample was treated with sulphuric acid (75%) and hydrofluoric acid (40%) and was evaporated on a hot plate to remove the silicon in the form of SiF_6. This procedure was repeated three times and the sample was ignited, cooled and weighed. The loss in weight gives the amount of silica present in the sample. The residue was fused with potassium pyrosulphate and dissolved in a known volume of water in a standard flask. It was then analyzed for

copper, iron, cobalt, silicon, sodium, potassium and aluminium by atomic absorption spectroscopy (Hitachi Model Z-8000).

2.3.2 X-ray fluorescence spectroscopy (XRF)

The XRF analyses were done using a Rigaku-3070, X-ray fluorescence spectrometer with a rhodium target energized at 50μv and 40 mA. The catalysts were ground to a fine powder and sieved through 160 mesh. They were then palletized by the borate fusion technique[8] using a hydraulic press and applying a pressure of 15 Kg/m^2. Si and Al were analyzed using a PET (pentaerythrital) crystal, while the lighter elements were analyzed using a TAP (thallium acethalate) crystal. Standard calibration curves were made and matrix correction was applied to increase the accuracy.

2.3.3 Adsorption and surface area measurements

Omnisorb 100 CX (COULTER Corporation, USA) was used for the measurements of nitrogen sorption and surface area of the samples. Prior to the adsorption measurements, the samples were activated at 373 K for 4 h, in high vacuum (1.33×10^{-6} Pa). After the evacuation, the samples were cooled to room temperature and the weight was taken. The samples were cooled to 78 K using liquid nitrogen and nitrogen gas was allowed to adsorb on them. The volume of N_2 adsorbed (cc/g at STP) and the BET surface areas were then measured. The sorption measurements for water, cyclohexane and n-hexane were carried out gravimetrically in a recording electromicrobalance (Model : Cahn-2000 G). The free metal complexes and the zeolite encapsulated metal complexes (about 60 mg) were pressed into a pellet and weighed into an aluminium bucket which was attached to the balance. The system was evacuated to a pressure of 10^{-6} Torr at 383 K using a two stage rotary and mercury diffusion pump. After 2 hrs, the temperature was lowered to the required value. The sorbate was admitted into the sample at a constant

temperature and pressure, and the weight gain was recorded as a function of time using a cathetometer (accuracy ± 0.01 mm). After the experiment was over, the catalyst was evacuated and heated to 383 K at 10^{-6} Torr for several hours. X-ray diffractograms were recorded for each sample before and after the sorption measurements to check the structure stability.

2.3.4 ESR spectroscopy

The ESR spectra of the solid catalysts were measured at room (300 K) and liquid N_2 (77 K) temperatures using a Bruker (E-2000) ESR spectrometer (200 D) at 9.7 MHz with a rectangular cavity ST_{9424}. The cavity input power was 20 Mw and the field modulation intensity was 1.25 Gpp. The instrument was calibrated with a standard sample of weak pitch (g = 2.0029). The frequency modulation was carried out at 100 kHz and a time constant of 10^3 msec was used. A standard calibration curve using different molar concentration of $CuSO_4.5H_2O$ (Aldrich) was drawn and the total number of spins of Cu^{2+} in the catalyst samples was estimated from the calibration curve. The second derivative spectra were calculated from the digitized absorption spectra.

2.3.5 X-ray diffraction

The solid catalyst samples were analyzed for qualitative and quantitative phase identification on a computer controlled automatic X-ray powder diffractometer (Rigaku Model D/MAX III VC, Japan). Ni filtered Cu-Kα radiation (λ = 1.5404 Å) was used with a curved graphite crystal monochromator and a NaI scintillator. All measurements were made at room temperature. Data were collected in the 2θ range 4-50 degrees at a scan rate of 4°/min. Silicon was used as the internal standard for calibrating the instrument. After background correction and Kα2 stripping were done, the peak positions were marked. The 'd' values and the relative intensities I/I_0 of the peaks were calculated. The interplanar

spacings 'd', were calibrated using silicon metal as the reference material and then used for the determination of unit cell paramaters. The latter were further refined by least square fitting programs. The crystalline phases were identified using a search-match technique. The catalysts were finely powdered and sieved through a 170 mesh before they were loaded in the sample compartment.

2.3.6 Infrared spectroscopy

The infrared spectra were recorded using a Perkin Elmer 1600 FTIR in the frequency range 4000-200 cm^{-1}. Nujol and fluorolube were used as the mulling agents. In the copper-acetate system, as the nujol peaks interfered with the acetate bands, fluorolube was used as the mulling agent. KCN was used as the internal standard for calibrating the instrument. Band intensities were expressed either as transmittance (T) or as absorbance (A). The IR crystallinity of the faujasite samples was determined using the formula[9]:

$$\text{IR crystallinity} = \frac{\text{peak area of the band at 550 cm}^{-1}\text{ of the product}}{\text{peak area of band at 550 cm}^{-1}\text{ of reference sample}} \times 100$$

The IR spectra of some samples were also recorded by the KBr pellet method over the same frequency range. The samples were prepared by grinding a mixture of the catalyst and spec-pure KBr powder in an agate mortar and pressing them using a hydraulic press at a pressure of 15 Kg/m^2.

2.3.7 UV-Vis spectroscopy

The diffuse reflectance UV-Vis spectra of the solid catalysts were recorded using a Shimadzu UV-2101 PC UV-Vis spectrophotometer in the range 180-800 nm. Anhydrous $BaSO_4$ was used as the reference material. UV spectra of liquid samples were measured in the 200-400 nm region. The computer processing of the spectra consisted of (i). subtraction of baseline (ii). conversion to wavenumber (iii). calculation of the Kubelka-

Munk function (iv). subtraction of the spectrum of the zeolite from that of the free complex. The values of the Kubelka-Munk function at the band maxima are used for quantitative diffuse reflectance spectroscopy.

2.3.8 X-ray photoelectron spectroscopy

XPS of the solid catalysts were recorded with a VG Scientific ESCA III Mark (II) with MgKα (1253.6 Å) as the excitation source. AlKα (1486.6 Å) was used for excitation and photoelectron kinetic energy was measured with reference to the Fermi energy. Binding energies were corrected with respect to the peak at 285.0 eV for carbon C_{1s} and the surface composition was determined from the observed peak intensity using known values of Scofield total cross section photoionisation constants of the individual atoms. The spectrometer was calibrated with values of the binding energies of Au $4f_{7/2}$ (84.0 eV), Ag $3d_{5/2}$ (368.3 eV) and Cu $2p_{3/2}$ (932.4 eV) using spectroscopically pure metals (Johnson and Matthey, UK). The samples were ground to a fine powder and a homogeneous mixture was made with isopropanol. It was deposited on a nickel strip for analysis. All XPS spectra were recorded under similar conditions (50 eV pass energy, 4 mm slit entrance, pressure 10^{-9} Torr.). In all cases, the samples were measured before and after argon ion sputtering. The peaks were resolved after background subtraction and a gaussian equation was used to fit the curves. The binding energy values were measured to a precision of ± 0.2 eV.

2.3.9 Scanning electron microscopy

Scanning electron micrographs of the solid catalysts were recorded on a Leica, Stereoscan-440, Cambridge, instrument. The crystal morphology and the average particle size of the catalysts were estimated by this technique The samples were dusted on alumina and coated with a thin film of gold to prevent surface charging and to protect the surface

material from thermal damage by the electron beam. In all analyses an uniform film thickness of about 0.1 mm was maintained.

2.3.10 Thermal analysis

Simultaneous TG-DTA-DTG analyses of the free metal complexes as well as the zeolite encapsulated metal complexes were recorded on an automatic derivatograph (Setaram TG-DTA 92). The thermograms of the samples were recorded under the following conditions :

Weight of the sample	= 30 mg
Heating rate	= 10 K min^{-1}
Sensitivity	
TG	= 25 mg
DTG	= 0.2 mv
DTA	= 0.1 mv
Atmosphere	= Air

Preheated and finely powdered α alumina was used as the reference material.

2.3.11 Computer Modeling

Molecular modeling studies were carried out on a Silicon Graphics, Indigo-2 workstation, using the Insight II software supplied by Biosym Inc[10]. The computer models of Pc and $Cl_{14}Pc$ were generated and their geometries optimized with respect to their strain energy using molecular mechanics and energy minimization procedures[11]. As a first approximation, it was assumed that CuPc and $CuCl_{14}Pc$ will have geometric strains similar to Pc and $Cl_{14}Pc$, respectively. This assumption is justified in view of the small volume occupied by the Cu^{2+} ion in the phthalocyanine complex. The interaction potentials of Cu^{2+} and the other atoms of the complex have not, so far, been reported in literature. Hence, Cu^{2+} is approximated by a pseudoatom with a charge of +2.

2.4 References

1. M.K. Rubin and P.Chu, *U.S. Patent No. 4,954,325* (1990).

2. L. Puppe and J. Weisser, *U.S. Patent No. 4,439,409* (1984).

3. R. Ravishankar, T. Sen, V. Ramaswamy, H.S. Soni, S. Ganapathy and S. Sivasanker, *Stud. Surf. Sci. Catal.*, **84 (A)** (1994) 331.

4. M.E. Davis, C. Saldarriaga, C. Montes, J. Garces, C. Crowder, *Nature,* **331** (1988) 698.

5. M.E. Davis, C. Saldarriaga, C. Montes, J. Garces, C. Crowder, *Zeolites* **8** (1988) 362.

6. M.E. Davis, C. Montes, J.M. Garces, in *"Zeolite Synthesis"*, ACS Symposium Series Vol. 398, in M.L. Occelli and H.E. Robson (Eds.) pg. 291, (1989).

7. J.M. Birchall, R.N. Hazeldine and O.J. Morley, *J. Chem. Soc C.*, (1970) 2667.

8. P.A. Gokhale and M.R. Wuensche, *Adv. in X-ray analysis*, **33** (1990) 679.

9. P.A. Jacobs, E.G. Derouane and J. Weitkamp, *J.Chem Soc., Faraday Trans I*, **57** (1981) 547.

10. *Insight II User guide*, version 2.3.5, San Diego, Biosym. Technologies (1994).

11. O. Ermer, *Structure and Bonding*, **27** (1976) 161.

CHAPTER-3

CATALYST CHARACTERIZATION

CATALYST CHARACTERIZATION

INTRODUCTION

3.1 Characterization of zeolite-encapsulated metal complexes

- 3.1.1 Chemical analysis
- 3.1.2 X-ray techniques
  - (a) X-ray diffraction
  - (b) EXAFS and XANES
- 3.1.3 Electronic spectroscopy
- 3.1.4 Vibrational spectroscopy
- 3.1.5 Surface characterization
  - (i) X-ray photoelectron spectroscopy
  - (ii) Scanning and Transmission electron microscopy
- 3.1.6 Electrochemical methods
- 3.1.7 Electron spin resonance
- 3.1.8 Surface area and sorption techniques
- 3.1.9 Nuclear magnetic resonance
- 3.1.10 Thermal methods
- 3.1.11 Molecular modeling

RESULTS

3.2 Copper-acetate system

- 3.2.1 Chemical analysis
- 3.2.2 X-ray diffraction
- 3.2.3 Infra-red spectroscopy
- 3.2.4 UV-Vis spectroscopy
- 3.2.5 ESR spectroscopy

3.3 Copper phthalocyanine system

- 3.3.1 Chemical analysis
- 3.3.2 X-ray diffraction
- 3.3.3 X-ray photoelectron spectroscopy
- 3.3.4 Scanning electron microscopy
- 3.3.5 Adsorption and surface area measurements
- 3.3.6 Infrared spectroscopy
- 3.3.7 UV-Vis spectroscopy
- 3.3.8 ESR spectroscopy
- 3.3.9 Thermal analysis
- 3.3.10 Computer modeling

3.4 References

3.1 Characterization of zeolite-encapsulated metal complexes

Characterization of zeozymes is quite complex and various techniques have to be used in tandem to characterize encapsulated coordination compounds and the support used for their encapsulation. After the surface species have been sufficiently removed by Soxhlet extraction, using a variety of solvents, the samples are dried in vacuum. As metallophthalocyanines strongly adsorb on the surface of oxides, sublimation and electrochemical procedures could be used after extraction for further removal of adsorbed complexes. Uncomplexed metal-Schiff-base complexes, however, could be removed by Soxhlet extraction only. In the characterization of metal complexes encapsulated within the restricted space of the pores, channels or cavities of the zeolites the following questions need to be considered :

(i). Does the organic ligand introduced form the desired compound? Are there any unreacted or uncomplexed remnants?

(ii). What is the yield of the desired material?

(iii). Where are the intrazeolite complexes located? Is there complete encapsulation or do we have species adsorbed on the external surface?

(iv). When the zeolite is prepared around the metal complex (as in the zeolite synthesis method) do the synthesis methods employed preserve the pore structure, crystallinity and other features characteristic of the host? In order to give an unequivocal answer to the above questions, several techniques must be used in conjunction.

3.1.1 Chemical Analysis

The bulk chemical composition of the zeozyme catalyst (concentration of the transition metal, degree of exchange and Si/Al ratio of the zeolite, the carbon and

nitrogen stoichiometry of the ligand, etc.) is the primary information needed for the characterization of the catalyst.

3.1.2 X-ray techniques

(a). X-ray diffraction

X-ray diffraction (XRD) is mainly used for the identification of the phase and purity of the zeolite matrix. It also provides information on the crystallinity and change in unit cell parameters arising as a result of encapsulation methods. Encapsulated metallophthalocyanines and their perhalogenated or nitrated analogues do not lead to any change in unit cell parameters of the zeolite even though they have a tight fit inside the supercage of the latter.[1-6] Zeolite crystallinity is preserved after encapsulation of metal-Schiff-base complexes as well as metal phthalocyanine complexes prepared by the above described methods.[4-6] Due to the low loading of the metal complex, they can be detected by this technique only in the cases of insufficient or unsuccessful synthesis.

(b). EXAFS and XANES

X-ray absorption fine structures (EXAFS) provides valuable information on the number and type of atoms as well as the distances between them. Intrazeolite carbonyl clusters are usually characterized by this technique.[7-12] X-ray absorption near-edge spectra (XANES) give an idea of the oxidation states. The formation of FePc in Na-Y was confirmed using these techniques.[13] The metal-nitrogen distances could be evaluated and they confirm distortion of these complexes in the supercage. Though these techniques do not confirm encapsulation, they are well in agreement with other spectroscopic techniques in confirming the structural integrity of the encapsulated complexes and indicating distortions in the geometry of the encapsulated complexes.

3.1.3 Electronic spectroscopy

Zeolites modified with phthalocyanine complexes are deep blue, green or brown in colour, depending on the nature of the substituents on the phthalocyanine ring. This intense colour which arises from ligand $\pi \rightarrow \pi^*$ transitions (known as Q band) is characteristic of both free and encapsulated complexes. So, UV/Vis spectroscopy provides an unique spectroscopic handle to characterize these intrazeolite complexes. This intense band is in the range of 600-900 nm. Zeolite encapsulated transition metal phthalocyanine complexes exhibit a Q band which is red-shifted relative to the free or physisorbed complexes.[3] This shift arises due to the distortion of the planar phthalocyanine ligand as a result of steric interactions within the supercage.[1] Computer modeling and molecular strain energy minimization calculations indicate that the geometric environment around the metal complex is distorted. To avoid overlap between the complex and the zeolite structure, planarity of the complex has to be distorted, since the dimensions of the phthalocyanine ligand (~ 14 Å) exceeds the effective diameter of the supercage of the faujasite. In the case of FePc encapsulated in zeolite Y, the central metal atom was located in the centre of the supercage and the bridging N atoms were oriented to the four rings of the cubo-octahedra.[4] The shift to lower energy for these ligand-based electronic transitions inside the zeolite is consistent with the distortion of the macrocycle from planarity. The UV-Vis spectra of the intrazeolite SALEN complexes are not as sensitive to structural perturbations.[14-17]

3.1.4 Vibrational spectroscopy

Infra-red spectroscopy can provide information on changes in the structural integrity of the guest metal complex on encapsulation, as well as the crystallinity of the host zeolite. IR spectroscopic studies for intra-zeolite metal phthalocyanine (MPc), substituted MPc and MSALEN complexes have been reported.[2, 4-6, 13, 18-24] Though the

various T-O vibrational modes associated with the zeolite dominate the spectral region, bands associated with C=N and C=C stretching modes for the phthalocyanine ligand are also observed and sometimes may show a shift to lower wavenumbers on encapsulation. Kimura et al[13] have attributed this shift to ligand distortion inside the supercage. However, if the intrazeolite metal complexes have been prepared by the template synthesis method, these bands could also arise due to uncomplexed or free Pc ligand molecules adsorbed or occluded in the zeolite pores. The encapsulation of metal-salen complexes results in a blue shift of a strong C=C stretching.[22-24]

3.1.5 Surface characterization

(i). X-ray photoelectron spectroscopy (XPS)

XPS is used to determine the composition of encapsulated phthalocyanine and SALEN complexes in the first few surface layers of the catalyst. The relative elemental concentration at the surface and oxidation states of the central metal atom of the complex can be found out by this method. A shift in the binding energy of the central metal atom and the nitrogen indicate encapsulation.[18-19,25-26] The distortion of the ligand on encapsulation sometimes gives rise to two types of nitrogen with differing binding energies for encapsulated MPc and MSALEN complexes[27-28]. The homogeneous distribution of the metal complex inside the zeolite framework can be estimated from the surface metal/Si or metal/Al ratios and bulk elemental analyses. Metal complexes encapsulated in the first few surface layers of the zeolite play a disproportionately important role in catalytic reactions due to the dominant influence of diffusion effects in zeolite catalysis.

(ii). Scanning and Transmission electron microscopy (SEM and TEM)

SEM or TEM is used to provide information on the metal complex or metal oxide formation and deposition on the external surface of the zeolite crystal. Careful study of

the morphology of the intrazeolite complexes can reveal the presence of uncomplexed or physisorbed material. Usually, after solvent extraction the external surface of the zeolite is smooth and clean.[3,25] SEM also provides information on the particle size and particle size distribution of encapsulated metal complexes as well as the zeolite martix.

3.1.6 Electrochemical methods

Cyclic voltametry can provide information on the redox properties of the central transition metal ion. Electrochemical data for such encapsulated metal complexes were obtained from zeolite/graphite composite electrodes.[29-32]

3.1.7 Electron spin resonance :

ESR studies can give information on the nuclearity (monomeric or dimeric structure) of encapsulated complexes in addition to the states of the metal in the zeolite-ship-in-bottle complexes. The structural integrity of the complexes on encapsulation can also be ascertained. The nature of adduct formation of adsorbed gases with the central metal atom of the complex can be seen. A dioxygen adduct of Co-salen encapsulated in Na-Y has been studied by EPR[33]

3.1.8 Sorption techniques

Sorption experiments can provide direct evidence for the presence of the complex inside the zeolite cavities and not merely on the external surface of the crystals. The extent of pore blocking can be ascertained from the decrease in the pore volume on encapsulation of the metal complex. Sorption data can also indicate the volume of the space available for substrate molecules. The BET surface area of zeolites X and Y is drastically reduced when metal phthalocyanine and porphyrin complexes[3,34] are incorporated.

3.1.9 Nuclear Magnetic Resonance

NMR can provide information on the deformation of the complexes on encapsulation. Na-Y encapsulated Li_2Pc, FePc, $Fe(NO_2)_4Pc$ and TiPc have been studied[35] using cross-polarization magic angle spinning ^{13}C MAS NMR. The distortion of the phthalocyanine ligand from planarity inside the supercage alters the hybridization automatically causing a shift in the carbon resonance frequencies. ^{7}Li-NMR spectra of encapsulated Na-Y indicate a shift ~ 1.8 ppm upfield for the intrazeolite complex which is attributed to the effects of the electrostatic field inside the zeolite.[35]

3.1.10 Thermal methods

Differential thermal analysis (DTA) and Thermogravimetric analysis (TGA) have been used to characterize metal complexes encapsulated in zeolites.[2,36] The metal complex loading can be estimated from the weight loss and is more accurate than the spectrophotometric methods or the chemical analysis methods after HF / H_2SO_4 dissolution of the zeolite. The encapsulated complexes generally decompose at a higher temperature than the free complexes. Hence this technique can also be used to estimate the amount of uncomplexed metal or ligand in the final catalyst.

3.1.11 Molecular Modeling.

Recently, mathematical and computerized tools such as computer graphics have been used for modeling phthalocyanine[1,4-5,37] as well as SALENS[23-24,33] in the faujasite supercage. Norman Herron[1] first showed that, in the case of zeolite encapsulated FePc, the central metal atom is at the centre of the supercage, the bridging N atoms being oriented to the four rings of the cubo-octahedra. The complex undergoes a saddle-deformation (< 20°) from planarity. In the case of VPI-5, which has cylindrical channels of 12.1 Å, the complex is not distorted and positioned between two opposite 6-rings.[4] Since the dimensions of the

phthalocyanine ligand (~ 14 Å) exceeds the effective diameter of Na-X or Na-Y supercage (~ 12 Å), the encapsulated complex molecule would be under significant geometric constraints leading to its distortion from planarity. In the case of $FeCl_{16}Pc$ in Na-Y, the lowest energy configuration was distorted by 34.5° from planarity.[4,23]

RESULTS

3.2 Copper-Acetate System

3.2.1 Chemical analysis

Table-1 gives the copper content of the four copper acetate-based catalysts which have been used in the present study.

Table-1

Copper content of the catalysts

Catalyst	Copper Content (% wt)
Cu-Na-Y	0.08
Cu-H-Y	0.12
Cu-MCM-22	0.05
Cu-VPI-5	0.06

3.2.2 X-ray diffraction

The X-ray diffractograms of the catalysts containing the complexes did not reveal any difference from those of the pure zeolites indicating that the molecular sieves had not undergone any significant structural changes during the incorporation of the copper acetate. Fig. 1 shows the X-ray diffractograms of Cu-Na-Y (A), Cu-MCM-22 (B) and Cu-VPI-5 (C), respectively. There were no changes in the unit cell parameters of the above zeolites.

3.2.3 *Infra-red spectroscopy*

Fig. 2 shows the infra-red spectra of the copper acetate complex (A) as well as the complex located in the molecular sieves, Cu-H-Y (B), Cu-MCM-22 (C) Cu-VPI-5 (D) and fluorolube (E), respectively. It is seen that the structure of the copper acetate is intact even when it is encapsulated in the molecular sieves. The bands at 2960 and 2920 cm^{-1} (due to the asymmetric and symmetric C-H vibrations of the CH_3 group) as well as those at 1630 cm^{-1} (due to the carboxylate group) are clearly seen in the spectra of Cu-H-Y, Cu-MCM-22 and Cu-VPI-5 (curves B, C and D, respectively).

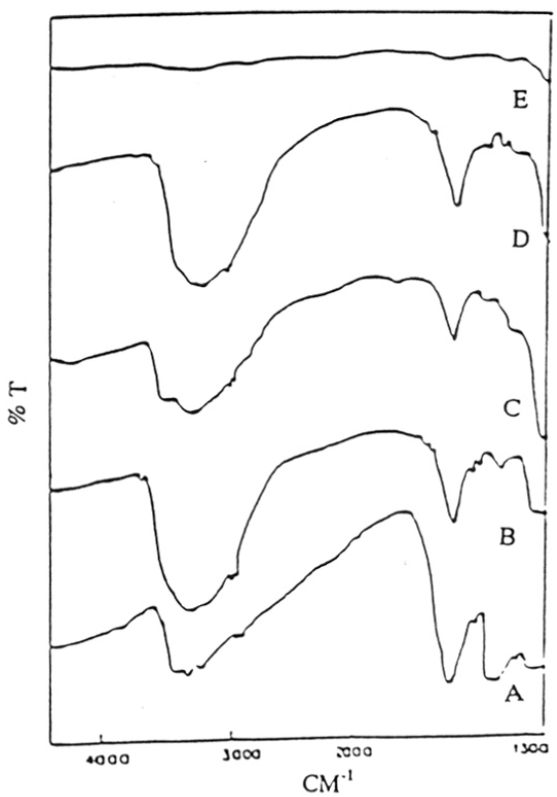

Fig. 2 IR spectra of catalysts : Curves A-E represent solid copper acetate monohydrate, Cu-H-Y, Cu-MCM-22, Cu-VPI-5 and fluorolube.

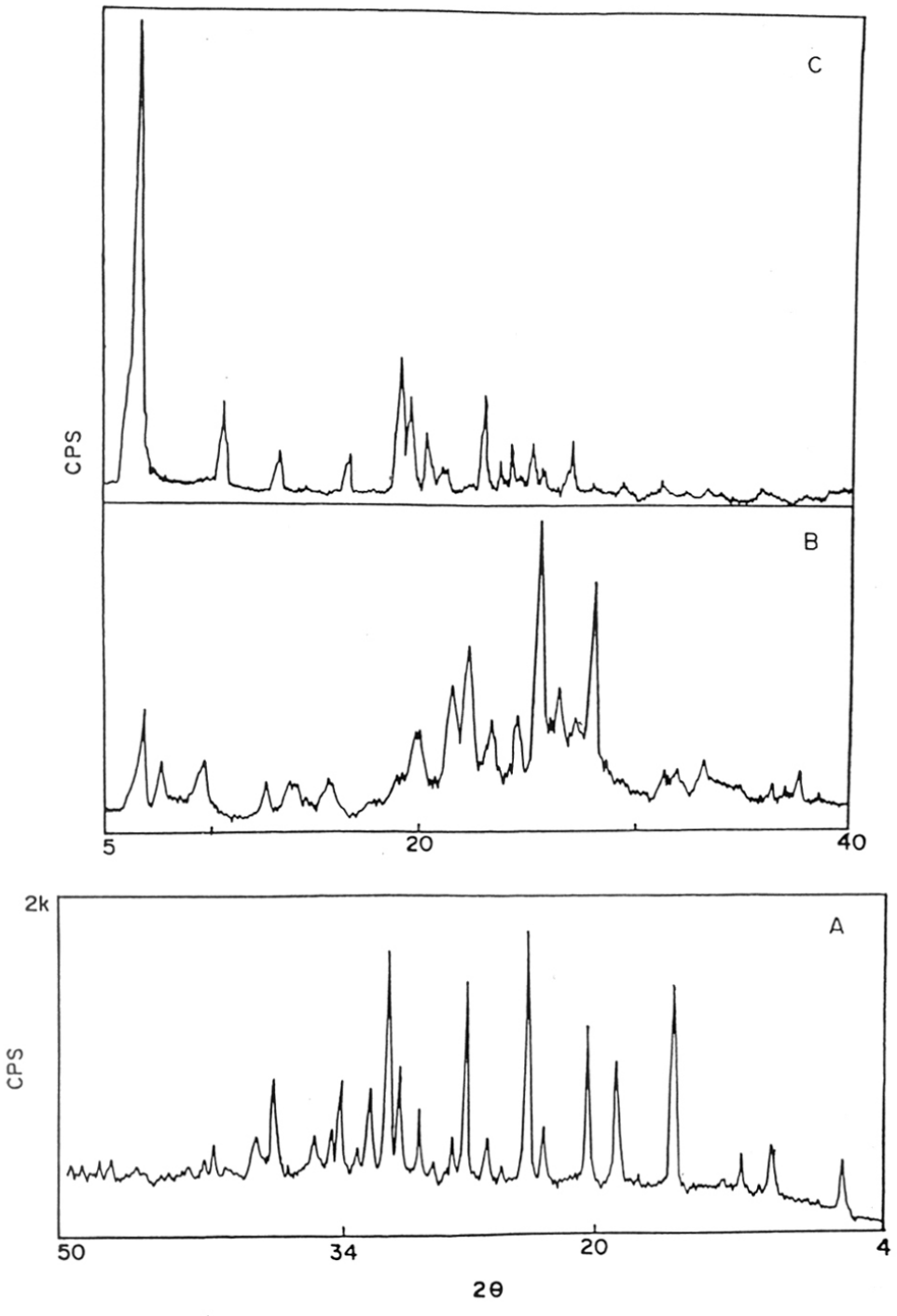

Fig. 1 X-ray diffractograms of Cu-H-Y (A), Cu-MCM-22 (B) and Cu-VPI-5 (C).

3.2.4 *UV-Vis spectroscopy*

The diffuse reflectance UV spectra of the molecular sieves with and without the copper complex (Fig. 3) also reveal the presence of copper acetate in the molecular sieves.

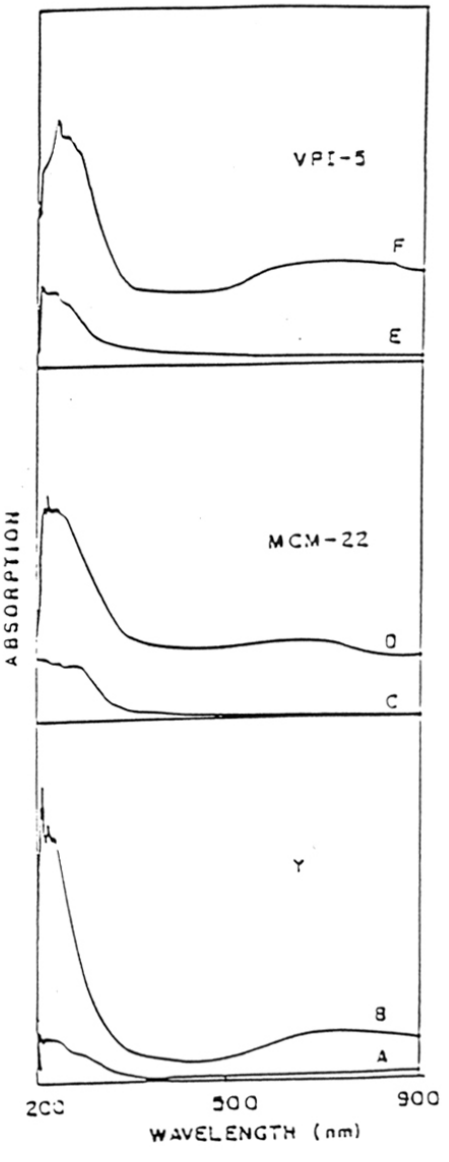

Fig. 3 Diffuse reflectance UV-Vis spectra of the catalysts. Curves A-F represent H-Y, Cu-H-Y, H-MCM-22, Cu-MCM-22, VPI-5 and Cu-VPI-5, respectively.

3.2.5 ESR spectroscopy

Having established the presence of copper (chemical analysis and XRF) and the structural and compositional integrity of copper acetate (IR and UV) in the catalysts, the next question is the nuclearity (monomeric or dimeric structure) of the copper acetate complex in the molecular sieves. ESR spectroscopy was used to elucidate this point. It is well known[38] (Fig. 4) that copper acetate monohydrate has a dimeric structure with four carboxylate groups

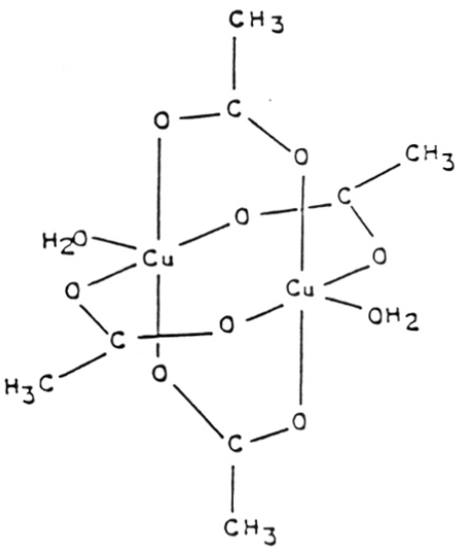

Fig.4. Structure of copper acetate monohydrate

bridging the two Cu (II) ions. The Cu-Cu distance is 2.616 Å. There is a weak antiferromagnetic coupling of the unpaired electrons, one on each Cu (II) ion, giving rise to a singlet ground state with a triplet state lying only a few kilojoules per mole above it. At room temperature the triplet is, thus, appreciably populated leading to the paramagnetism of copper acetate. At 298 K, μ_{eff} is typically about 1.4 BM per copper atom.[38] A

distinguishing characteristic of the dimeric copper acetate species is the presence of a seven line hyperfine structure in their ESR spectra.[39-40] The ESR spectra of our catalysts (Fig. 5) exhibit this seven-line pattern and, hence, indicate unequivocally the presence of a

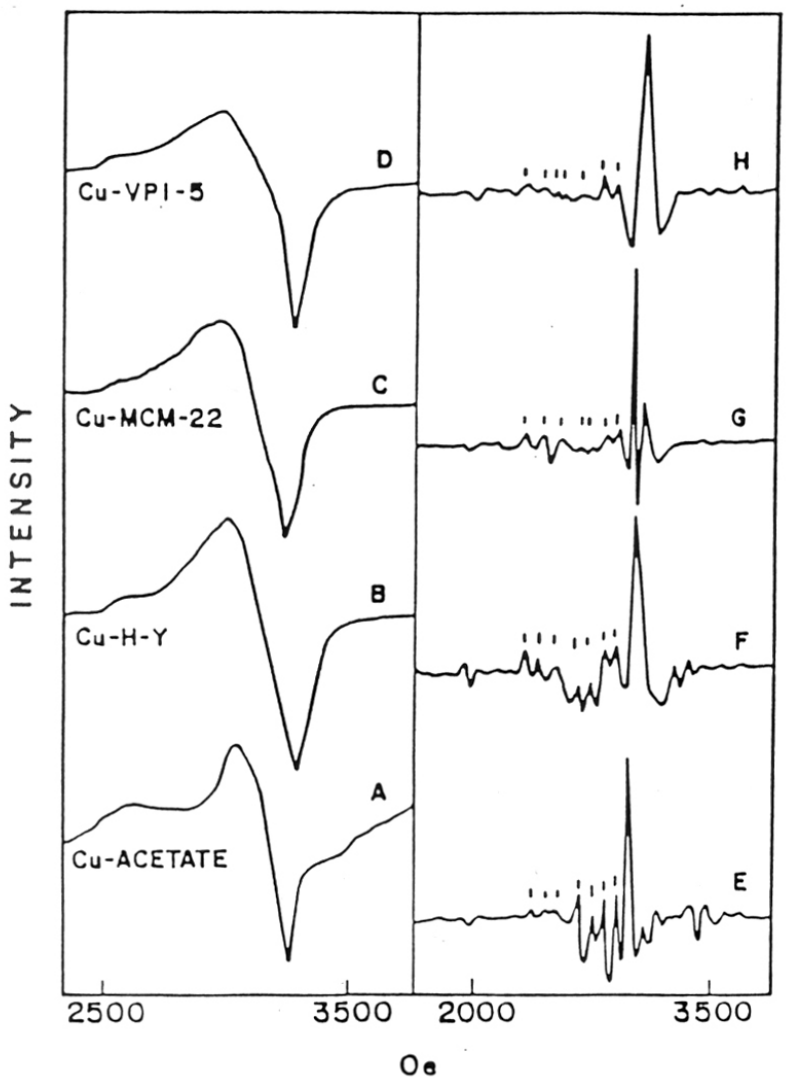

Fig. 5 ESR spectra of the catalysts. Curves A-D refer to the absorption curves of copper acetate monohydrate, Cu-H-Y, Cu-MCM-22 and Cu-VPI-5, respectively. Curves E-H refer to their corresponding second derivative spectra.

dimeric copper acetate complex similar to that present in copper acetate monohydrate. The ESR parameters for Cu-MCM-22 for example, were $g_{\perp}$= 2.02, $g_{\parallel}$= 2.21, $A_{\perp}$= 50 and $A_{\parallel}$= 55 G. The corresponding values for copper acetate monohydrate are 2.03, 2.21, 36 and 63, respectively. The latter set of values match very well with those in the literature for copper acetate monohydrate.[39-40] The ESR parameters of copper acetate and copper acetate incorporated molecular sieves at 298 K are given in Table-2.

Table-2

ESR parameters (at 298 K) of copper acetate incorporated in molecular sieves.

System	$g_{\perp}$	$g_{\parallel}$	$A_{\perp}$	$A_{\parallel}$	FWHM[a]
Cu-Ac	2.03	2.21	36	63	106
Cu-H-Y	2.00	2.22	43	58	147.15
Cu-MCM-22	2.02	2.21	50	55	141.2
Cu-VPI-5	2.03	2.22	43	66	164.8

[a] FWHM = full width at half maximum (Oe)

The presence of a seven-line pattern in the spectra of all the catalysts (Fig. 5) is a confirmatory evidence for the *dimeric* copper structure of the incorporated complex. The dimeric structure was maintained in the solid catalyst both before and after the catalytic reactions.

3.3 Copper phthalocyanine system

3.3.1 Chemical composition

The amount of metal and chemical composition of the phthalocyanine-based catalysts, were determined as described in Sections 2.3.1 and 2.3.2 and are given in Table-3.

Table-3

Metal content of the phthalocyanine-based catalyst

Catalyst	Metal (% wt)
$CuCl_{14}Pc$-Na-Y	0.11
$CuCl_{14}Pc$-Na-Y	0.17
$CuCl_{14}Pc$-Na-Y	0.26
$CuCl_{14}Pc$-Na-Y	0.27
$CuCl_{14}Pc$-Na-X	0.14
$CuCl_{16}Pc$-Na-X	0.27
$CuCl_{16}Pc$-Na-X	0.28
$CuCl_{16}Pc$-Na-Y	0.11
$CuCl_{16}Pc$-Na-X	0.28
$Cu(NO_2)_4Pc$-Na-Y	0.09
$Cu(NO_2)_4Pc$-Na-Y	0.16
$Cu(NO_2)_4Pc$-Na-X	0.11
$Cu(NO_2)_4Pc$-Na-X	0.14
$CuCl_{16}Pc$-K-L	0.10
$CuCl_{16}Pc$-ZSM-5	0.10
$CuCl_{16}Pc$-ZSM-5	0.17
$CoCl_{16}Pc$-Na-X	0.27
$FeCl_{16}Pc$-Na-X	0.16

3.3.2 X-ray diffraction

The X-ray diffractograms of the catalysts containing the copper complexes did not reveal any significant differences from those of the pure zeolites indicating that the molecular sieves had not undergone any major structural changes due to the encapsulation of the complexes, copper hexadeca chloro phthalocyanine ($CuCl_{16}Pc$) or copper tetra nitro phthalocyanine ($Cu(NO_2)_4Pc$). X-ray diffractograms of $CuCl_{16}Pc$ encapsulated in the

zeolite Na-X (A), $Cu(NO_2)_4Pc$ encapsulated in Na-Y (B), $CuCl_{16}Pc$ encapsulated in K-L (C) and ZSM-5 (D) are shown in Fig. 6.

3.3.3 X-ray photoelectron spectroscopy (XPS)

The XPS binding energies of copper in the molecular sieves were also similar to the values in the *neat* complexes. There is however a major difference in the XPS spectra of copper ions in $CuCl_{16}Pc$ and $Cu(NO_2)_4Pc$. While all the copper ions in $Cu(NO_2)_4Pc$ are in the divalent state (B.E. = 937.2 eV), the XPS data indicate that about 25 % of the copper ions in $CuCl_{16}Pc$ are in the monovalent state (B.E. = 935.8 eV) {Fig. 7 B}. In the non-chlorinated precursor CuPc, however, there is no evidence for the presence of monovalent copper {Fig. 7 A}. On treatment of $CuCl_{16}Pc$ with O_2 at 373 K for 3 h *in situ* in the ESCA spectrometer, the peak at 935.8 eV (due to Cu^{+1}) disappeared. The binding energy of Cu^{-2} in $CuCl_{16}Pc$ is 937.2 eV. Its value in the chlorine-free CuPc {Fig. 7 A} is 936.9 eV.

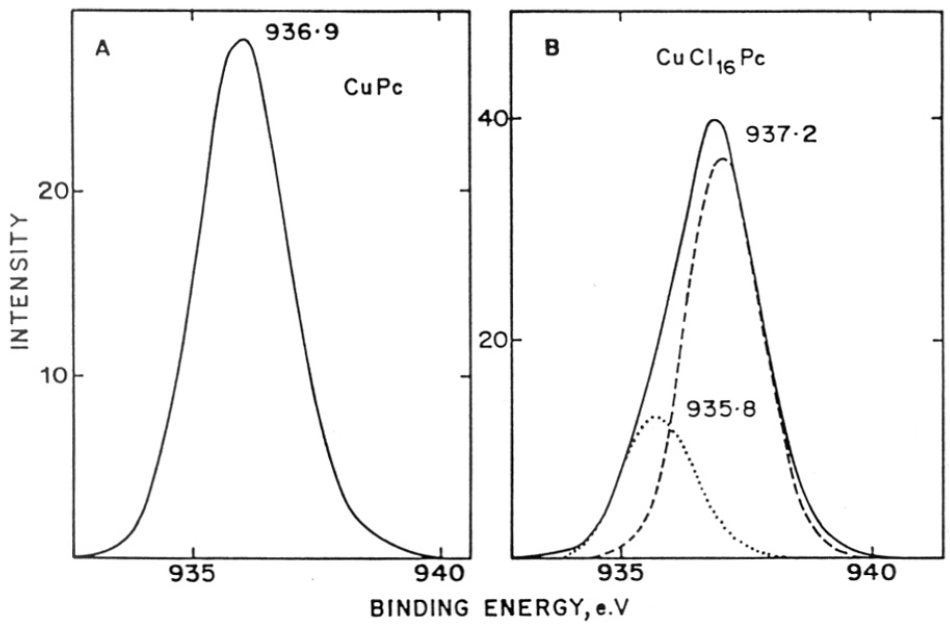

Fig. 7. XPS spectra of CuPc (Fig. A) and $CuCl_{16}Pc$ (Fig. B) at 298 K

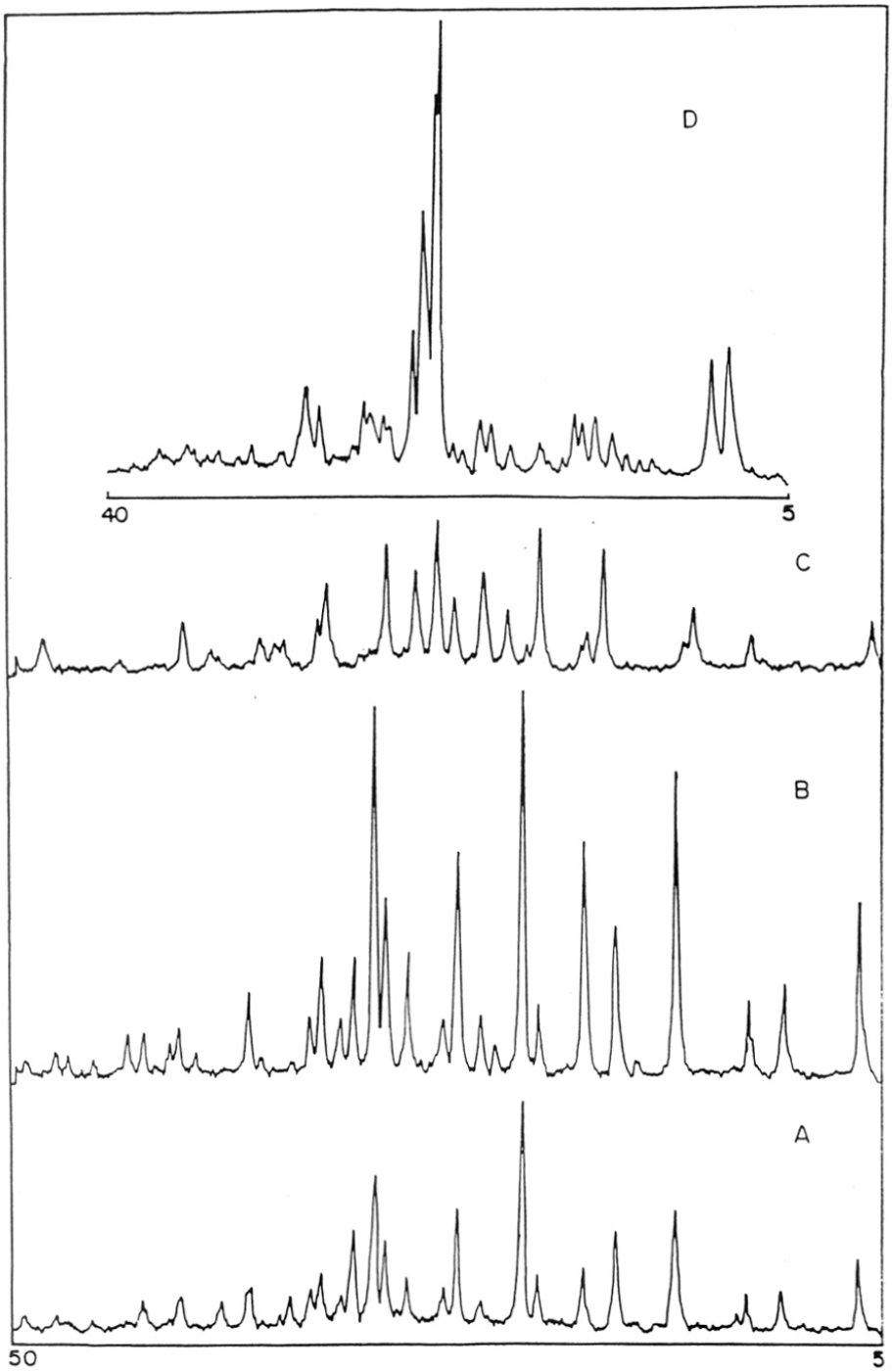

Fig. 6. X-ray diffractograms of $CuCl_{16}Pc$ encapsulated in Na-X (A), $Cu(NO_2)_4Pc$ encapsulated in Na-Y (B), $CuCl_{16}Pc$ encapsulated in K-L (C) and ZSM-5 (D).

3.3.4 Scanning electron microscopy

The encapsulation of the copper complexes inside the zeolite cavities is suggested by the absence of extraneous material by scanning electron microscopy. The SEM photographs of $CuCl_{16}$Pc-Na-Y (0.17) and $Cu(NO_2)_4$Pc-Na-X (0.14) {Fig. 8} indicate the presence of well defined zeolite crystals without any patches of phthalocyanine complexes overlaid on their external surface.

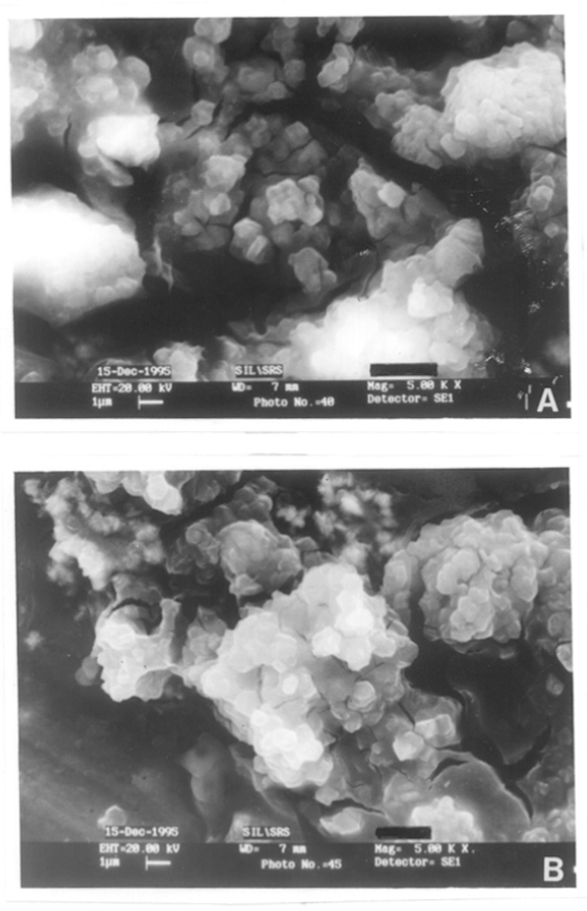

Fig. 8 Scanning electron micrographs of $CuCl_{16}$Pc-Na-Y (0.17) (A) and $Cu(NO_2)_4$Pc-Na-X (0.14) (B).

3.3.5 *Adsorption and surface area measurements*

N_2 adsorption data for $CuCl_{16}Pc$-Na-Y (0.17) {Fig. 9,C} confirm the presence of the copper complex inside the zeolite cavities. When $CuCl_{16}Pc$ was merely impregnated on the external surface of Na-Y (curve B, Fig. 9), there was no significant reduction in the volume of N_2 adsorbed, indicating that the large pore volume is still accessible to N_2. However, there is a drastic reduction in the pore volume in the case of samples containing the encapsulated copper complex, wherein the zeolite was synthesized in the presence of the metal complexes, as described in section 2.2, (curve C, Fig. 9), providing direct evidence for the presence of the copper complex inside the zeolite cavities and not merely on the external surface of the zeolite crystals. Similar results were observed in the case of $Cu(NO_2)_4Pc$-Na-X (0.14) and other encapsulated transition metal complexes.

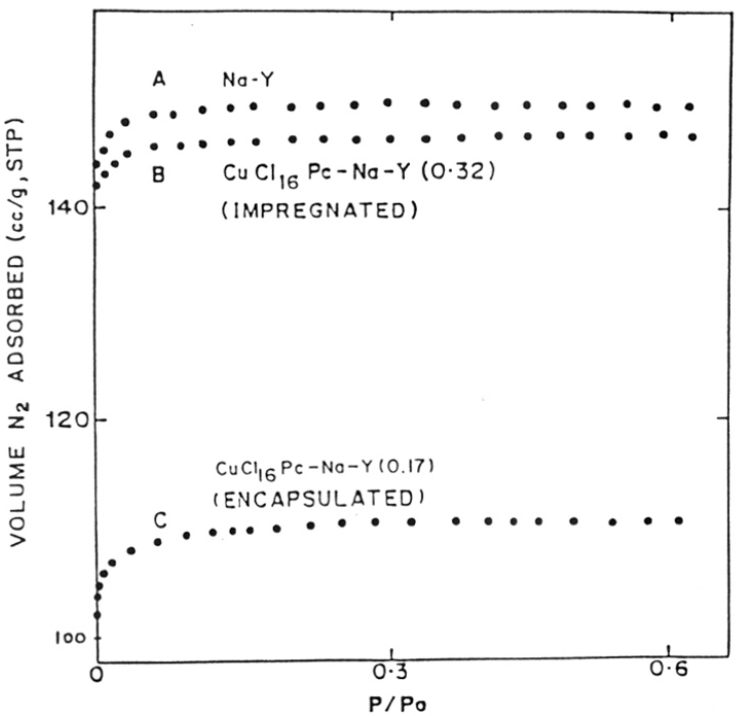

Fig. 9 N_2 adsorption isotherms at liquid nitrogen temperature of Na-Y (A), $CuCl_{16}Pc$-Na-Y (0.32) {impregnated} and $CuCl_{16}Pc$-Na-Y (0.17) {encapsulated}

The volume of N_2 adsorbed and the BET surface areas for $CuCl_{16}Pc$, $Cu(NO_2)_4Pc$, $CuCl_{16}Pc$-Na-Y (0.17) and $Cu(NO_2)_4Pc$-Na-X (0.14) are given in Table-4. The BET surface areas and micropore volume are drastically reduced when $CuCl_{16}Pc$ or $Cu(NO_2)_4Pc$ are encapsulated in the supercage of the faujasites or in ZSM-5. On the other hand, when $CuCl_{16}Pc$ is merely impregnated ($CuCl_{16}Pc$-Na-Y (0.32) {impregnated}) on the external surface of the zeolites, there is no significant reduction in the BET surface area and micropore volume. It is possible to achieve high loadings of the metal complex in ZSM-5 using the seeded method as compared to the non-seeded method. The drastic decrease in the surface area and micropore volume, using the seeded method, is an indication of the filling of the channels by the metal complex.

Table-4

Surface area and micropore volume of the different copper catalysts

Catalyst	S_{BET} (m^2/g)	S_t[a] (m^2/g)	Micropore Volume (ml/g)
CuPc	49.4	45.5	-
$CuCl_{16}Pc$	24	26	-
$CuCl_{16}Pc$-Na-Y (0.32) (Impregnated)	183	7.51	0.0731
$CuCl_{16}Pc$-Na-Y (0.17) (Encapsulated)	13.6	0.91	0.020
$CuCl_{16}Pc$-ZSM-5 (0.10) (non-seeded)	220	-	0.09
$CuCl_{16}Pc$-ZSM-5 (0.17) (Seeded)	52	-	0.04
$Cu(NO_2)_4Pc$	31	26	-
$Cu(NO_2)_4Pc$-Na-X (0.14) (Encapsulated)	9.5	0.25	0.023

[a] mesopore area

The sorption measurements for water, cyclohexane and n-hexane were carried out as described in section 2.3.3 and are presented in Table-5. The sorption values for n-hexane, cyclohexane and cumene are significantly reduced as compared to Na-Y[41] and ZSM-5[42] when $CuCl_{16}Pc$ is either impregnated or encapsulated in the zeolite. Zeolite Y is known to have particularly good adsorption characteristics. Further, the sorption values on encapsulation are still lower than on impregnation, as the internal void volume or channel of the zeolite is occupied by the metal complex and is inaccessible to the sorbate molecule.

Table-5

Sorption capacities of copper phthalocyanine-based catalysts

Catalyst	n-hexane (% wt adsorbed)	Cyclohexane (% wt adsorbed)	Cumene (% wt adsorbed)
CuPc	1.9	1.8	2.9
$CuCl_{16}Pc$	1.2	1.4	1.2
Na-Y	15.8	14.5	12.5
ZSM-5	13.5	7.1	6.2
$CuCl_{16}Pc$-Na-Y (0.32) (Impregnated)	8.2	9.5	9.3
$CuCl_{16}Pc$-Na-Y (0.17) (Encapsulated)	6.4	6.2	6.4
$CuCl_{16}Pc$-ZSM-5 (0.10) (Non-seeded)	3.5	1.5	-
$CuCl_{16}Pc$-ZSM-5 (0.17) (Seeded)	1.5	0.5	-
$Cu(NO_2)_4Pc$	0.8	0.9	0.9
$Cu(NO_2)_4Pc$-Na-X (0.14) (Encapsulated)	2.1	2.5	2.3

3.3.6 Infrared spectroscopy

Fig. 10 shows the infrared spectra of $CuCl_{14}Pc$, $Cu(NO_2)_4Pc$, $CuCl_{14}Pc$-Na-Y(0.26) and $Cu(NO_2)_4Pc$-Na-X (0.16). The IR bands of CuPc, $CuCl_{14}Pc$ and $CuCl_{14}Pc$-Na-Y(0.26) are given in Table-6. The structures of both the chloro- and nitro- complexes are seen to be intact even when they are encapsulated in the molecular sieves.

Table-6

FTIR results : Infrared bands (cm^{-1}) for CuPc, $CuCl_{14}Pc$, $CuCl_{14}Pc$-Na-Y(0.26)

CuPc	$CuCl_{14}Pc$	$CuCl_{14}Pc$-Na-Y(0.17)
2952	2953	2954
2916	2919	2922
1616	1618	1620
1508	1509	1512
1463	1466	1472
1445	1449	1454
1421	1422	1422
1377	1377	1378
1334	1336	1338

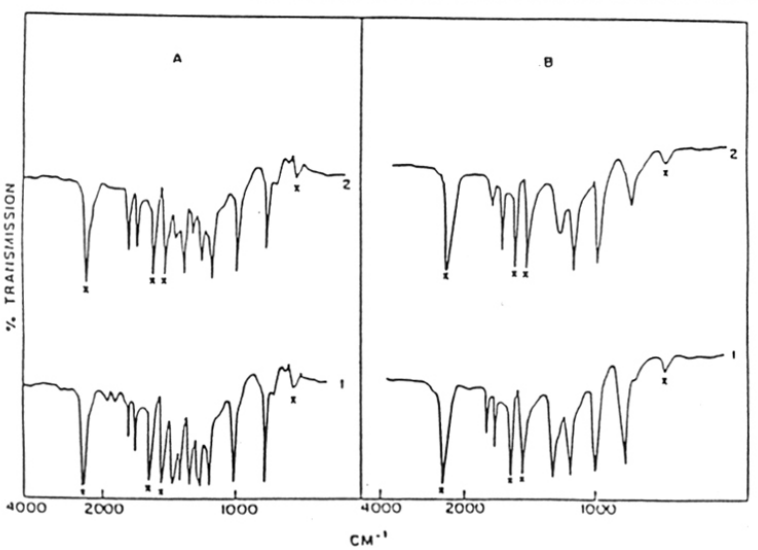

Fig.10 IR spectra of the catalysts : $CuCl_{14}Pc$ (A,1), $CuCl_{14}Pc$-Na-Y (0.26) (A,2), $Cu(NO_2)_4Pc$ (B,1) and $Cu(NO_2)_4Pc$-Na-Y (0.16) (B,2). x is used to denote the peaks due to nujol.

3.3.7 UV-Vis spectroscopy

The diffuse reflectance UV-Vis spectra of both the chloro- and nitro- complexes in the *neat* as well as well as in the encapsulated states also reveal that the integrity and structure of the complexes are more or less, preserved when they are encapsulated in the zeolites. Fig. 11 shows the diffuse reflectance UV-Vis spectra of Na-Y, $CuCl_{14}Pc$, $CuCl_{14}Pc$-Na-Y(0.26), $Cu(NO_2)_4Pc$ and $Cu(NO_2)_4Pc$-Na-X (0.16). The absorption maxima for $CuCl_{14}Pc$-Na-Y(0.26) are at 681.0 and 384 nm, respectively. The corresponding values for $CuCl_{14}Pc$ are 665.5 and 374 nm, respectively. Similarly the values for $Cu(NO_2)_4Pc$ and $Cu(NO_2)_4Pc$-Na-X (0.16) are 628.5, 354 and 652, 373 nm, respectively. There is, hence, a shift to lower energy for these ligand-based electronic transitions ($\pi \rightarrow \pi^*$) on

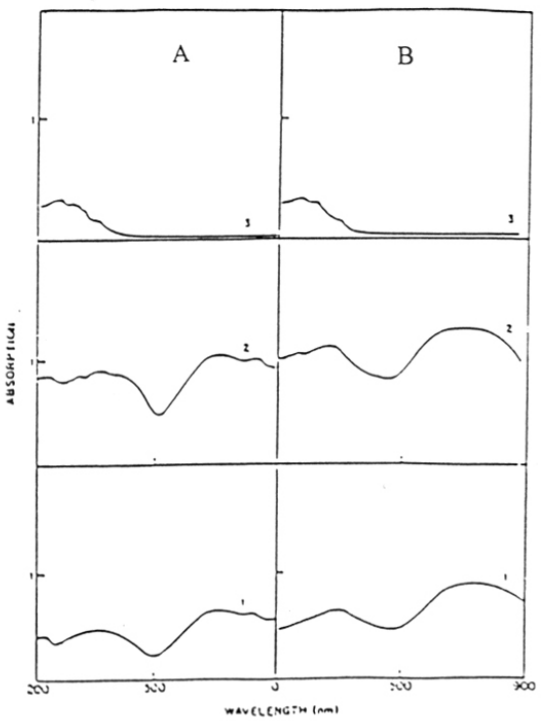

Fig. 11 Diffuse reflectance UV-Vis spectra of the catalysts : {Fig. A} Curves 1-3 represent $CuCl_{14}Pc$, $CuCl_{14}Pc$-Na-Y(0.26) and Na-Y, respectively. {Fig. B} Curves 1-3 represent $Cu(NO_2)_4Pc$ and $Cu(NO_2)_4Pc$-Na-X (0.16) and Na-Y, respectively.

encapsulation of the complexes inside the zeolite cavities. Balkus et al[6] had also observed a similar phenomena in the case of cobalt (II) and copper (II) perfluoro phthalocyanines encapsulated in Na-Y zeolites. They attributed this red shift to the distortion of the phthalocyanine ligand in the supercage of the zeolite. It may be noted that the size of the planar phthalocyanine ligand (~ 14 Å) exceeds the effective dimensions of the zeolite supercage (about 12 Å). The red shift in the UV-Vis spectra, due to the deformation of the planar phthalocyanine ligand, is indicative of the encapsulation of the copper complex inside the zeolite cavities and not merely adsorbed on the external surface of the zeolite.

3.3.8 ESR spectroscopy

The integrity of the copper complexes is also supported by their ESR spectra and the ESR parameters. Fig. 12 shows the ESR absorption spectra of $CuCl_{14}Pc$, $CuCl_{14}Pc$-Na-Y(0.26), $Cu(NO_2)_4Pc$ and $Cu(NO_2)_4Pc$-Na-X (0.16) at 298 K. Table-7 lists the ESR parameters at 298 K of the above catalysts. These parameters confirm that there are no major, significant differences on encapsulation of these complexes in the faujasite structure.

Table-7

ESR parameters at 298 K of $CuCl_{14}Pc$ and $Cu(NO_2)_4Pc$ encapsulated in Na-Y zeolite.

System	$g_\perp$	$g_\parallel$	$A_\perp$	$A_\parallel$
$CuCl_{14}Pc$	2.08	2.12	45	61
$Cu(NO_2)_4Pc$	2.06	2.16	38	58
$CuCl_{14}Pc$-Na-Y (0.17)	2.04	2.12	51	66
$Cu(NO_2)_4Pc$-Na-Y (0.16)	2.03	2.16	44	62

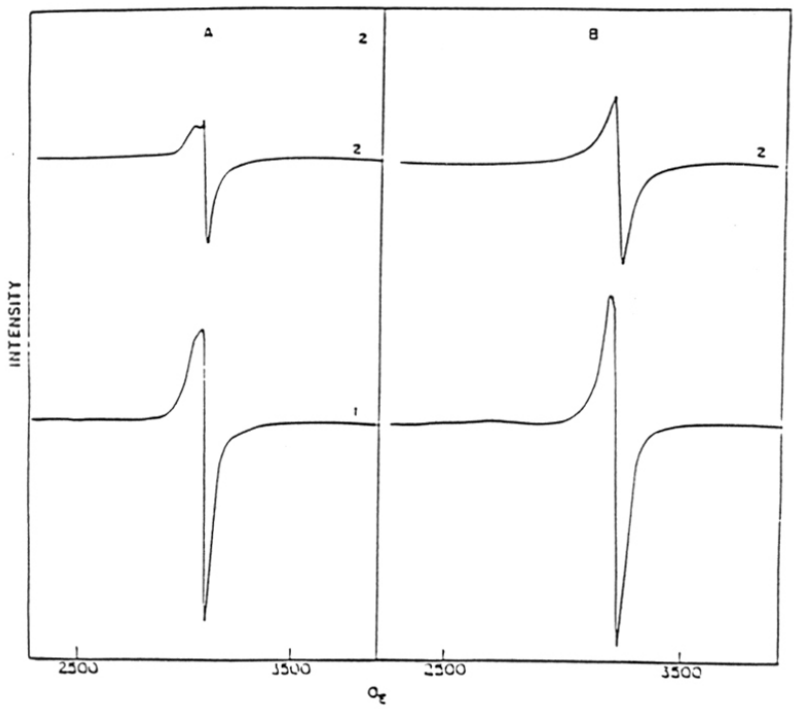

Fig. 12 ESR spectra of the catalysts : Curves 1-2 (Fig. A) refer to the absorption curves of $CuCl_{14}Pc$, $CuCl_{14}Pc$-Na-Y(0.26), respectively, at 298 K; Curves 1-2 refer to the absorption spectra of $Cu(NO_2)_4Pc$ and $Cu(NO_2)_4Pc$-Na-X (0.16), respectively at 298 K.

3.3.9 Thermal analysis

Simultaneous TGA and DTG of $CuCl_{16}Pc$ and $CuCl_{16}Pc$ encapsulated in Na-X is shown in Fig. 13 A and 13 B. respectively. $CuCl_{16}Pc$ is stable upto 703 K and undergoes decomposition at this temperature (Fig. 13 A). The weight loss at 373 K is due to water. While the neat $CuCl_{16}Pc$ complex decomposes at 703 K, encapsulation in zeolite matrices

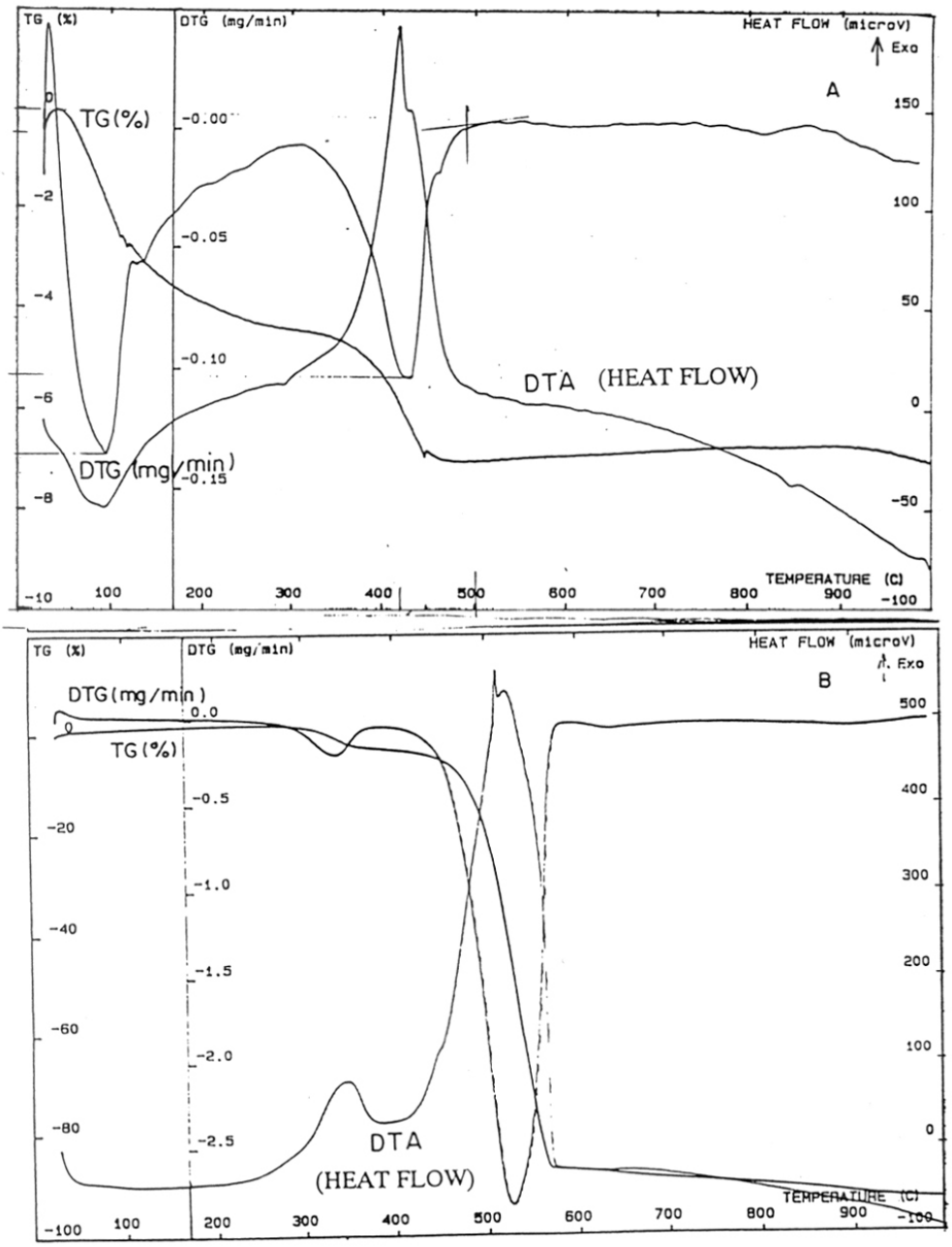

Fig. 13. TGA and DTG of $CuCl_{16}Pc$ (A) and $CuCl_{16}Pc$-Na-X (0.28) (B).

increases the stability of the catalyst and prevents decomposition of the complex via bimolecular pathways. $CuCl_{16}Pc$-Na-X (0.28) was activated at 373 K for 8 h, prior to measurements to remove water. 92 % of the encapsulated complex decomposes at 798 K, in the case of $CuCl_{16}Pc$-Na-X (0.28). Since thermal stability of the material improves on encapsulation, these zeolite encapsulated metal complexes can be used as catalysts at higher temperatures in catalytic reactions.

3.3.10 Computer Modeling

The dimensions of phthalocyanine (Pc) and tetra deca chloro phthalocyanine ($Cl_{14}Pc$) were measured as the extents of molecules fitting in the smallest possible rectangular box with dimensions a,b,c. It was found that their dimensions were (13.22, 12.94, 3.89 Å) and (14.60, 14.34, 4.26 Å), respectively and their respective strain energies were 395.70 and 413.53 K. cal/mol. The strain energy values were calculated using the central valence force field potential (CVFF)[44] described in the Insight II/Discover molecular modeling software package supplied by Biosym. Inc[45]. The molecular fitting of CuPc and $CuCl_{14}Pc$ were tried in the supercages of the faujasite structure. Fig. 14 A and 14 B represent the computer graphics picture of CuPc and $CuCl_{14}Pc$ inside the supercage of the faujasite structure. It is obvious that the latter cannot fit into the supercage without significant strain in the geometry, while the former just fits into the supercage. It was found that it is possible to achieve a suitable geometry for the $CuCl_{14}Pc$ which can fit into the supercage of the faujasite structure with minimum strain energy {Fig. 15}. Molecular strain energy minimization calculations indicate that the geometric environment around the copper is distorted from the square planar symmetry (of the free complex) when encapsulated in the supercage of the faujasite (Fig. 15). The copper atom is now at the

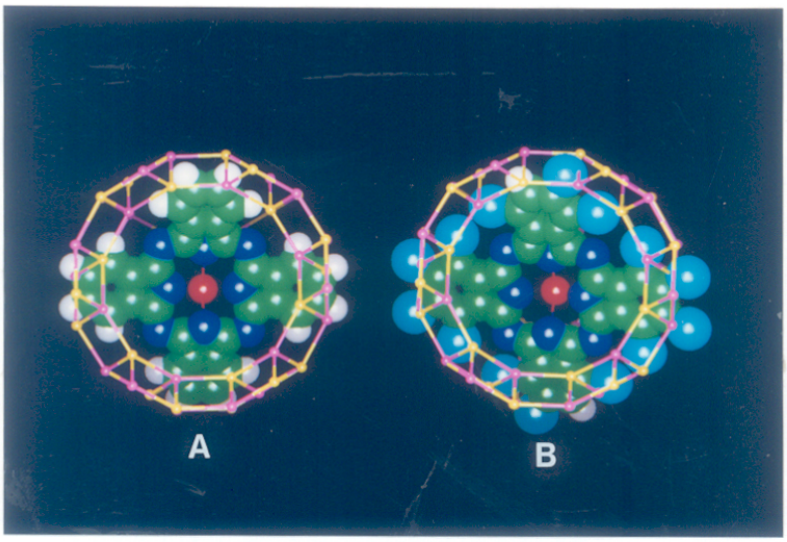

Fig. 14. CuPc (A) and $CuCl_{14}Pc$ (B) inside the supercage of the faujasite structure.
red - copper, dark blue - nitrogen, green - carbon, white - hydrogen, light blue - chlorine

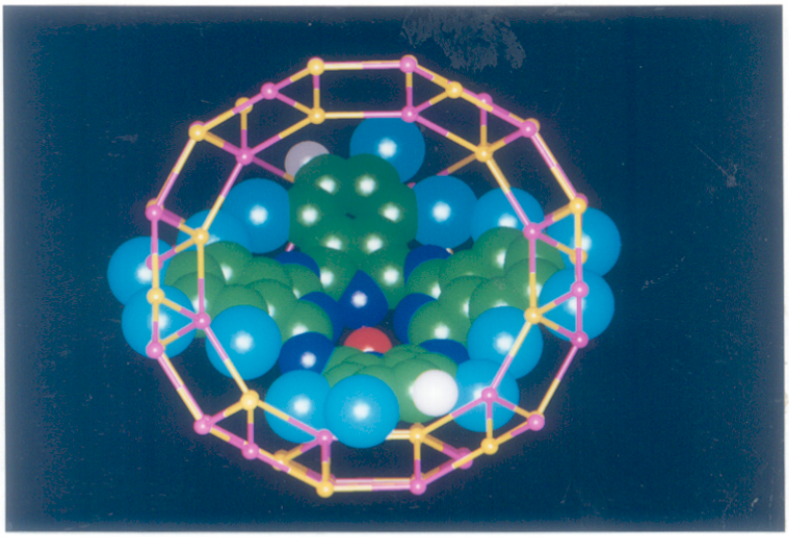

Fig. 15. Distorted $CuCl_{14}Pc$ inside the supercage of the faujasite structure.
red - copper, dark blue - nitrogen, green - carbon, white - hydrogen, light blue - chlorine

bottom of a *hydrophobic bowl*. The red shift observed in the UV-Vis spectra provides experimental evidence for this molecular distortion. The additional strain energy required for this distortion (3.6 K cal/mol), is available to the system during the synthesis

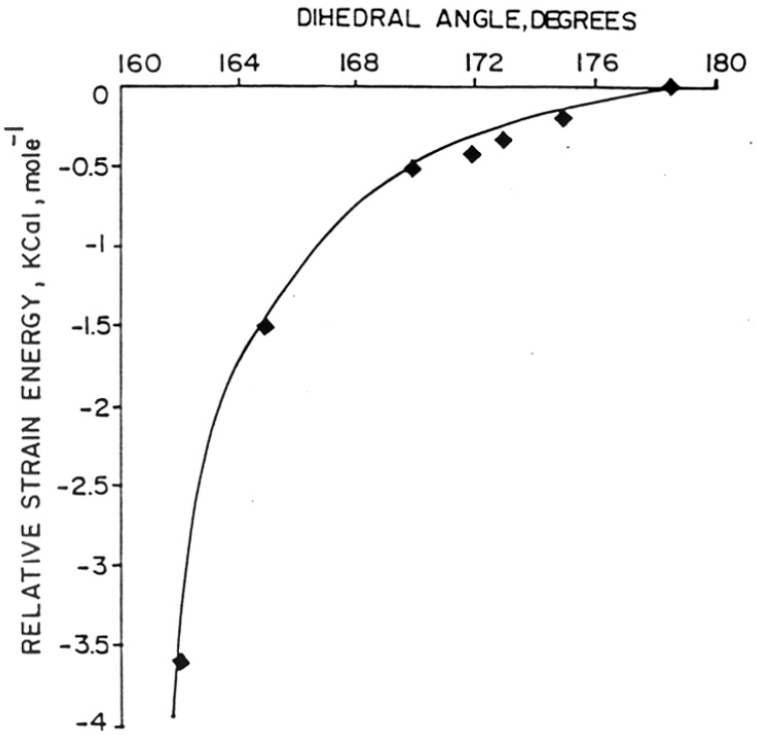

Fig.16 Plot of relative strain energy versus non-planarity in $CuCl_{16}Pc$.

of the encapsulated catalyst. Such distortions in the symmetry of the complex from square planarity to quasi-tetrahedral symmetry will admix the d_{xy} orbital with the d_{z2} orbital leading to a lower electron density on the metal ion thereby enhancing the reactivity of the complex towards molecular O_2[43] in general and oxidation reactions, in particular.

3.4 References

1. N. Herron, *J. Coord. Chem.*, **19** (1988) 25.

2. K.J. Balkus, Jr., A.A. Welch and B.E. Gnade, *J. Inclus. Phenom. Molec. Recog. Chem.*, **10** (1991) 141.

3. H. Diegruber, P.J. Plath, E.G. Schulz-Elkoff and M. Mohl, *J. Mol. Catal.*, **24** (1984) 115.

4. R.F. Parton, L. Utytterhoeven and P.A. Jacobs, *Stud. Surf. Sci. Catal.*, **59** (1991) 395.

5. A.G. Gabrielov, K.J. Balkus, Jr., F. Bedioui and J. Devynck, *Micropor. Mater.*, **2** (1994) 119.

6. K.J. Balkus, Jr., A.G. Gabrielov, F. Bedioui and J. Devynck, *Inorg. Chem.*, **33** (1994) 67.

7. S. Kawi and B.C. Gates, *J. Chem. Soc. Chem. Commun.*, (1992) 702.

8. N. Takahashi, A. Mijin, H. Suematsu, S. Shinohara and H. Matsuoka, *J. Catal.*, **177** (1989) 348.

9. A. Fukuoka, L.F. Rao, N. Kosugi, H. Kuroda and M. Ichikawa, *Appl. Catal.*, **50** (1989) 295.

10. T. Bein, S.J. Mc Lain, D.R. Corbin, R.D. Farlee, K. Moller, G.D. Stucky, G. Woolery and S. Sayers, *J. Am. Chem. Soc.*, **110** (1988) 1801.

11. A. De Mallmann and D. Barthomeuf, *Catal. Lett.*, **5** (1990) 293.

12. G.J. Li, T. Fujimoto, A. Fukuoka and M. Ichikawa, *J. Chem. Soc. Chem. Commun., (1991)* 1337.

13. T. Kimura, A. Fukuoka and M. Ichikawa, *Catal. Lett.*, **4** (1990) 279.

14. N.C. Eickman, R.S. Himmelwright and E.I. Solomon, *Proc. Natl. Acad. Sci., USA* **76** (1979) 2094.

15. K. Magnus and H. Ton-That, *J. Inorg. Biochem.*, **47** (1992) 20.

16. H.S. Mason, *Nature* **177** (1956) 79.

17. A.C. Rosenzweiz, C.A. Frederick, S.J. Lippard and P. Nordlund, *Nature*, **366** (1993) 537.

18. B.V. Romanovsky and A.G. Gabrielov, *Stud. Surf. Sci. Catal.*, **72** (1992) 443.

19. B.V. Romanovsky and A.G. Gabrielov, *J. Mol. Catal.*, **74** (1992) 293.

20. M. Ichikawa, T. Kimura and A. Fukuoka, *Stud. Surf. Sci. Catal.*, **60** (1991) 335.

21. C. Bowers and P.K. Dutta, *J. Catal.*, **122** (1990) 271.

22. K.J. Balkus, Jr., A.A. Welch and B.E. Gnade, *Zeolites*, **10** (1990) 722.

23. D.E. De Vos and P.A. Jacobs, in *Proceedings from the 9th International Zeolite Conference*, R. Von Ballmoos, J.B. Higgins and M.M.J. Treacy (Eds); Butterworth-Heinemann, Boston, Vol. 2 (1992) pp. 615.

24. L. Gaillon, N. Sajot, F. Bedioui, J. Devynck and K.J. Balkus, Jr., *J. Electroanal. Chem. Interface. Electrochem.*, **345** (1993) 157.

25. G. Meyer, D. Wohrle, D. Mohl and G. Schultz-Ekloff, *Zeolites*, **4** (1984) 30.

26. K. Putyera, G. Plesch, L. Benco, J. Dobrovodsky, A.V. Tchuvaev, V.I. Nefedov and M. Zikmund, *Proc. 12th Conf. Coord. Chem.*, (1990) 295.

27. E.S. Shpiro, G.V. Antoshin, O.P. Tkachenko, S.V. Gudkov, B.V. Romanovsky and Kh. M. Minachev, *Stud. Surf. Sci. Catal.*, **18** (1984) 31.

28. A.G. Gabrielov, A.N. Zakharov and B.V. Romanovsky, O.P. Tkachenko, E.S. Shpiro and Kh. M. Minachev, *Koord. Khim.*, **14** (1988) 821.

29. M. Nakamura, T. Tatsumi and H. Tominaga, *Bull. Chem. Soc. Jpn.*, **63** (1990) 3334.

30. G.A. Ozin, A. Kuperman and A. Stein, Angew. *Chem. Int. Ed. Engl.*, **28** (1989) 359.

31. D.R. Rolisson, *Chem. Rev.*, **90** (1990) 867.

32. A.J. Bard and T.E. Mallouk, in R.W. Murray (Ed); "*Molecular design of electrode surfaces*" Wiley, New York, (1992) pp. 271.

33. N. Herron, *Inorg. Chem.*, **25** (1986) 4717.

34. N. Herron, G.D. Stucky and C.A. Tolman, *J. Chem. Soc., Chem. Commun.*, (1986) 1521.

35. R. Parton, D. De Vos and P.A. Jacobs, in E.G. Derouane, F. Lemos, C. Naccache and R.F. Ribeiro (Eds); "*Zeolite Microporous Solids : Synthesis, Structure and Reactivity*," Khumer Academic Publishers, London (1991) 555.

36. K.J. Balkus, Jr., and J.P. Ferraris, *J. Phys. Chem.*, **94** (1990) 8019.

37. M.G.B. Drew in *"Spectroscopic and Computational Studies of Supramolecular Species*," J.E.D. Davies (Ed); Kluwer, Dordrecht (1992) pp. 207.

38. F.A. Cotton and G. Wilkinson, "*Advanced Inorganic Chemistry*", 5th Ed; John Wiley and Sons, New York (1988) pp. 772.

39. B. Bleaney and K.D. Bowers, *Proc. Roy. Soc. A*, **214** (1952) 451.

40. H. Abe and J. Shimada, *J. Chem. Phys.*, (1953) 316.

41. D.W. Breck, *U.S. Patent*, 3,130,007 (1964).

42. A.N. Kotasthane, V.P. Shiralkar, S.G. Hegde and S.B. Kulkarni, *Zeolites*, **6** (1986) 253.

43. M.M. Bhadbhade and D. Srinivas, *Inorg. Chem.*, **32** (1993) 5458.

44. O. Ermer, *Structure and bonding*, **27** (1976) 161.

45. Insight II User guide, Version 2.3.5, San Diego, Biosym. Technologies (1994).

CHAPTER-4

OXIDATION OF ALKANES

4.0 Oxidation of alkanes

4.1 Introduction

The chemical inertness of alkanes is reflected in their old name *paraffins* from the Latin *parum affins* - without affinity. Hence, most of the alkane reactions usually require strong reagents like strong oxidants, superacids, free atoms, radicals and carbenes or proceed at high temperatures. One of the major problems in catalysis (and heterogeneous catalysis, in particular) remains the development of catalytic methods for the selective oxidation of the unactivated C-H bonds in alkanes at relatively low temperatures. The oxidation of hydrocarbons is highly exothermic, about 105 Kcal/mole of O_2 consumed, accounting for their use, by combustion, to power automobiles, airplanes, trains and ships, as well as to generate much of our electricity. In spite of this favorable thermodynamics, the kinetics of oxidation at low temperatures is rather unfavorable due to a spin conservation selection rule against direct reactions of triplet O_2 with singlet hydrocarbons. Hence, a suitable catalyst is necessary to overcome this kinetic barrier at low temperatures.

During the past two decades, this problem has been addressed by various strategies. The homogeneous catalytic functionalisation of alkanes by metalloporphyrins[1], Schiff base complexes[2-5] and their related heterogenised analogs are some of the efforts in this

direction. These systems oxidize alkanes by C-H bond hydroxylation through the intermediacy of oxometal species, in a way analogous to oxidation by enzymes like cytochrome P-450[6-7]. Some of these enzymes, like the omega hydroxylases,[8] are capable of selectively hydroxylating the terminal methyl groups of straight chain normal paraffins to primary alcohols.

An important step in mimicking cytochrome P-450 was taken in 1979 by Groves at al[9] who used iodosobenzene as an oxygen atom donor for iron porphyrins as catalysts. The latter accept the singlet oxygen atom and are transformed to an active form capable of epoxidising olefins and hydroxylating alkanes. Suslick[10] has shown in his work that it is possible to achieve C_1 hydroxylation by going to a tetraphenyl porphyrin system which has bulky phenyl groups in all the ortho positions. However, these complexes require (a). stoichiometric oxygen atom donors, other than oxygen, (b). sacrificial co-reductants, (c). electrochemical reduction and (4). photolytic assistance. Romanovsky[1] was the first to encapsulate porphyrin complexes in zeolite matrices in an attempt to mimic the catalytic activity and selectivity of cytochrome P-450. In later studies, Herron et al[11] prepared an active catalyst and showed that terminal hydroxylation is preferred in the hydroxylation of n-octane. Their catalyst system comprised of Fe (II)-Pd (0) on zeolite A, using a mixture of H_2 and O_2 as oxidants. Pd (0) and H_2 reduced the O_2 to H_2O_2, which reacts with the Fe (III) to form a reactive ferryl. In the case of Fe/ZSM-5 catalyst with H_2O_2 as the oxidant, the major product in the case of n-octane oxidation was 1-octanol.[12] More recently, Ellis and Lyon[13] as well as Balkus et al[14] have reported the oxidation of alkanes by iron, ruthenium, manganese and copper porphyrin and phthalocyanine complexes encapsulated in zeolites X and Y.

In the present chapter, the synthesis, characterization and catalytic properties (in selective hydrocarbon oxidation reactions) of copper, iron and cobalt phthalocyanine complexes encapsulated in molecular sieves Na-X and Na-Y is reported. Molecular oxygen and singlet oxygen sources like aqueous H_2O_2 and tert. butyl hydroperoxide (TBHP) have been used as the oxidants. The results obtained using n-hexane, cyclohexane and methane indicate that copper, iron and cobalt complexes with appropriately chosen ligands and incorporated in molecular sieves are a novel class of catalysts which can selectively oxidize a wide variety of organic substrates using O_2, TBHP and H_2O_2 as oxidants. Regioselectivity was observed in the case of oxidation of n-hexane with molecular O_2. The values of methane conversion, TON and selectivity over these solid catalysts are comparable if not better, than most of the results published, so far.

4.2. Experimental

4.2.1 Materials

The *neat* $CuCl_{16}$ Pc, $Cu(NO_2)_4Pc$ and $FeCl_{16}$ Pc (where Pc stands for phthalocyanine) complexes were synthesized according to the procedure reported in Sections 2.2.1 (Chapter-2). CuPc, CoPc and $CoCl_{16}Pc$ complexes were obtained from M/s. Lona Industries, Bombay.

The $CuCl_{16}Pc$, $CuCl_{14}Pc$, $Cu(NO_2)_4Pc$, $FeCl_{16}Pc$ or $CoCl_{16}Pc$ complexes were encapsulated in zeolites NaX and Na-Y and K-L and ZSM-5 as described in Sections 2.2.1, (Chapter-2). NaX and Na-Y samples with varying loadings of $CuCl_{16}Pc$, $CuCl_{14}Pc$, $Cu(NO_2)_4Pc$, $FeCl_{16}Pc$ or $CoCl_{16}Pc$ were prepared similarly.

4.2.2 Procedures

Catalytic Reactions

Detailed procedures of the catalytic reaction using n-hexane, cyclohexane or methane as the substrates are described in Section 2.2.2.1 (Chapter-2).

Product analysis

Detailed description of the analyses of the products of the oxidation of n-hexane, cyclohexane and methane is given in Section 2.2.2.1 (Chapter-2).

4.3 n-hexane Oxidation

Oxidation with O_2

Table 1 illustrates the oxidation of n-hexane with O_2 (from air) over $CuCl_{14}Pc$, $Cu(NO_2)_4Pc$ and the two complexes encapsulated in Na-Y. One interesting finding is that both $CuCl_{14}Pc$ and its encapsulated analog are able to oxidize even the primary C-H bonds of the end-methyl groups of n-hexane to C-OH groups and the corresponding aldehyde (Table 1). The nitro complex, on the other hand, is unable to oxidize the CH_3 groups. In this context, the halogenated phthalocyanines seem to be more active than their porphyrin analogs in activating primary C-H bonds. Lyons et al[13] found that, while their perfluoro porphyrin complexes were active catalysts for the oxidation of unactivated acyclic alkanes having either secondary or tertiary C-H bonds, the primary C-H bonds were quite resistant to oxidative attack in the presence of their catalysts. It may be noted from Table 1 that though the *neat* complexes are more active than their encapsulated analogs on a weight basis, the catalytic efficiency of the latter (in terms of activity per copper atom) is higher than the former. This is, probably, due to the isolation of the copper sites in the zeolite cavities. An additional feature of the results in Table 1 is that

Table-1

Oxidation of n-hexane with O_2 over phthalocyanines

Catalyst	Temp	nC_6	Products (%)					
	(K)	Conv. (%)	1-ol	ald	2-ol	2-on	3-ol	3-on
	333	15.7	4.9	6.2	3.0	1.6	-	-
$CuCl_{14}Pc$	343	18.8	4.7	6.9	2.1	3.5	1.0	0.6
	353	19.5	2.7	6.4	2.3	5.4	1.2	1.5
$CuCl_{14}Pc$-Na-Y	333	8.9	2.8	6.1	-	-	-	-
(0.26)	353	10.2	4.6	5.6	-	-	-	-
$CuCl_{16}Pc$-ZSM-5	353	6.4	1.3	2.0	0.7	1.9	0.5	
(0.10)								
$Cu(NO_2)_4Pc$	333	6.2	-	-	1.7	2.6	1.2	1.7
	353	8.1	-	-	1.2	3.1	1.4	2.4
$Cu(NO_2)_4Pc$-Na-Y	333	4.8	-	-	0.7	1.2	0.9	2.0
(0.16)	353	6.9	-	-	1.4	1.6	1.7	2.2

Reaction conditions : n-hexane = 15 g; catalyst = 1.2 g; air = 500 psi; acetonitrile = 45 g; reaction time = 8 hrs;

oxidation at the 3-position increases with temperature. Similar results were observed in the oxidation of n-alkanes in Pd-Fe-zeolites by the DuPont workers[15] who attributed it to the end-on diffusion of the linear paraffins in the narrow channels of the molecular sieve.

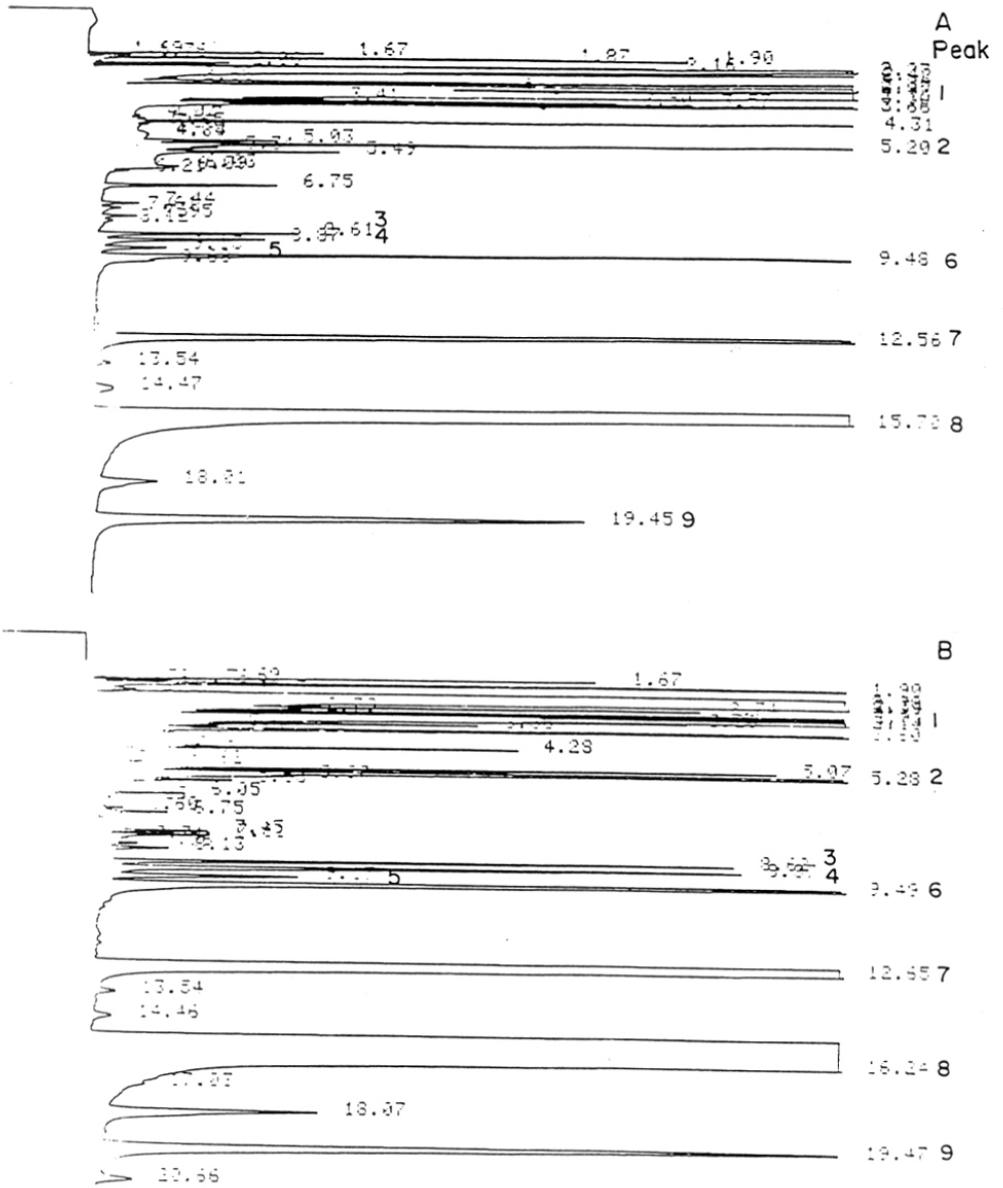

Fig. 1 Typical GC chromatograms of the products of oxidation of n-hexane. A and B represent the top and bottom layers of the reaction mixture : Peaks 1-9 represent n-hexane, t-butanol, 3-ol, 2-ol, 3-one, 2-one, 1-ald, 1-ol and hexanoic acid, respectively.

Oxidation with H_2O_2

Oxidation of n-hexane with a singlet oxygen source, H_2O_2, as the oxidant, is illustrated in Table 2. The most striking difference between the oxidation (of n-hexane) with O_2 and H_2O_2 (Tables 1 and 2, respectively) is the total absence of n-hexan-1-ol and the n-hexan-1-aldehyde when H_2O_2 is used as the oxidant in the case of both $CuCl_{14}Pc$ and $CuCl_{14}Pc$-Na-Y (0.26). By contrast, these two compounds were the most important constituents of the products when O_2 was the oxidant (Table 1). Another notable feature of Table 2 is the higher concentration of the 3-ol and 3-on at high conversion levels, especially with $CuCl_{14}Pc$-based catalysts. There is no significant variation in the ratio of (2+3)-ol / (2+3)-on between the chloro- and nitro complexes as well as at different temperatures. (The value varies between 0.8 and 1.0). This is not surprising since the rate of oxidation of the secondary alcohol to the ketone is expected to be much faster than that of n-hexane to the alcohol.

Table-2

Oxidation of n-hexane with H_2O_2 over phthalocyanines

Catalyst	Temp	nC_6	Products (%)			
	(K)	Conv. (%)	2-ol	2-on	3-ol	3-on
$CuCl_{14}Pc$	333	19.2	6.5	8.9	2.1	1.7
	343	22.5	9.2	11.0	1.7	0.6
	353	26.2	7.1	8.3	5.9	4.9
$CuCl_{14}Pc$-Na-Y (0.26)	333	16.5	6.1	7.2	1.1	2.1
	343	19.1	6.8	9.1	1.6	1.6
	353	22.4	6.2	7.6	4.1	4.5

$CuCl_{16}Pc$-ZSM-5 (0.10)	353	9.9	4.2	1.1	3.3	1.2
$Cu(NO_2)_4Pc$	333	10.5	1.9	3.1	3.2	2.3
	353	11.2	2.2	4.6	1.7	2.7
$Cu(NO_2)_4Pc$-Na-Y (0.16)	333	6.3	1.1	1.7	2.0	1.5
	353	8.2	1.2	1.9	2.9	2.2

Reaction conditions : n-hexane = 15 g; n-hexane/H_2O_2 = 3 mole; acetonitrile = 45 g; reaction time = 8 hrs.

4.4 Cyclohexane Oxidation

The oxidation of cyclohexane to cyclohexanol and cyclohexanone, under mild conditions has an important industrial significance. More than 10^6 tonnes of cyclohexanol and cyclohexanone are made world-wide per year for the production of Nylon-6 and Nylon-6-6. Enzymes are capable of oxidizing cyclohexane to cyclohexanol at room temperature with high selectivity[16]. The best known and most interesting enzymes are cytochrome P-450[17], methane monooxygenase[18], proyl 4-hydroxylase[19], isopeniciline N-synthase[20], γ-butyl-obetaine hydroxylase[21] and bleomycine[22]. The ability of cytochrome P-450 to activate oxygen for hydrocarbon oxidation has motivated many studies involving metalloporphyrin catalysts.[23-25]

Industrially, cyclohexane is oxidized at 423-433 K and 0.9 MPa air, in the presence of cobalt naphthenate, or metaboric acid to form a mixture of cyclohexanol and cyclohexanone[26] (the so-called K-A oil).

Recently, Barton and his co-workers[27] have developed the *Gif System* which allows the oxidation and functionalisation of saturated hydrocarbons under mild reaction

conditions, ambient temperatures and atmospheric pressures. These systems contain a pyridine-acetic acid solution of a hydrocarbon, which is to be oxidized in the presence of an oxidant, an iron-based catalyst and an electron source. Gif systems were designed to emulate non-heme enzymatic oxidations of alkanes. This reaction which proceeds by a radical mechanism involves, (1). the activation of the dioxygen molecule as an Fe=O species (2). activation of the hydrocarbon through insertion of the Fe (V)=O species into the carbon-hydrogen bond and (3). Insertion of dioxygen in a carbon-hydrogen bond and formation of products from the alkyl hydroperoxide intermediate.

A major drawback of the Gif system is that during the oxidation, radical reactions become more important causing over-oxidation and coupling of the products with pyridine.[28] Moreover, the water formed during the oxidation process causes hydrolysis of the catalyst and phase separation, thereby leading to its deactivation. An interesting feature of the Gif system is that the iron salt can be substituted by a copper salt.[29] This system was less efficient than the iron system, although more selective for oxidation of cyclohexane to cyclohexanone.

Encapsulated Fe (II) phthalocyanines have shown promise as catalysts for the oxidation of cyclohexane, using alkyl peroxides or iodosyl benzene as the oxidants.[30-32] Iodosyl benzene, however, leads to zeolite pore blockage and alkyl peroxides can bleach the catalyst. Parton et al[33], recently circumvented the above problem by incorporating the zeolite encapsulated FePc complex in a polymer matrix. The polymer serves to inhibit the preferential adsorption of the peroxide over the alkane, and thereby enhances catalyst stability. Balkus et al[34], have shown that $RuF_{16}Pc$ complexes encapsulated in Na-X are also effective catalysts for the oxidation of cyclohexane at room temperature.

Catalytic activity

Experimental evidence to show that the oxidation of cyclohexane is indeed catalyzed by the solid zeolite catalyst containing the encapsulated metal complex and not by the free complex dissolved in solution is presented in Fig. 2. In one set of two identical experiments, the solid catalyst {$CuCl_{16}$Pc-Na-X (0.28)} was removed by centrifugation after a reaction time

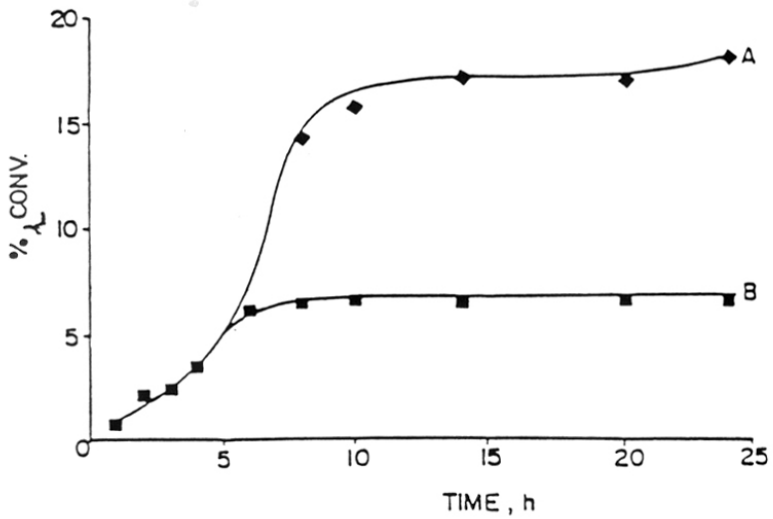

Fig.2 Kinetics of cyclohexane oxidation in the presence of $CuCl_{16}$Pc-Na-X (0.28) {curve A} and when the catalyst is removed from the reaction mixture at 6h reaction time {curve B}.

of 6 h (curve B, Fig. 2). While the conversion of cyclohexane proceeded further in the presence of the solid catalyst (curve A, Fig. 2), there was no further conversion of cyclohexane when the catalyst was removed from the reaction system (curve B, Fig. 2). This indicates that : (1). the solid catalyst is essential for the oxidation of cyclohexane; (2). oxidation of cyclohexane by free metal complex or dissolved copper complexes leached out from the zeolite matrix is negligible. This conclusion was independently

confirmed by the analysis of the reaction products for copper (by atomic absorption spectroscopy). The absence of copper in the filtrate was confirmed; (3). in the absence of the catalyst, molecular oxygen as well as TBHP are unable to oxidize cyclohexane to any significant extent. In independent experiments carried out in the absence of the catalyst, the conversion of cyclohexane under otherwise identical experimental conditions to those of Fig. 2, was about 0.6 % mole. When TBHP was used as the oxidant, the cyclohexane conversion in the absence of the catalyst was only 0.5 % mole. The zeolites alone, without the encapsulated metal complexes, were also catalytically inactive. Thus, we may conclude, that the oxidation of cyclohexane reported in the present study, are indeed catalyzed by the metal complexes encapsulated in the zeolite matrix.

The results of the oxidation of cyclohexane using O_2 as the oxidant and TBHP as the initiator (2 % by weight) and acetonitrile as the solvent at 343 K over the various copper, iron, cobalt, nickel and aluminium phthalocyanines both in the neat and in the encapsulated states are presented in Table-3. The following points may be noted : (1). The unsubstituted metal phthalocyanines have a low activity; only cyclohexanol and cyclohexanone are formed. (2). Copper, cobalt and iron phthalocyanines containing electron withdrawing groups (like -Cl or -NO_2) were most active, by an order of magnitude, than their non-substituted analogs. The electron withdrawing groups enhance the electrophilic character of the active oxygen species and consequently its reactivity. This is comparable with what is reported in literature for porphyrins.[35] (3). The intrinsic catalytic activity (turnover number, TON = moles of cyclohexane converted per mole of copper) of the neat chloro complexes of iron, copper and cobalt are of similar magnitude.

Table-3

Oxidation of cyclohexane with O_2 over phthalocyanines

Catalyst	TON	Products (%)				
		A	B	C	D	Others[1]
CuPc	0.036	70.0	30.0	-	-	-
CoPc	0.050	41.6	58.4	-	-	-
$CuCl_{16}Pc$	1.15	37.7	44.2	6.9	7.2	4.0
$Cu(NO_2)_4Pc$	0.31	46.1	53.9	-	-	-
$FeCl_{16}Pc$	1.02	38.5	41.0	5.0	13.4	2.1
$CoCl_{16}Pc$	1.30	13.5	53.6	6.0	23.9	3.0
$NiCl_{16}Pc$	0.15	47.6	-	-	-	52.4
$AlCl_{16}Pc$	0.08	-	-	-	-	100
$CuCl_{16}Pc$-Na-X (0.28)	1342.4	28.1	48.5	7.0	16.4	-
$CuCl_{16}Pc$-Na-Y (0.11)	3246.1	30.2	48.3	12.7	8.8	-
$CuCl_{16}Pc$-K-L (0.10)	1101.6	72.7	22.7	-	-	4.6
$Cu(NO_2)_4Pc$-Na-X (0.14)	1056.3	78.9	21.2	-	-	-
$FeCl_{16}Pc$-Na-X (0.16)	1568.8	33.0	47.8	7.8	11.4	-
$CoCl_{16}Pc$-Na-X (0.27)	1472.3	19.4	51.1	8.8	20.7	-
No Catalyst	0	-	-	-	-	100

Reaction conditions : cyclohexane = 15 g; catalyst wt = 0.75 g; reaction time = 8 h; Temp = 343 K; solvent = acetonitrile = 45 g; A = cyclohexanol; B = cyclohexanone; C = valeraldehyde; D = adipic acid; [1]Others = mainly succinic and glutaric acids. TON = moles of cyclohexane converted per mole of copper in the catalyst. Air = 800 psi; TBHP = 0.40 g.

(4). It may be noted that though the neat complexes are more active than their encapsulated analogs (for e.g. the cyclohexane conversions using $CuCl_{16}Pc$ and $CuCl_{16}Pc$-

Na-X (0.28) were 17.2 and 14.9 % wt; and using $Cu(NO_2)_4Pc$ and $Cu(NO_2)_4Pc$-Na-X (0.14) were 6.5 and 5.7 % wt) on a weight basis, the catalytic efficiency of the encapsulated catalysts (in terms of activity per copper atom) is higher than that of the neat complexes. This is, probably, due to the isolation of the copper sites in the zeolite cavities (5). The central transition metal of the phthalocyanine complex is, the seat of the catalytic activity. $Cl_{16}Pc$ or phthalocyanines of non-transition metals (like Al) had negligible oxidation activity (The conversion of cyclohexane using $Cl_{16}Pc$ as the catalyst was 0.5 % wt). (6). Glutaric and succinic acids were not detected on encapsulation of the neat $CuCl_{16}Pc$, $CoCl_{16}Pc$ or $FeCl_{16}Pc$ complexes in the supercages of zeolites as can be seen from Table-3.

Even though cyclohexane could be oxidized over the above catalysts (Table-3) using air alone, the conversion levels were below 3 %. There is, hence, a synergistic enhancement in TON when both O_2 and TBHP were used as the oxidants. Since there is a direct dependence of cyclohexane conversion levels on TBHP, the reaction is probably, of a radical nature. When cyclohexane is oxidized over $CuCl_{16}Pc$-Na-X (0.28) in the absence of O_2, substituting N_2 for air under otherwise identical conditions of Table-3, the TON was 9.2 instead of 1342.4 (Table 3, row 9). The concentration of cyclohexanol and cyclohexanone in the products was 57.1 and 42.9 % wt, respectively.

The kinetics of oxidation of cyclohexane using $CuCl_{16}Pc$-Na-X (0.28) as the catalyst is illustrated in Fig. 3. Cyclohexanol and cyclohexanone were the major products at lower conversion levels and residence times. When the reaction is continued beyond 14 h significant amounts of adipic, glutaric and succinic acids start appearing in the reaction mixture. At 48 h, there is almost complete conversion of the cyclohexanol and cyclohexanone to adipic and other acids. In independent experiments carried out,

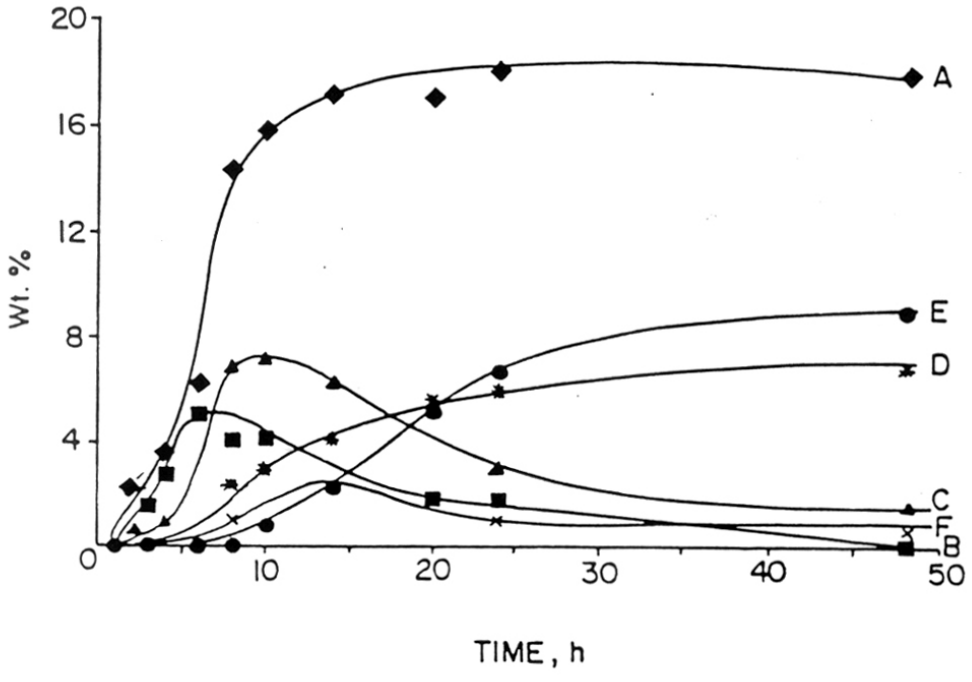

Fig. 3 Kinetic plots for the oxidation of cyclohexane using $CuCl_{16}Pc$-Na-X (0.28) as the catalyst; cyclohexane = 15 g; catalyst wt = 0.75 g; Temp = 343 K; solvent = acetonitrile = 45 g; Air = 800 psi; TBHP = 0.40 g. Curves A-F indicate cyclohexane conversion (A), and the yields of cyclohexanol (B), cyclohexanone (C), adipic acid (D), glutaric plus succinic acids (E) and valeraldehyde (F).

where cyclohexanol or cyclohexanone were taken as the substrates, there was conversion of the above substrates to acids.

The catalytic nature of the reaction is confirmed by the data in Fig. 4 which illustrates the influence of catalyst weight on cyclohexane conversion and product distribution. Cyclohexane conversion is negligible in the absence of any catalyst and no oxidation products are formed. The conversion increases linearly with increase in catalyst concentration (Fig. 4) and levels off beyond 2 g. The presence of acids is also negligible at lower conversion levels.

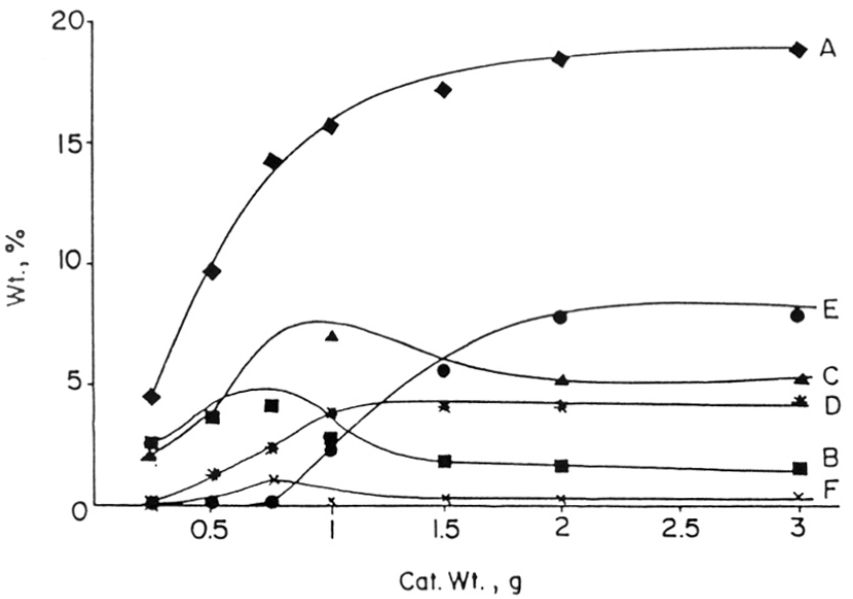

Fig. 4 Influence of catalyst weight on cyclohexane conversion (A) and formation of cyclohexanol, cyclohexanone, adipic acid, glutaric plus succinic acids, and valeraldehyde (mole %, curves B-F, respectively). cyclohexane = 15 g; reaction time = 8 h; Temp = 343 K; solvent = acetonitrile = 45 g; Air = 800 psi; TBHP = 0.40 g.

The influence of temperature on the rate and product distribution (in the oxidation of cyclohexane) is shown in Fig. 5. At high temperatures large amounts of adipic, glutaric

and succinic acids are produced, probably due to the further oxidation of the cyclohexanol formed. Beyond 353 K, there is a gradual decrease in quantity of cyclohexanol in the reaction mixture, but an increase in the acid concentration in the products.

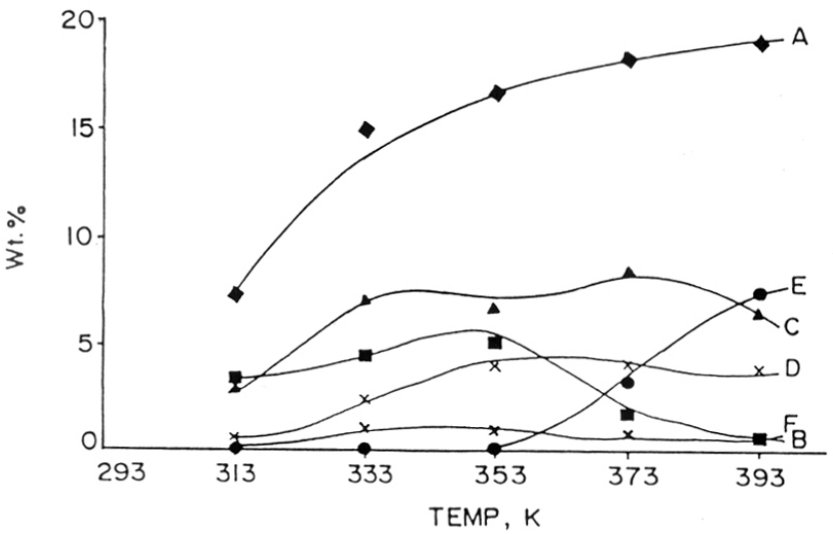

Fig. 5 Influence of temperature on cyclohexane conversion (A), and formation of cyclohexanol, cyclohexanone, adipic acid, glutaric plus succinic acids and valeraldehyde (mole %, curves B-F, respectively); catalyst weight = 0.75 g. cyclohexane = 15 g; reaction time = 8 h; solvent = acetonitrile = 45 g; Air = 800 psi; TBHP = 0.40 g.

Fig. 6 shows a typical GC chromatogram of the products of the oxidation of cyclohexane. The unesterified upper and lower layers of the reaction mixture are shown in Figs. 6A and

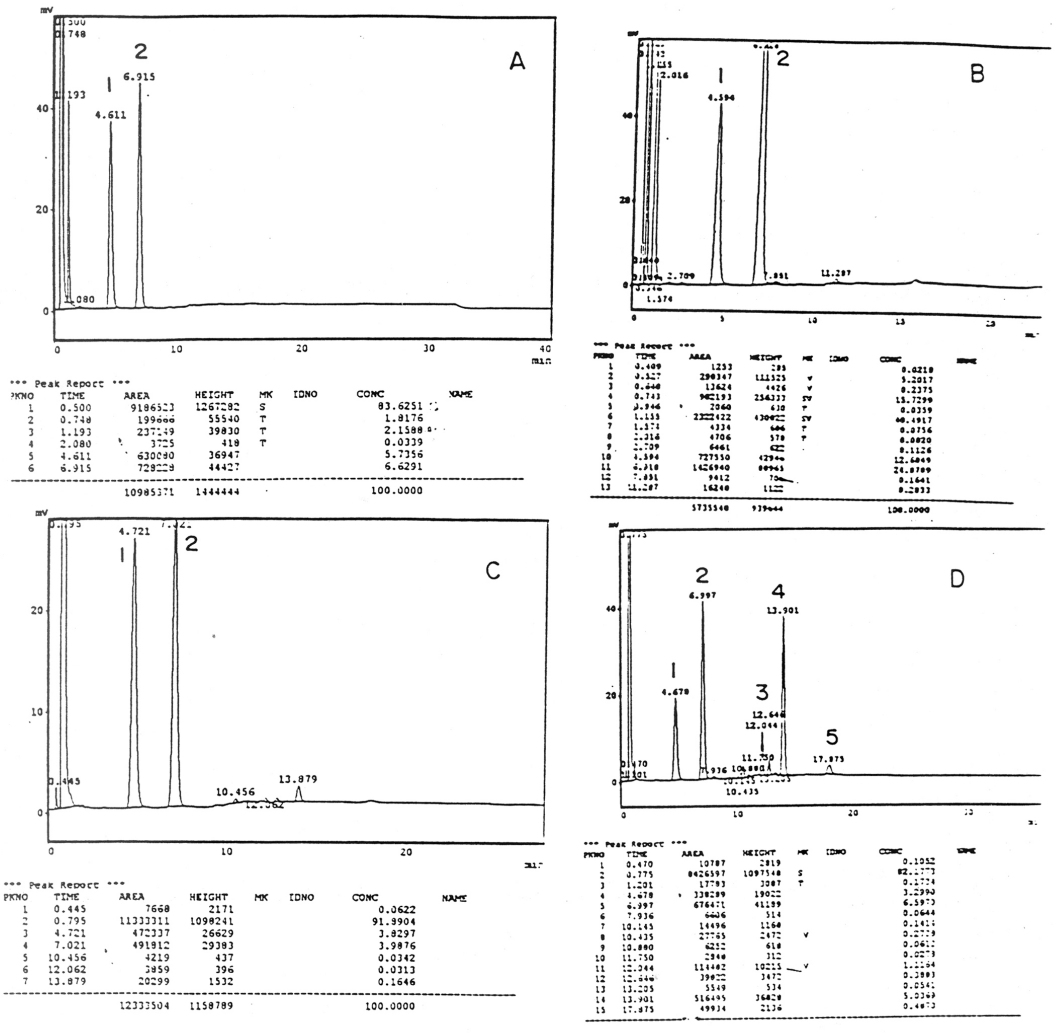

Fig. 6 GC chromatograms of the products of the oxidation of cyclohexane. Chromatograms A and B represent the reaction mixture (upper and lower layers) before esterification, while chromatograms C and D, represent the corresponding esterified samples. The peaks 1-5 represent the products, cyclohexanol, cyclohexanone, valeraldehyde, dimethyl adipate and di methyl succinate, respectively.

6B, respectively, and the corresponding esterfied upper and lower layers of the reaction mixture are shown in Figs. 6C and 6D, respectively. The presence of acids was confirmed *only* on esterification of the reaction mixture as can be seen from Fig. 6C and 6D, respectively. Without esterification of the reaction mixture, cyclohexanol and cyclohexanone were the primary products as can be seen from Figs. 6A and 6B.

The influence of concentration of the oxidant, TBHP, on cyclohexane conversion and product formation over $CuCl_{16}Pc$-Na-X (0.28) is given in Table-4. The results

Table-4

Influence of Cyclohexane : TBHP ratio

Cyclohexane : TBHB ratio (mole)	TBHP efficiency (%)	TON	Products (% mole)				
			A	B	C	D	Others[1]
1 : 5	35.6	3209.0	1.9	18.5	5.3	32.3	42.0
1 : 2	34.7	3127.2	1.5	25.6	4.6	33.1	35.2
1 : 1	29.5	2657.5	3.0	31.2	2.7	30.1	33.0
2 : 1	52.8	2378.7	7.5	33.7	18.1	19.6	21.1
3 : 1	64.5	1936.3	22.3	41.8	12.1	18.1	5.7
5 : 1	91.0	1639.3	23.0	41.2	12.0	22.0	1.8

The cyclohexane : TBHP ratio was varied by changing [TBHP]. Air was not used as the oxidant; cyclohexane = 15 g; catalyst wt, $CuCl_{16}Pc$-Na-X (0.28) = 0.75 g; reaction time = 8 h; Temp = 343 K; solvent = acetonitrile = 45 g.; A = cyclohexanol; B = cyclohexanone; C = valeraldehyde; D = adipic acid; [1]Others = mainly succinic and glutaric acids. TON = moles of cyclohexane converted per mole of copper in the catalyst.

indicate that for maximum utilization of TBHP in the conversion of cyclohexane (to cyclohexanol, cyclohexanone and adipic acid) and minimum formation of succinic and glutaric acids, the cyclohexane : TBHP (mole) ratio should be kept as high as possible. The formation of acids increased with increasing the concentration of TBHP. At the end of the oxidation reaction, TBHP was converted to tert. butanol. Other singlet oxygen sources like H_2O_2, cyclohexyl hydroperoxide or cumene hydroperoxide readily oxidized cyclohexane even in the complete absence of molecular oxygen as can be seen from Table-5. Large amounts of acids are formed, even at low conversion levels, when H_2O_2 was used as the oxidant. Large amounts of byproducts such as glutaric and succinic acids were

Table-5

Influence of oxidant

Oxidant	TON	Products (% mole)				
		A	B	C	D	Others[1]
TBHP	1936.3	22.3	41.8	12.1	18.1	5.7
Cumene hydroperoxide	1496.0	13.2	19.2	7.2	29.5	30.9
H_2O_2	817.8	13.2	20.8	21.9	3.3	40.8
Cyclohexyl hydroperoxide	2454.4	7.0	44.8	3.3	18.4	26.5

Air was not used as the oxidant; catalyst wt, $CuCl_{16}Pc$-Na-X (0.28) = 0.75 g; reaction time = 8 h; Temp = 343 K; solvent = acetonitrile = 45 g; cyclohexane : oxidant = 3 : 1. A = cyclohexanol; B = cyclohexanone; C = valeraldehyde; D = adipic acid; [1]Others = mainly succinic and glutaric acids. TON = moles of cyclohexane converted per mole of copper in the catalyst.

formed when cumene hydroperoxide, H_2O_2 or cyclohexyl hydroperoxide were used as the oxidants.

The effect of solvents on the oxidation of cyclohexane using O_2 as well as TBHP as the oxidants is illustrated in Tables 6 and 7. The conversion was the highest when pyridine

Table-6

Effect of solvent using $CuCl_{16}$Pc-Na-X (0.28) and O_2

Solvent	TON	Products (% mole)				
		A	B	C	D	Others1
Pyridine	1612.0	7.8	44.1	1.1	16.7	30.3
Acetic acid	1560.0	17.9	20.2	11.5	15.6	34.8
Acetonitrile	1342.4	28.1	48.5	7.0	16.4	-
Methanol	1145.6	18.1	32.2	-	41.1	8.6
Ethanol	881.6	56.1	25.5	-	-	18.4
Methyl Ethyl Ketone	876.0	61.8	7.2	-	21.6	9.4
Water	651.2	38.8	26.3	-	9.7	25.2

cyclohexane = 15 g; catalyst wt, $CuCl_{16}$Pc-Na-X (0.28) = 0.75 g; reaction time = 8 h; Temp = 343 K; solvent = 45 g; A = cyclohexanol; B = cyclohexanone; C = valeraldehyde; D = adipic acid; [1]Others = mainly succinic and glutaric acids. TON = moles of cyclohexane converted per mole of copper in the catalyst. Air = 800 psi; TBHP = 0.40 g.

or acetic acid were used as the solvents. However, large amounts of succinic and glutaric acids were formed when using these solvents. When acetonitrile was used as the solvent,

there was negligible formation of succinic and glutaric acids. The conversion dropped when water was used as the solvent. Valeraldehyde was not detected when methanol, ethanol, methyl ethyl ketone or water were used as the solvents in the presence of O_2. Irrespective of the type of solvent, higher turnover numbers were observed, when TBHP was used as the oxidant (Table-7).

Table-7

Effect of solvent using $CuCl_{16}$Pc-Na-X (0.28) and TBHP

Solvent	TON	Products (% mole)				
		A	B	C	D	Others1
Acetic acid	2496.8	5.8	17.6	17.6	22.7	36.3
Acetonitrile	1936.3	22.3	41.8	12.1	18.1	5.7
MEK	1803.2	10.0	12.0	37.5	19.5	21.0
Water	1396.8	11.0	11.0	18.7	27.0	32.3

catalyst wt, $CuCl_{16}$Pc-Na-X (0.28) = 0.75 g; reaction time = 8 h; Temp = 343 K; solvent = 45g; A = cyclohexanol; B = cyclohexanone; C = valeraldehyde; D = adipic acid; [1]Others = mainly succinic and glutaric acids. TON = moles of cyclohexane converted per mole of copper in the catalyst; Cyclohexane : TBHP = 3 (mole).

The influence of site isolation of the copper complexes $CuCl_{16}$Pc (Fig. 7A) and $Cu(NO_2)_4$Pc (Fig. 7B) encapsulated in the faujasite structure on the TON of oxidation of cyclohexane using O_2 as the oxidant clearly indicates that the isolated metal complex is the active site in the oxidation reactions.

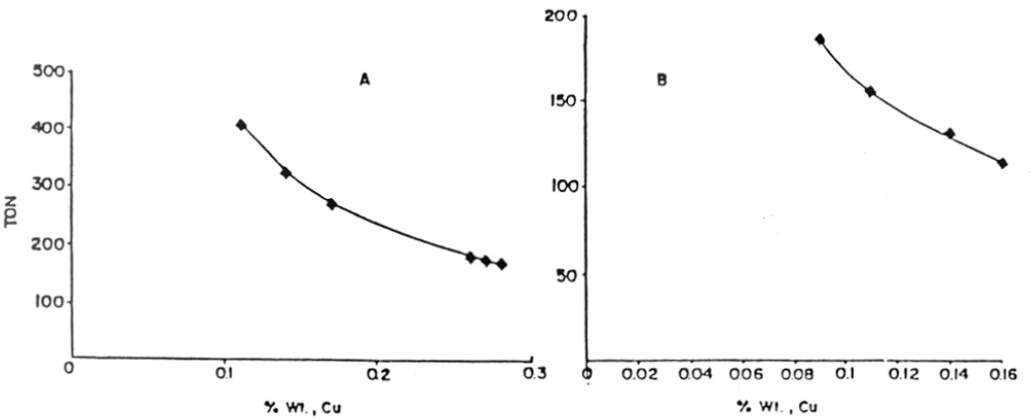

Fig. 7 Influence of site isolation of the copper complexes $CuCl_{16}Pc$ (Fig. 7A) and $Cu(NO_2)_4Pc$ (Fig. 7B) encapsulated in the faujasite structure on the TON of oxidation of cyclohexane.

The probable reaction sequence for the oxidation of cyclohexane is given in Fig. 8. Cyclohexane is first oxidized to cyclohexanol and cyclohexanone. Cyclohexanone is further oxidized to a di-ketone which is the reaction intermediate, before the cyclohexanone cleaves to give adipic acid. The rate of oxidation of this di-ketone to adipic acid is very fast and therefore not observed in the reaction products. Adipic acid cleaves on further oxidation to give glutaric and succinic acids.

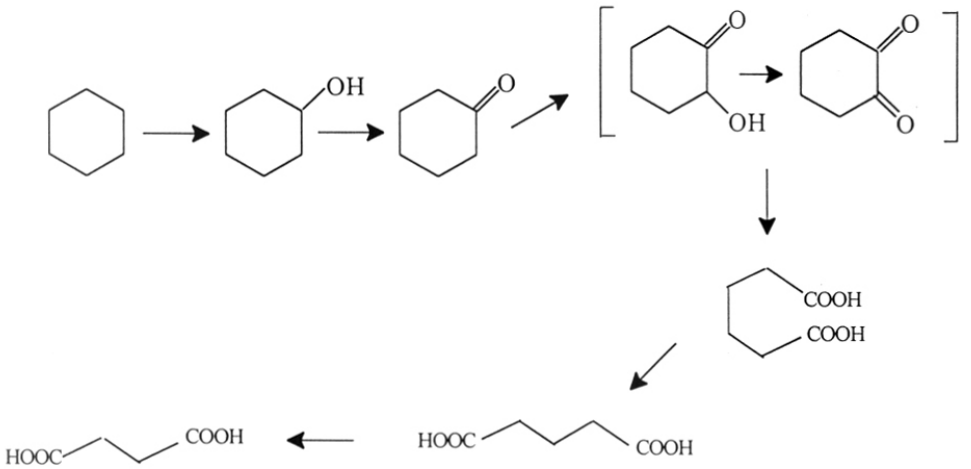

Fig. 8 Reaction sequence for the oxidation of cyclohexane

4.5 Oxidation of methane

Current technology for the conversion of methane to methanol is based on steam reforming or partial oxidation to syngas ($CO + H_2$) followed by methanol synthesis. Although significant advance has been made in conventional syngas technology, there is no escaping the fact that it is first necessary to conduct an energy intensive endothermic steam reforming step followed by a subsequent catalytic conversion which has equilibrium limitations. Hence, worldwide research is underway to oxidize methane in a single exothermic step directly to methanol in high yield. Calculations indicate that the yield of methane by the direct non-catalytic oxidation through gas radical processes is too low to be economically attractive.[36] The catalytic oxidation of methane to methanol at high temperatures has been claimed by many authors.[37-39] However, both conversion and, especially, selectivity values are too low. Typically the selectivity for methanol is below 50 % at a maximum conversion of methane of 5.0 %[37]. CO_2 formation is significant at

high temperatures. Selective oxidation at low temperatures seems to be the only route to avoid excessive formation of CO_2. Such reports of selective, low-temperature (say below 373 K) oxidation are rather limited.[40-42] Periana et al[41] reported the conversion of methane by using stoichiometric quantities of concentrated sulphuric acid to methyl bisulfate, water and SO_2 at 453 K catalyzed by mercuric triflate in triflic acid medium. The molar productivity was 10^{-7} moles ml^{-1} s^{-1} and the turnover number (TON) { based on the catalyst, Hg (II) } was about 3-4 h^{-1}. Since (1) methyl bisulfate can be subsequently hydrolyzed to methanol and sulfuric acid and (2) SO_2 can be oxidized by O_2 to SO_3 and further converted to H_2SO_4 and recycled, the net reaction may be considered as the oxidation of CH_4 to CH_3OH. While the productivity and TON values are a distinct improvement over prior-art results, further work is needed to develop systems which might be able to use molecular oxygen directly and which might work in less corrosive environment.

4.5.2 Catalytic activity

Experimental evidence that the oxidation of methane is indeed catalyzed by the solid zeolite containing the encapsulated complex is presented in Fig.9. In one set of two identical experiments, the solid catalyst was removed by centrifugation at a reaction time of 8 hrs. While the methane conversion continued in the presence of the catalyst (curve A), there was no further conversion of the methane when the catalyst was removed from the reaction system (curve B). This indicates that :

(1). the solid catalyst is essential for the oxidation reaction to occur;

(2). Oxidation of methane by dissolved copper complexes leached out from the solid material is negligible; The latter conclusion was independently confirmed by the absence of copper in the filtrate (atomic absorption spectroscopy) and that

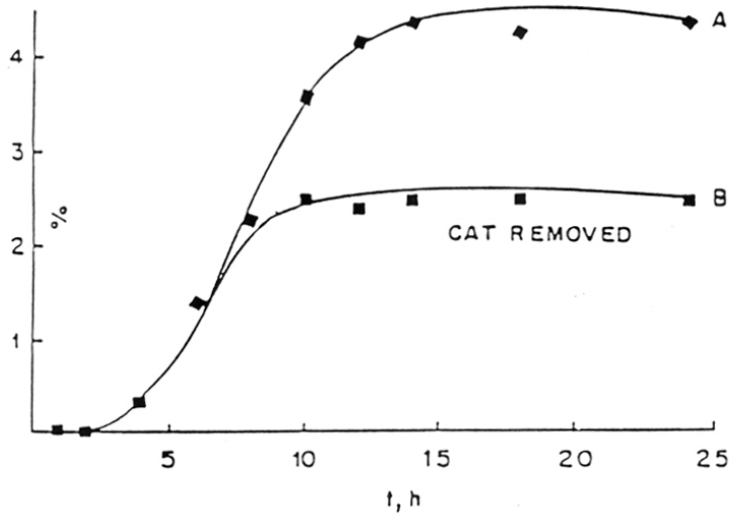

Fig. 9. Kinetics of methane oxidation in the presence of the solid catalyst $CuCl_{16}Pc$-Na-X (0.28) (curve A) and when the catalyst is removed from the reaction mixture at 8 hrs reaction time (curve B).

(3). In the absence of the catalyst, O_2 /TBHP are unable to oxidize methane to any significant extent. In independent experiments carried out in the absence of the catalyst, the conversion of methane was less than 0.1 % mole under otherwise identical conditions of Fig. 9.

The results of the oxidation of methane using O_2 / TBHP as the oxidants and acetonitrile as the solvent at 273 K over the various copper, iron, cobalt and nickel phthalocyanine complexes both in the neat and encapsulated states, are presented in Table-8. The following points may be noted :

(1). The unsubstituted metal phthalocyanines have a low activity

(2). The intrinsic catalytic activity (TON) of the neat chloro complexes of iron, copper and cobalt are of similar magnitude. Nickel chlorophthalocyanine has a low activity.

(3). There is a dramatic increase in turnover number (by more than two orders of magnitude) when the halogenated or nitrated complexes are encapsulated in the cavities of X, Y or L;

(4). The central transition metal of the phthalocyanine complex is the seat of the catalytic activity. $Cl_{16}Pc$ or phthalocyanines of non-transition metals (like Al) had negligible oxidation activity.

Table-8

Methane oxidation
Comparison of catalysts

Catalyst	TON	Products (% mole)			
		CH_3OH	HCHO	HCOOH	CO_2
CuPc	0.09	-	20	-	80
CoPc	0.08	-	-	-	100
$Cu(NO_2)_4Pc$	0.20	-	-	90	10
$CuCl_{16}Pc$	0.72	40.2	47.5	7.2	5.1
$CoCl_{16}Pc$	0.41	10.2	80.5	7.3	2.0
$FeCl_{16}Pc$	0.90	41.2	42.0	8.3	8.5
$NiCl_{16}Pc$	0.07	-	-	-	100
$Cu(NO_2)_4Pc$-Na-X (0.16)	17.7	-	20.5	72	7.5
$CuCl_{16}Pc$-Na-X (0.28)	48.5	51.5	41.7	4.1	2.7
$CuCl_{16}Pc$-Na-Y (0.11)	74.3	53.5	42.5	3.0	1.0
$CuCl_{16}Pc$-K-L (0.10)	32.2	10.7	5.6	62.5	21.2

$CoCl_{16}Pc$-Na-X (0.27)	30.5	12.5	72.2	10.9	4.4
$FeCl_{16}Pc$-Na-X (0.16)	107.2	52.6	42.3	3.2	1.9

Temp, K = 273; Duration, h = 12; Catalyst = 0.75 g; TBHP = 0.5 g; methane = 50 psig; Air = 100 psig; CH_3CN = 99.5 g

(5). There is no apparent direct correlation between CO_2 formation and the extent of conversion of methane. The identity of the catalyst (metal, zeolite type, nature of substituent on the phthalocyanine, etc.) is the predominant factor in the formation of CO_2.

(6). The TON values are higher than most of the values reported, so far.[40,42]

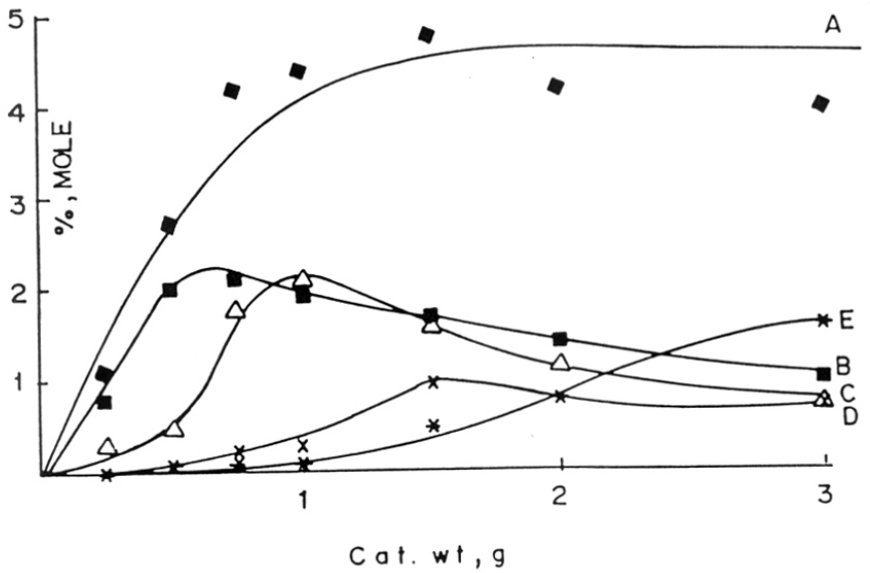

Fig. 10. Influence of catalyst weight on methane conversion (A), and formation of methanol, formaldehyde, formic acid and CO_2, (mole %, B-E, respectively). Temp, K = 273; Duration, h = 12; Catalyst = $CuCl_{16}Pc$-Na-X (0.28); TBHP = 0.5 g; methane = 50 psig; Air = 100 psig; CH_3CN = 99.5 g

The influence of catalyst weight on the reaction is illustrated in Fig.10 for $CuCl_{16}Pc$-Na-X (0.28). The conversion levels off above 1 g of catalyst. However, CO_2 formation increases significantly at high catalyst concentrations.

The kinetics of oxidation of methane is shown in Fig. 11. A surprising feature in Fig. 11 is the significant formation of *both* methanol and formaldehyde even at low conversion levels of methane. This may arise due to (1). the faster rate of oxidation of

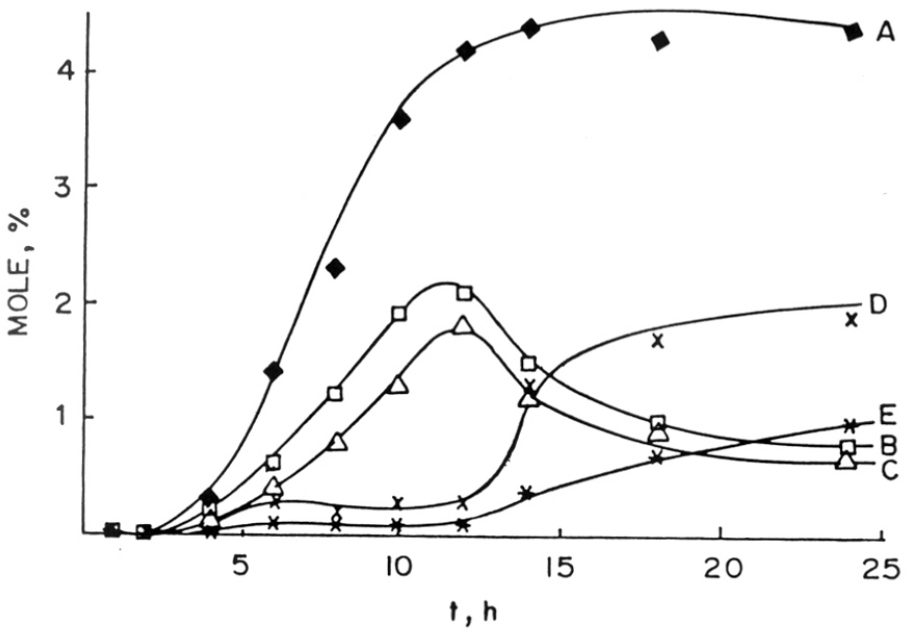

Fig. 11. Kinetic plots for the oxidation of methane over $CuCl_{16}Pc$-Na-X (0.28); Curves A-E indicate methane conversion and the yields of methanol, formaldehyde, formic acid and CO_2 (mole %) formed, respectively. Temp, K = 273; Catalyst = $CuCl_{16}Pc$-Na-X (0.28) = 0.75g; TBHP = 0.5 g; methane = 50 psig; Air = 100 psig; CH_3CN = 99.5 g

methanol to formaldehyde (compared to methane oxidation to methanol) or (2). the direct simultaneous formation of both methanol and formaldehyde from methane. As expected,

the formation of formic acid and CO_2 is enhanced at prolonged contact times (Fig. 11). Another surprising feature of the present catalytic system is the large variation in the formation of CO_2 with the solvent (Table-9). Over $FeCl_{16}Pc$-Na-X (0.16), and at similar conversion levels the

Table-9

Oxidation of methane over $FeCl_{16}Pc$-Na-X (0.16)

Influence of solvent

Solvent	TON	Products (% mole)			
		CH_3OH	HCHO	HCOOH	CO_2
Acetonitrile	57.9	61.7	19.5	18.8	-
Acetic acid	62.4	63.0	10.0	20.2	6.8
Pyridine	66.0	1.5	2.8	75.5	20.2
Water	19.2	15.1	12.5	52.9	19.5

Oxidant = TBHP only; CH_4 : TBHP = 5 : 1 (mole); Temp, K = 273; Catalyst = $CuCl_{16}Pc$ Na-X (0.28) = 0.75g; methane = 50 psig; Air = 100 psig; Solvent = 99.5 g; reaction time = 12 h.

formation of CO_2 was completely suppressed in acetonitrile, while is was significant in acetic acid and excessive in pyridine. The ability to modulate CO_2 selectivity levels by proper choice of solvents is an interesting finding useful in development of a technology for methane conversion. Even though methane could be oxidized over our catalysts using O_2 alone, the conversion levels were below 1 % and CO_2 was the only product. On the

other hand, sources of singlet oxygen like TBHP readily oxidized methane to methanol and formaldehyde even in the complete absence of molecular oxygen. The influence of the CH_4 : TBHP molar ratio on activity and selectivity is shown in Table-10. At low concentrations of TBHP, methanol was the major product. The formation of formic acid and CO_2 increased with increasing concentration of TBHP. At the end of the oxidation reaction, TBHP was converted into tert. butanol. There is a synergistic enhancement in TON when both O_2 and TBHP are used as the oxidants. When methane was oxidized over $CuCl_{16}Pc$-Na-X (0.28) in the absence of O_2, substituting N_2 for air under otherwise identical conditions of Table-8, the TON was 21.5 instead of 48.5 (Table-8, row 9). The concentration of CH_3OH, HCHO, HCOOH and CO_2 in the product were 50.5, 48.2, 1.0 and 0.3 % (mole), respectively.

Table-10

Methane oxidation
Influence of CH_4 : TBHP ratio

Catalyst	CH_4 : TBHP (mole)	TON	Products (% mole)			
			CH_3OH	HCHO	HCOOH	CO_2
$CuCl_{16}Pc$-Na-X (0.28)	5 : 1	50.3	63.2	28.2	8.6	-
	3 : 1	52.7	62.5	24.5	10.0	3.0
	2 : 1	54.2	56.4	19.7	16.4	7.5
	1 : 1	57.5	49.9	10.2	27.2	12.5
	1 : 3	66.6	48.7	8.3	27.5	15.5
	1 : 5	69.8	43.5	6.4	30.1	20.0

$FeCl_{16}Pc$-Na-X (0.16)	15 : 1	9.9	64.0	34.5	1.5	-
	10 : 1	22.2	62.5	33.3	4.2	-
	5 : 1	57.9	61.7	19.5	18.8	-
	2 : 1	62.5	59.5	16.5	14.3	9.7
	1 : 1	70.2	54.1	3.5	28.5	13.9
	1 : 3	73.5	51.2	10.0	26.6	12.2
	1 : 5	77.2	46.6	5.7	29.5	18.2

The CH_4 : TBHP ratio was varied by changing [TBHP]. The amount of CH_3CN + TBHP was kept constant at 100 g. Air was not used as the oxidant; Temp, K = 273; Catalyst = $CuCl_{16}Pc$ Na-X (0.28) = 0.75g; methane = 50 pig; Air = 100 psig; Solvent = 99.5 g; reaction time = 12 h.

4.6 Summary and conclusions

The selective oxidation, with molecular dioxygen as well as TBHP and aqueous H_2O_2, of n-hexane, cyclohexane and methane has been studied. Phthalocyanines of Fe, Cu and Co, wherein all or most of the ring hydrogens have been substituted by electron withdrawing groups like the halogens or nitro groups, when encapsulated in zeolites X, Y, L or ZSM-5, possess high catalytic activity and stability in the selective oxidation of n-hexane, methane and cyclohexane. The integrity of the copper complexes in the cavities of the molecular sieves was confirmed by IR, UV-Vis , ESCA and ESR spectroscopic techniques. An unique feature of halogenated copper phthalocyanines is that they are able to oxidize the C-H bonds of even the primary carbon atoms, including those in the $-CH_3$ groups in normal paraffins, using O_2 as the oxidant. In the case of $FeCl_{16}Pc$-Na-X (0.16)

turnover numbers exceeding 100 (mole/mole) have been obtained in the oxidation of methane (Table-8). These values are amongst the highest reported, so far, for the catalytic oxidation of methane at ambient temperatures. A particularly advantageous feature is that even at these high conversion values, the selectivity for CO_2 was only 1.9 % mole (Table-8). This is the first *solid* catalyst system to exhibit such high activity and selectivity in direct methane oxidation at ambient and sub-ambient temperatures. One distinguishing and unique feature of all the copper-based catalyst systems studied in this Chapter is that the catalyst remains in the solid phase during the entire course of the reaction and can be easily filtered off after the reaction is over, thereby providing significant processing advantages in their large scale application.

4.7 References

1. B.V. Romanovsky, *Proc. Int. Symp. of zeolite catalysis*, Siofok, (1985) 215.
2. "Activation and functionalisation of alkanes", C.L. Hill (Ed)., Wiley (1989).
3. I. Tabushi, *Coord. Chem. Revs.*, **86** (1988) 1.
4. D. Mansuy, *Pure Appl. Chem.*, **59** (1987) 759.
5. J. Green and H. Dalton, *J. Biol. Chem.*, **264** (1989) 17698.
6. R.E. White and M.J. Coon, *Ann. Rev. Biochem.*, **49** (1980) 315.
7. I.C. Gunsales and S.C. Sligar, *Adv. Enzymology.*, **47** (1978) 1.
8. M. Hamburg, B. Samuelsson, I. Bjorkhem and H. Danielsson, in O. Hayaishi (Ed); "*Molecular mechanism of oxygen activation*" Academic Press, New York, (1974) 29.
9. J.T. Groves, T.E. Nemo and R.S. Myers, *J. Am. Chem. Soc.*, **101** (1979) 1032.
10. B.R. Cook, T.J. Reinert and K.S. Suslick, *J. Am. Chem. Soc.*, **108** (1986) 7281.
11. N. Herron and C.A. Tolman, *J. Am. Chem. Soc.*, **109** (1987) 2837.
12. N. Herron, *New. J. Chem.*, **13** (1989) 761.
13. J.E. Lyons, P.E. Ellis Jr. and H.K. Myers Jr., *J. Catal.*, **155** (1995) 59.
14. K.J. Balkus, Jr., A.G. Gabrielov, F. Bedioui and J. Devynck, *Inorg. Chem.*, **33** (1994) 67.
15. D.R. Corbin and N. Herron, *J. Mol. Catal.*, **86** (1994) 343.
16. P.A. Frey, *Chem. Rev.*, **90** (1990) 1343.
17. M. Ingelman-Sundberg, "Cytochrome P-450 - Structure, mechanism and biochemistry" in O. de Montellano (Ed)., Plenum, New York, (1986) pg. 119-160.
18. M.P. Woodland, D.S. Patil, and R. Cammack, *Biochim. Biophys Acta.*, (1986) 2330.
19. K.I. Kivirkko, R. Myllyla and T. Pihalajaniems, *FASEB,* **3** (1983) 1609.
20. J.E. Baldwin, *Heterocycle Chem.*, **27** (1990) 71.
21. D.C. Ziering, R.A. Pascal Jr., *J. Am. Chem. Soc.*, **112** (1990) 834.
22. A. Suga, T. Sugiyama, M. Otsuka, M.Y. Sugiura and K. Maeda, *Tetrahedron*, **47** (1991) 1191.
23. D. Mansuy, *Pure Appl. Chem.*, **62** (1990) 741.
24. M.D. Assis, O.A. Serra, Y. Iamamota and O.R. Nascimento, *Inorg. Chim. Acta.*, **187** (1991) 107.

25. M. Nakamura, T. Tatsumi and H. Tominaga, *Bull. Chem. Soc., Japan*, **63** (1990) 3334.

26. D.E. Danly, C.R. Campbell in H.F. Mark et al (Ed), "Kirk Othmer Encyclopedia of Chemical Technology", 3 rd edition, Wiley, New York, Vol. 1 (1979) pg. 510.

27. D.H.R. Barton, F. Halley, N. Ozbalik, M. Schmilt, E. Young and G. Balavoine, *J. Am. Chem. Soc.*, **111** (1989) 7144.

28. U. Schuchardt, E.V. Spinace and V. Mano, "Dioxygen activation and homogeneous catalytic oxidation" in L.I. Simandi (Ed), Elsevier Science Publishers, B.V. Amsterdam (1991) pg. 41.

29. U. Schuchardt, C.E.Z. Krahembuhl and W.A. Carvalho, "New developments in selective oxidation" in V. Cortes Coberan and S.V. Bellon (Ed)., Elsevier Science Publishers, B.V. Amsterdam (1994) pg. 647.

30. C.A. Tolman, J.D. Druliner, M.J. Nappa and N. Herron, "Activtion and functionalisation of alkanes" Chapter 10, in C.L. Hill (Ed)., New York, Wiley, (1989) pg. 303.

31. M. Ichikawa, T. Kimura and A. Fukuoka, *Stud. Surf. Sci. Catal.*, **60** (1991) 335.

32. P.P. Knops-Gerrits, M.L. Abbe, W.H. Leung, A.M. Van Bavel, G. Langouche, I. Bruynseraede and P.A. Jacobs, *Stud. Surf. Sci. Catal.*, **101** (1996) 811.

33. R.F. Parton, I.F.J. Vankelcom, M.J.A. Casselman, C.P. Bezouhanova, J.B. Utterhoeven and P.A. Jacobs, *Nature*, **570** (1994) 541.

34. K.J. Balkus Jr., M. Eissa and R. Levado, *J. Am. Chem. Soc.*, **117** (1995) 10753.

35. P.E. Ellis Jr. and J.E. Lyons, *Coord. Chem. Rev.* **105** (1990) 181.

36. J.A. Labinger, *Catal. Lett.*, **371** (1988)

37. U.S. Patent 5,220,080.

38. U.S. Patent 5,347,057.

39. U.S. Patent 5,406,017.

40. L.C. Kao, A.C. Hutson and A. Sen, *J. Am. Chem. Soc.*, **113** (1991) 700.

41. R.A. Periana, D.J. Tanbe, E.R. Evitt, D.G. Löffler, P.R. Wertreck, G. Voss and T. Masuda, *Science*, **259** (1993) 340.

42. G.A. Olah, D.G. Parker and N. Yoveda, *Angew. Chem. Int. Ed. Engl.* **17** (1978) 909.

CHAPTER-5

OXIDATION OF AROMATIC HYDROCARBONS

5. Oxidation of Aromatic Hydrocarbons

5.1 Introduction

Selective oxidation of aromatic substrates using solid catalysts, preferably at near-ambient conditions and using *clean oxidants* like O_2 or H_2O_2 is a research area of growing importance in recent years. Both the hydroxylation and ring cleavage of aromatic compounds are of widespread occurrence in nature, whereas such processes are relatively uncommon in the laboratory. Nevertheless, a number of chemical systems which bring about these reactions are known. The best known and most extensively studied system which brings about the hydroxylation of aromatic compounds is the *Fenton's reagent* which consists of ferrous ion and hydrogen peroxide. The essential feature of this system is that the metal ion takes part in the one-electron redox changes with the production of free radicals[1]. According to the Haber-Weiss[2] mechanism, both the hydroxyl radical (· OH) as well as the perhydroxyl radical (· O_2H) are generated as intermediates in aromatic hydroxylations by the Fenton's reagent. Fenton's reagent has been employed for the hydroxylation of both benzenoid[3,4] and heteroaromatic compounds[5]. It was later confirmed[6] that hydroxylation of aromatic compounds is brought about by free hydroxyl radicals (and not those complexed with the metal ion) and the reaction occurs through the formation of an adduct of this radical with the aromatic ring.

Peracids also bring about the oxidation of aromatic compounds and such processes usually involve an electrophilic attack on the ring[7]. The peroxy bond has a tendency to undergo heterolysis, thereby generating an electrophile (OH^+). This would probably account for the greater effectiveness of trifluoro peracetic acid in comparison with other peracids[8]. The electrophilic nature of aromatic oxidation by peracids could be interpreted in terms of the reagent's being an electrophilic radical (·OH) as of its being an electrophile (OH^+).

The *Hamilton-Friedmann*[9] system was first used for the hydroxylation of anisole by hydrogen peroxide in aqueous solution at pH 4, in the presence of catalytic quantities of ferric ion and catechol. Since product patterns are different from that observed with the Fenton's system, it is not the free hydroxyl radicals that bring about the hydroxylation in this system. The ferric ion forms a complex with the phenol and the hydroxylation which is effected catalytically by the complex consists overall of the reduction of the hydrogen peroxide by the aromatics undergoing oxidation ($ArH + H_2O_2 \rightarrow ArOH + H_2O$) and apparently this reaction is facilitated by the ability of the catalyst to provide one electron which it subsequently regains.

Cupric ion, oxygen and morpholine have been used to oxidize phenols to ortho quinone derivatives[10]. Since only cupric ions are effective and only ortho hydroxylation occurs, this system was regarded as a model for tyrosinase. The mechanism for the hydroxylation has a formal similarity to that of the Hamilton system.

Udenfriend and his co-workers[11] have found that aromatic compounds can be hydroxylated by a system comprising of ferrous ion, EDTA, ascorbic acid and oxygen. Here, the hydrogen peroxide is replaced by molecular oxygen, which is reduced to hydrogen peroxide by ascorbic acid. The hydroxylation is brought about by the hydroxyl

radical which is formed by the interaction of H_2O_2 with the ferrous ion[12]. Ascorbic acid, also regenerates the ferrous ion by reducing the ferric ion formed. The role of EDTA is to reduce the oxidation potential of the ferrous-ferric couple. Of all the chemical systems discussed above, the Udenfriend system clearly comes nearest to being a suitable model for biological processes, as it requires molecular oxygen, utilizes an electron donor (ascorbic acid) and involves a transition metal ion.

Eventhough Cytochrome P-450 model systems have been extensively in the oxidation of alkanes,[13-15] very few data is available on the activation of aromatics[16-18] in the open literature. Kimura et al[19], first showed that it was possible to achieve selective hydroxylation of aromatics with Ni (II) polyamines. This monooxygenase model activates coordinating of the oxygen in the complexes, which then selectively attacks aromatic substrates resulting in their hydroxylation. Formation of the oxygen adduct is essential, prior to the oxygenation. Iron and manganese porphyrins bearing halogen substituents on the pyrrole and meso-aryl groups have been used for the oxidation of anisole, naphthalene and phenanthrene using PhIO or H_2O_2 as the oxidants[17]. Chlorinated manganese tetraphenyl porphyrin[18] was effective for the monohydroxylation of aromatic compounds in the presence of N-methyl imidazole, colloidal Pt, O_2 and H_2. Halogenated Fe^{III} tetraphenyl porphyrin selectively oxidized anisole, toluene and naphthalene using PhIO as the oxidant[20]. Most of the above mentioned aromatic hydroxylations have been carried out using the more expensive PhIO or H_2O_2. The use of H_2O_2 is, however, not economically favourable in many oxidation processes and there is still a need for solid catalyst systems capable of utilizing O_2 in selective aromatic hydroxylations.

In this chapter the catalytic properties (in selective oxidation and hydroxylation of aromatic hydrocarbons, like benzene, naphthalene, toluene and ethyl benzene) of copper

tetradecachlorophthalocyanine and copper tetranitrophthalocyanines encapsulated in zeolites Na-X and Na-Y are described. Both molecular dioxygen and aqueous H_2O_2 have been used as the oxidants. The results indicate that copper complexes with appropriately chosen ligands and incorporated in molecular sieves are a novel class of selective catalysts accomplishing both the ring hydroxylation and side chain oxidation of aromatic hydrocarbons.

5.2 Experimental

5.2.1 Materials

The *neat* $CuCl_{16}$ Pc, $CuCl_{14}Pc$, $Cu(NO_2)_4Pc$ and $FeCl_{16}$ Pc (where Pc stands for phthalocyanine) complexes were synthesized according to the procedure reported in Sections 2.2.1 (Chapter-2). CuPc, CoPc and $CoCl_{16}Pc$ complexes were obtained from M/s. Lona Industries, Bombay.

The $CuCl_{16}Pc$, $CuCl_{14}Pc$, $Cu(NO_2)_4Pc$, $FeCl_{16}Pc$ or $CoCl_{16}Pc$ complexes were encapsulated in zeolites NaX and Na-Y and K-L and ZSM-5 as described in Sections 2.2.1, (Chapter-2). NaX and Na-Y samples with varying loadings of $CuCl_{16}Pc$, $CuCl_{14}Pc$, $Cu(NO_2)_4Pc$, $FeCl_{16}Pc$ or $CoCl_{16}Pc$ were prepared similarly.

5.2.2 Procedures

Catalytic Reactions

Detailed procedures of the catalytic reaction using benzene, toluene, ethyl benzene and naphthalene as the substrates are described in Section 2.2.2.1 (Chapter-2).

Product analysis

Detailed description of the procedures of analyses of the products of oxidation of benzene, toluene, ethyl benzene and naphthalene is given in Section 2.2.2.1 (Chater-2).

5.2.3 *Catalyst Characterization*

The physicochemical properties of the catalysts are described in Chapter-3.

5.3 Results and Discussion

5.3.1 *Catalytic Activity*

Table 1 compares the intrinsic catalytic efficiencies of the various complexes and their encapsulated analogs in the oxidation of ethyl benzene and toluene using O_2 as the

Table-1

Oxidation of ethyl benzene (EB) and toluene with air : Comparison of catalysts

S. No.	CATALYST	TON[a]	
		EB	TOLUENE
A	No Catalyst	0.0	0.0
B	$Cl_{14}Pc$	0.0	0.0
C	CuPc	1.64	1.8
D	CoPc	2.65	1.7
E	Cu $Cl_{14}Pc$	19.4	22.5
F	$Cu(NO_2)_4Pc$	10.7	21.3
G	Co $Cl_{14}Pc$	37.2	21.2
H	Fe $Cl_{16}Pc$	16.3	14.26
I	Ni $Cl_{16}Pc$	8.3	2.0
J	Al $Cl_{16}Pc$	0.20	0.40
K1	Cu $Cl_{14}Pc$-Na-Y (0.11)	1838.4	2869.2
K2	Cu $Cl_{14}Pc$-Na-Y (0.17)	1245.0	1905.0
K3	Cu $Cl_{14}Pc$-Na-Y (0.26)	1055.3	1257.3
K4	Cu $Cl_{14}Pc$-Na-Y (0.27)	1050.3	1255.8
L1	Cu $Cl_{14}Pc$-Na-X (0.14)	1437.5	2375.7
L2	Cu $Cl_{14}Pc$-Na-X (0.28)	1036.3	1238.6
M1	$Cu(NO_2)_4Pc$-Na-Y (0.09)	920.7	1981.1
M2	$Cu(NO_2)_4Pc$-Na-Y (0.16)	611.0	1301.1
N1	$Cu(NO_2)_4Pc$-Na-X (0.11)	784.6	1692.3

N2	$Cu(NO_2)_4Pc$-Na-X (0.14)	654.0	1393.1
O	Co $Cl_{14}Pc$-Na-X (0.27)	991.2	790.1
P	Fe $Cl_{16}Pc$-Na-X (0.16)	1209.1	1506.9

Note : 1. [a]TON = turnover number, mole of substrate converted per mole of metal;

2. Reaction conditions : catalyst wt. = 0.75 g; substrate = 15 g; reaction time = 8 h; temp = 348 K; pressure (Air) = 300 psig; solvent (acetonitrile) = 45 g;

oxidant. The following points may be noted from Table 1 :

(1). There was negligible conversion in the absence of any catalyst. For example, the conversion of toluene did not exceed 0.2 % wt even after a prolonged period of reaction under the conditions mentioned in Table 1. Benzaldehyde was the only product. Similarly, the zeolite matrices without their encapsulated transition metal complexes, were also inactive in the oxidation reactions.

(2). The central transition metal of the phthalocyanine complex is, the seat of the catalytic activity. $Cl_{14}Pc$ or phthalocyanines of non-transition metals (like Al) had negligible oxidation activity;

(3). Copper phthalocyanines containing electron withdrawing groups (like -Cl or $-NO_2$) were more active, by an order of magnitude, than their non-substituted analogs.

(4). At similar levels of substitution by chlorine ($CuCl_{14}Pc$, $CoCl_{14}Pc$, $FeCl_{16}Pc$ and $NiCl_{16}Pc$), the intrinsic activities in ethyl benzene (which contains secondary $-CH_2-$ hydrogen atoms) conversion decrease in the order Co > Cu > Fe > Ni. For the oxidation of toluene the corresponding order is Co ≈ Cu > Fe > Ni.

(5). There is a dramatic increase in the turnover number (by two orders of magnitude) when the halogenated or nitrated complexes are encapsulated in the cavities of zeolites Y or X;

(6). The turnover numbers decrease with increasing loading of the zeolite cavities with the metal complex in the case of both $CuCl_{14}Pc$ and $Cu(NO_2)_4Pc$. This phenomenon is observed for both Na-Y and Na-X zeolites.

The detailed product distribution from the oxidation of the various aromatic hydrocarbons over $CuCl_{14}Pc$-Na-Y (0.17), using O_2 or aqueous H_2O_2 as the oxidants, is given in Table 2. Both ring hydroxylation and side chain oxidation of alkyl aromatics are observed in the oxidation of various aromatic substrates over $CuCl_{14}Pc$-Na-Y (0.17) using O_2 or H_2O_2 as the oxidants (Table 2). In the case of benzene oxidation,

Table-2

Oxidation of aromatic hydrocarbons over $CuCl_{14}Pc$-Na-Y (0.17)

Substrate	Oxidant	Conv (%)	Products (% wt)
Benzene	H_2O_2	6.2	Phenol (95); CAT + HQ (5)
	O_2	5.4	Phenol (100)
Toluene	H_2O_2	23.6	ϕ CH_2OH (68.6); ϕ CHO (8.8); ϕ COOH (16.5); Cresols (5.9)
	O_2	22.9	ϕ CH_2OH (4.3); ϕ CHO (15.7) Cresols (80)
Ethyl benzene	H_2O_2	31.6	ϕ $COCH_3$ (19.7); ϕ $CHOHCH_3$ (20.9); ortho + para hydroxy EB (58.6) para hydroxy acetophenone (0.9)
	O_2	16.2	ϕ $COCH_3$ (80.2); ϕ $CHOHCH_3$ (9.27); ortho + para hydroxy EB (4.3)

			ortho + para hydroxy acetophenone (6.2)
Naphthalene	H_2O_2	7.9	α naphthol (7.8); β naphthol (53.6) NQ (1.1); phthalic anhydride (37.4)
	O_2	5.4	β naphthol (100)

Note: Reaction conditions : substrate/H_2O_2 = 3 mole; temp = 348 K; reaction; time = 8 h; solvent (acetonitrile) : 45 g for 15 g of substrate; catalyst : 0.75 g. O_2 (air) as oxidant; NQ = naphthaquinones; See Table 1, experimental for other details.

hydroquinone and catechol are formed by the further oxidation of phenol. In the case of toluene, while ring hydroxylation (to yield cresols) was the predominant reaction when O_2 was used as the oxidant (80 % wt, yield of cresols), the oxidation of the methyl group to benzyl alcohol, benzaldehyde and benzoic acid (total selectivity = 94.1 % wt) predominated with H_2O_2 as the oxidant. When the aromatic substrate molecule contains a secondary -CH_2 group [(as in ethyl benzene) in addition to the aromatic C-H and primary (methyl) C-H bonds (as in toluene)] interesting differences in both reactivity and product selectivity are observed between O_2 and H_2O_2; H_2O_2 being the more reactive oxidant. Moreover, while oxidation of the secondary -CH_2- group (to 1-phenylethanol and acetophenone) is predominant with O_2, ring hydroxylation to hydroxy ethyl benzene is significant with H_2O_2. Similarly, H_2O_2 is the more reactive oxidant of naphthalene. Further, in addition to the primary oxidation product (the naphthols), secondary oxidation proceeds to a significant extent yielding naphthaquinone and phthalic anhydride when H_2O_2 is the oxidant. Beta naphthol was the only product at a relatively low (5.4 % wt) conversion level obtained in the case of O_2. A surprising observation in the oxidation of

naphthalene (Table 3) is the preponderance of the beta rather than the alpha isomer among the naphthol products. The latter would have been the predominant species if the attacking moiety had been a simple electrophilic cation (like HO^+, for example). Molecular modeling calculations explain this surprising (namely, selectivity for the beta rather than the alpha naphthol) feature. The molecular model for naphthalene oxidation using $CuCl_{14}Pc$ encapsulated in faujasites is shown in Fig.1. The naphthalene molecule enters the faujasite structure with its β position towards the metal complex. Since it is the β position that comes into contact with the active metal centre, the preponderance of the β naphthol (rather than the α isomer) in the products is understandable.

Table-3

Oxidation of naphthalene with H_2O_2 over phthalocyanines

Catalyst	Temp	Naphth.	Products (%) wt			
	(K)	Conv. (%)	A	B	C	D
	353	3.1	1.8	0.7	0.3	0.2
$CuCl_{14}Pc$	363	5.6	2.1	1.8	0.8	0.9
	373	7.2	4.2	1.7	0.5	0.6
$CuCl_{14}Pc$-Na-Y (0.26)	373	6.8	3.8	2.0	0.7	0.2
$CuCl_{14}Pc$-Na-X (0.28)	373	7.1	4.6	1.1	0.9	0.3

Reaction conditions : naphthalene = 15 g; naphthalene/H_2O_2 = 3 mole; acetonitrile = 15 g; reaction time = 8 hrs; A = beta naphthol; B = alpha naphthol; C = naphthaquinones; D = phthalic anhydride.

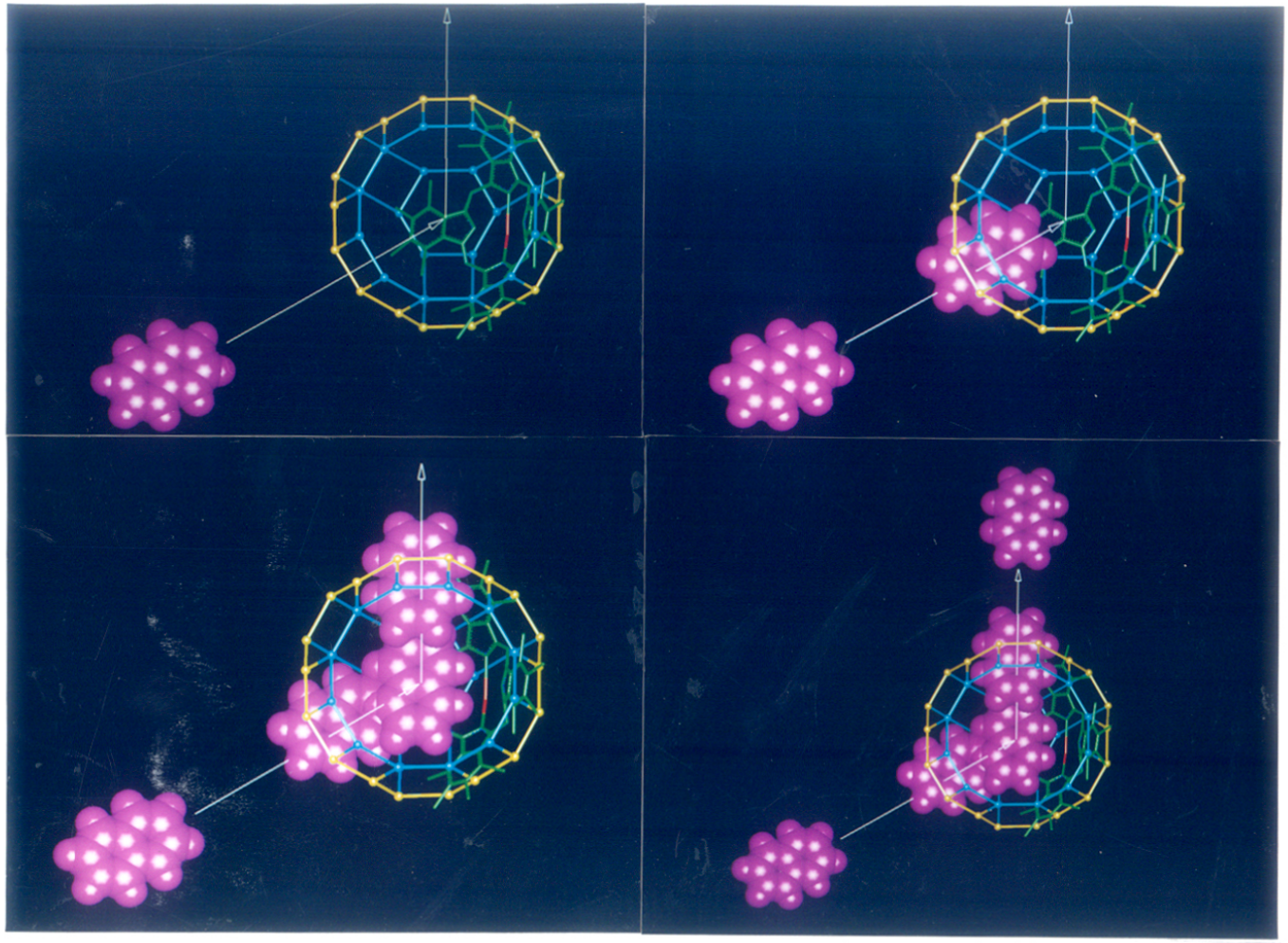

Fig.1 Molecular model of naphthalene oxidation using $CuCl_{14}Pc$ encapsulated in faujasites

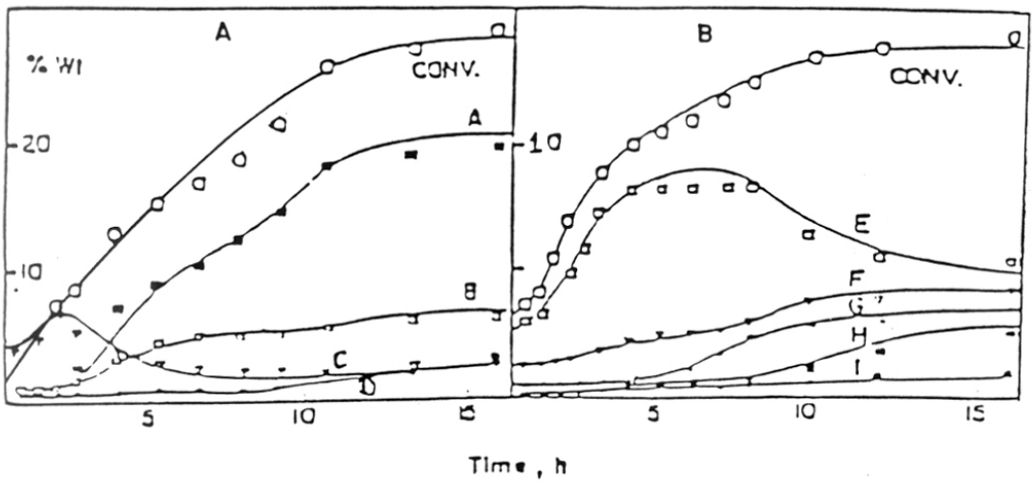

Fig.2 Kinetics of oxidation of toluene A) and ethyl benzene (B) with air over $CuCl_{14}$Pc-Na-Y (0.17); catalyst wt. = 0.75 g; substrate = 15 g; temp = 348 K; pressure (Air) = 300 psig; solvent (acetonitrile) = 45 g; CONV = substrate conversion; Curves A-I refer to p-cresol (A), benzaldehyde (B), o-cresol (C), benzyl alcohol (D), acetophenone (E), 1-phenylethanol (F), p-hydroxy acetophenone (G), p-hydroxy ethyl benzene (H), and (o-hydroxy acetophenone plus o-hydroxy ethyl benzene (I), respectively. See Experimental for reaction conditions

The kinetics of oxidation of toluene and ethyl benzene with O_2 (air) over $CuCl_{14}$Pc-Na-Y (0.17) is illustrated in Fig. 2. Even though the formation of o-cresol (from toluene) is significant at low (below about 5 %) levels of conversion, the fraction of p-cresol increases steadily with conversion and is the predominant product above a conversion level

of 15 %. It may be noted here that higher yield of p-cresol (rather than the ortho isomer) was observed even in the case of the *neat* complex, $CuCl_{14}Pc$. Hence, the higher para selectivity of the encapsulated complex is not due to the shape selectivity of the zeolite matrix and is an inherent property of the copper phthalocyanine complex itself. Acetophenone is the major product of oxidation of ethyl benzene. It is oxidized further to p-hydroxy acetophenone at higher (above 20 %) conversion levels.

Solvents exert a major influence on product distribution (at similar conversion levels) in the oxidation of toluene (Table 4). While ring hydroxylation predominates over

Table-4

Oxidation of toluene over $CuCl_{14}Pc$-Na-Y (0.17) using O_2 as the oxidant

Influence of solvent

Solvent	Toluene	Products (% wt)				
	Conv (%wt)	ϕCH_2OH	ϕ CHO	ϕ COOH	o-cresol	p-cresol
Acetonitrile	22.9	4.3	15.7	-	4.5	75.5
CCl_4	18.1	12.1	36.5	10.5	6.1	34.8
t-butanol	23.6	10.6	21.2	8.9	6.8	52.5
Acetone	15.4	29.2	46.7	-	1.9	22.2
Methanol	18.8	20.7	32.4	6.4	3.7	36.7

catalyst wt. = 0.75 g; substrate = 15 g; temp = 348 K; reaction time = 8 h; pressure (Air) = 300 psig; solvent = 45 g; See Table-1 for reaction conditions

acetonitrile and t-butanol, side-chain oxidation is significant in the case of CCl_4, acetone and methanol. The isolated metal complex is the active site in the oxidation reactions (Fig.3). At low loadings of the metal complex in the zeolite, the active sites are well isolated leading to a higher TON. As the loading is increased, the TON decreases. At high loadings there is no site isolation leading to a lower TON.

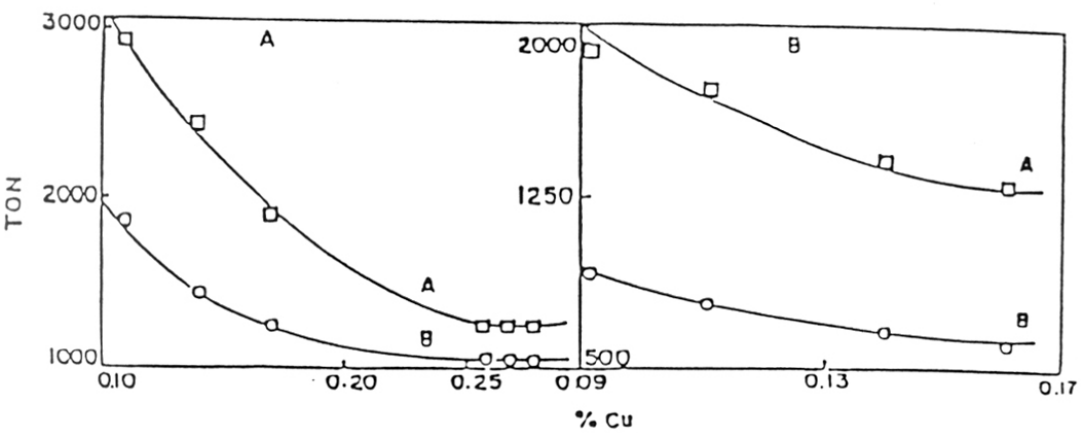

Fig. 3 Influence of site isolation of the copper complexes $CuCl_{14}Pc$ (A) and $Cu(NO_2)_4Pc$ (B) in the faujasite structure on the TON of oxidation of toluene (A) and ethyl benzene (B) in the presence of O_2. The TON values are from Table-2.

5.4 Summary

The selective, low temperature oxidation of benzene, toluene, ethyl benzene and naphthalene over chloro- and nitro substituted phthalocyanine complexes of copper encapsulated in zeolites X and Y, using molecular oxygen as well as aqueous H_2O_2 as the oxidants, has been studied. The integrity of the copper complexes in the supercage of the faujasite zeolites was confirmed by IR, UV-Vis , ESCA and ESR spectroscopic techniques. The catalytic efficiency (turnover numbers) of the copper atoms are higher in the encapsulated state compared to that in the *neat* copper phthalocyanines. The isolated metal complex is the active site in the oxidation of aromatic hydrocarbons. While benzene was oxidized to phenol, both ring hydroxylation as well as side chain oxidation were observed in the case of alkyl aromatics such as toluene. Ethyl benzene was oxidized to acetophenone and 1-phenylethanol in the presence of molecular oxygen, while ring hydroxylation products (ortho and para hydroxy ethyl benzene) were observed when H_2O_2 was used as the oxidant. β naphthol was the major product in the oxidation of naphthalene, using O_2 as the oxidant. Chloro- and nitro substituted complexes of copper, cobalt and iron encapsulated in molecular sieves are promising, selective catalysts for the oxidation and hydroxylation of aromatics.

5.5 References

1. W.G. Barb, J.H. Baxendale, P. George and K.R. Hargrave, *Trans. Faraday Soc.*, **47** (1951) 462.

2. F. Haber and J. Weiss, *Proc. Royal Soc. (London),* **A147** (1934) 332.

3. J.H. Merz and W.A. Waters, *J. Chem. Soc.*, (1949) 2427.

4. A. Cier and C. Nofre, *Bull. Soc. Chim., France* (1959) 1523.

5. R.O.C. Norman and G.K. Radda, "Free radical substitutions of heteroaromatic compounds," in A.R. Katritzky, Ed., Advances in Heterocyclic Chemistry, Vol. 2, Academic Press, New York, 1963 p. 167.

6. J.R. Lindsay Smith and R.O.C. Norman, *J. Chem. Soc.,* (1963) 2897.

7. I.M. Roitt and W.A. Waters, *J. Chem. Soc.,* (1949) 3060.

8. R.D. Chambers, P. Goggin and W.K.R. Musgrave, J. Chem. Soc., (1959) 1804.

9. G.A. Hamilton and J.P. Friedmann, J. Am. Chem. Soc., 85 (1963) 1008.

10. W. Brackman and E. Havinga, Res. trav. Chim., 74 (1955) 937.

11. S. Udenfriend, C.T. Clark, J. Axelrod and B.B. Brodie, J. Biol. Chem., 208 (1954) 731.

12. R.C. Krueger, Federation Proc.,

13. J.T. Groves, T.E. Nemo and R.S. Myers, *J. Am. Chem. Soc.*, **101** (1979) 1032.

14. J.E. Lyons, P.E. Ellis Jr. and H.K. Myers Jr., *J. Catal.*, **155** (1995) 59.

15. C.A. Tolman, J.D. Druliner, M.J. Nappa and N. Herron, "Activtion and functionalisation of alkanes" Chapter 10, in C.L. Hill (Ed)., New York, Wiley, (1989) pg. 303

16. S.V. Barkanova, V.M. Derkacheva, O.V. Dololova, V.D. Li, V.M. Grimovsky, O.L. Kaliya and E.U. Lukyanets, *Tett. Lett.,* 37 (10) (1996) 1637.

17. M. Carrier, C. Scheer, P. Goouvine, J. Bartoli, P. Battioni and D. Mansuy, *Tett. Lett.,* 31 (1990) 6645.

18. I. Tabushi and K. Morimitsu, *Tett. Lett.*, 27 (1986) 51.

19 E. Kimura and R. Machida, *J. Chem. Soc. Chem. Commun.*, (1984) 499.

20. J.R. Lindsay Smith and P.R. Sleath, *J. Chem. Soc. Perkin Trans. II*, (1982) 1009.

CHAPTER-6

OXIDATION OF PHENOLS

6.0 Oxidation of Phenols

Phenols were oxidized over two catalyst systems based on copper : (1). dimeric copper acetate complexes encapsulated in zeolites Na-Y, MCM-22 and VPI-5 and (2). copper phthalocyanines encapsulated in zeolites X, Y and ZSM-5.

6.1 Oxidation over copper acetate-based catalysts

6.1.1 Introduction

Copper dioxygen coordination chemistry is an exciting area of research. While a great deal is known concerning the binding and activation of molecular oxygen (dioxygen) by hemoproteins and porphyrin containing metal complexes,[1-2] the chemistry of related processes using non-heme iron or copper proteins and complexes is considerably less

developed. The ability of heme enzymes to incorporate oxygen atoms from molecular oxygen into organic substrates (oxygenase activity) and to use H_2O_2 and other peroxides to oxidize substrates (peroxidase activity) illustrates the catalytic versatility of heme-containing enzymes. Both synthetic and natural complexes which reversibly bind dioxygen are termed *oxygen carriers*. Interest in catalytic aspects of dioxygen complexes has intensified in recent years.[3-7] In an attempt to prepare analogs of hemoglobin and myoglobin which can reversibly bind O_2, cobalt salen complexes were encapsulated in the supercages of zeolite Y. Such encapsulated complexes formed adducts with dioxygen which were more stable than those formed by the same complex in free solution[8]. Metal complexes or polyamines and related ligands have been successfully employed to promote reactions similar or identical with those promoted in biological systems.[9-12] Apart from their catalytic properties, they also exhibit a wide range of interesting structural and electronic properties, reactivities and stabilities which vary predictably with changes in the ligands employed.

Compared to the wealth of information available on binding and activation of dioxygen by Fe-containing hemoproteins and porphyrin- containing complexes, the chemistry of copper complexes and copper proteins in such processes is known in less detail.[13-15] Tyeklar and Karlin[16] have reported extensive studies on the biomimetic binding and activation of dioxygen by various copper complexes in the homogeneous phase. Copper-containing monooxygenase enzymes, like tyrosinase, (EC 1.14.18.1) reversibly bind O_2 and catalyze two different reactions;[17,18] the hydroxylation of monophenols to o-diphenols (monophenolase activity) and the oxidation of o- diphenols to o- quinones (diphenolase activity) both using molecular oxygen. The active site contains a pair of antiferromagnetically-coupled copper ions[19]. The oxygenated form (oxytyrosinase)

consists of two tetragonal Cu(II) ions each coordinated by two strong equatorial and one weaker axial N_{His} ligand. The exogenous oxygen molecule is bound as peroxide {with a side-on, (μ-η^2-η^2) rather than an end-on (cis-μ-1,2) geometry} and bridges the two copper centres[20]. During hydroxylation, the phenol molecule, coordinates directly to the copper ion, leading to transfer of electron density from the phenol to the Cu ions and weakening of both the O-O and Cu-O bonds. Oxygen transfer to the ortho position in phenol occurs subsequently. The resultant, coordinated catecholate, transfers two electrons to the binuclear cupric site, leading to the dissociative elimination of the o-quinone product and the formation of the deoxy site for further turnover.[21]

In the search for an inorganic mimic of tyrosinase to oxidize phenols the following points were kept in mind : (1) the complex should contain a pair of copper atoms separated by about 2-3 Å, (2) for utilization in industrial applications, it would be preferable if during the oxidation reaction, the binuclear complex of copper remains in the solid state or can be encapsulated in the microcavities of porous solids like zeolites for easy catalyst separation and recycle, (3) the complex should be relatively easy and inexpensive to prepare and rugged to use and (4) the ligands attached to the copper ions should have coordinating properties somewhat similar to the histidine groups in tyrosinase. Neither a heterogeneous solid mimic of tyrosinase nor a molecular sieve containing an encapsulated complex of a transition metal capable of aromatic hydroxylations using O_2 as the oxidant has, so far, been reported in the literature.

In the present section, a novel catalytic system consisting of dimeric complexes of copper acetate located in molecular sieves Y, MCM-22 and VPI-5 which utilize O_2 in the hydroxylation of the aromatic nucleus (in L-tyrosine, phenol and cresols) thereby

mimicking, in a restricted sense, the catalytic properties of the enzyme tyrosinase, is reported.

6.1.2 Experimental

Five solid catalysts were used : (1). solid copper acetate monohydrate (CuAc), and copper acetate encapsulated in (2). Na-Y (designated as Cu-Na-Y), (3). H-Y (designated as Cu-H-Y), (4). MCM-22 (designated as Cu-MCM-22) and (5). in the aluminophosphate molecular sieve VPI-5 (designated as Cu-VPI-5). Details of the synthesis have been described in the earlier section (Section 2.1.1, Chapter 2.). The substrates chosen were monohydroxy aromatic compounds like L-tyrosine, phenol, ortho and meta cresols. Detailed procedures of the catalytic reaction and product analysis are described in Sections 2.1.2 (Chapter 2). The physicochemical chemical properties of the neat copper acetate as well as the encapsulated catalysts are described in Section 3.2 (Chapter-3).

6.1.3 Results and Discussion

6.1.3.1 Catalyst characterization

The catalysts used for the activation of dioxygen in the oxidation of phenols have been characterized using a wide variety of physicochemical techniques as described in Chapter-3.

Catalytic activity

6.1.3.2 Oxidation of L-tyrosine

Typical HPLC chromatograms of the products of the oxidation of L-tyrosine to L-DOPA with O_2 over the solid catalysts are shown in Fig.1 along with their UV spectra. For comparison, the results for the enzyme tyrosinase are also illustrated. The reaction

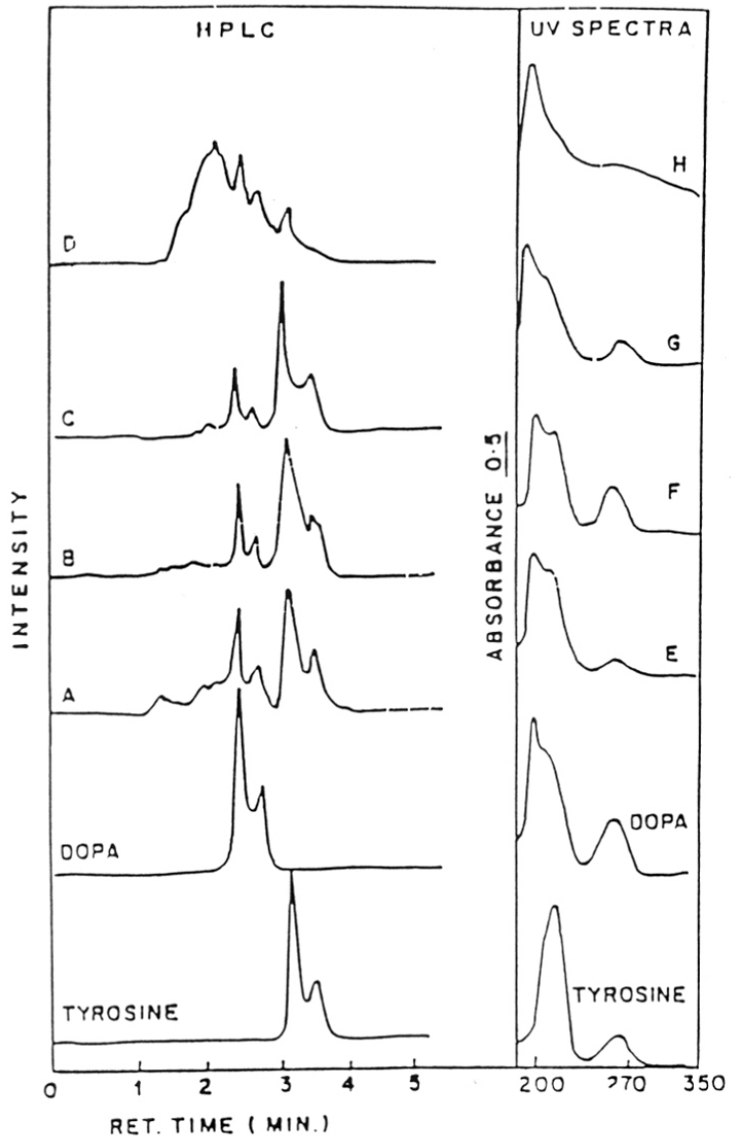

Fig. 1 HPLC chromatograms (left) and UV spectra (right) of the reactant (L-tyrosine) and products (L-DOPA and o-quinones). Curves A-D represent HPLC chromatograms of the products from copper acetate monohydrate (A), Cu-MCM-22 (B), Cu-Na-Y (C), and the enzyme tyrosinase (D), respectively. Curves E-H represent the corresponding UV spectra of the products.

time, at 298 K, was 24 hrs in all cases. The minor (about 22%) peak (at 3.85 min) in the HPLC spectrum of L-tyrosine is due to the presence of D-tyrosine formed by racemisation of the L-isomer in the phosphate buffer even in the absence of any catalyst. The separation of the L- and D-tyrosine over the C_{18} columns (used in the HPLC separation in the present study) has been reported earlier[22]. The D-isomer was also oxidized to D-DOPA (retention time = 2.85 min., Fig.5) under our experimental conditions. The identity of L- and D-DOPA in the products was also confirmed by ^{1}H NMR spectroscopy of the lyophilized samples in D_2O medium. The relative proportions of L-DOPA (and D-DOPA) and quinones in the products varied with reaction conditions like catalyst quantity, reaction time, temperature, O_2 partial pressure, etc. The concentration of the quinones was negligible at low temperatures, low catalyst content or short reaction time. The catalytic activity of the various catalysts are compared in Table 1.

Table-1

Oxidation of phenols (TON[1]) with O_2 over copper acetate-based catalysts at 298 K

Catalyst	TON[1]			
	phenol	o-cresol	m-cresol	L-tyrosine
Cu-Ac	3.76	7.20	5.20	2.85
Cu-Ac-Na-Y	19.71	18.61	21.62	12.90
Cu-Ac-H-Y	22.10	56.42	50.94	15.15
Cu-Ac-MCM-22	35.60	71.5	55.80	27.61
Cu-Ac-VPI-5	20.20	45.73	33.80	10.46

substrate = 4 dM solution in 0.05 M phosphate buffer (pH = 6.5, 10 ml). Catalyst = 0.020 g; Temp = 298 K, pressure (O_2) = 100 psi; reaction time = 24 h; See Experimental for other reaction conditions, TON[1] : moles of substrate converted per mole of copper in the catalyst

All the solid catalysts exhibit both cresolase (tyrosine to L-DOPA) and catecholase (L-DOPA to o-quinones) activities similar to the enzyme tyrosinase[23]. There was neither any conversion of tyrosine in the absence of catalysts nor was there any product other than L-DOPA or the quinones in striking similarity to the behavior of the enzyme. When L-DOPA, instead of L-tyrosine, was taken as the substrate, its further oxidation to the quinones was observed. The influence of catalyst concentration and temperature (Fig.2) further confirms the catalytic nature of the reaction.

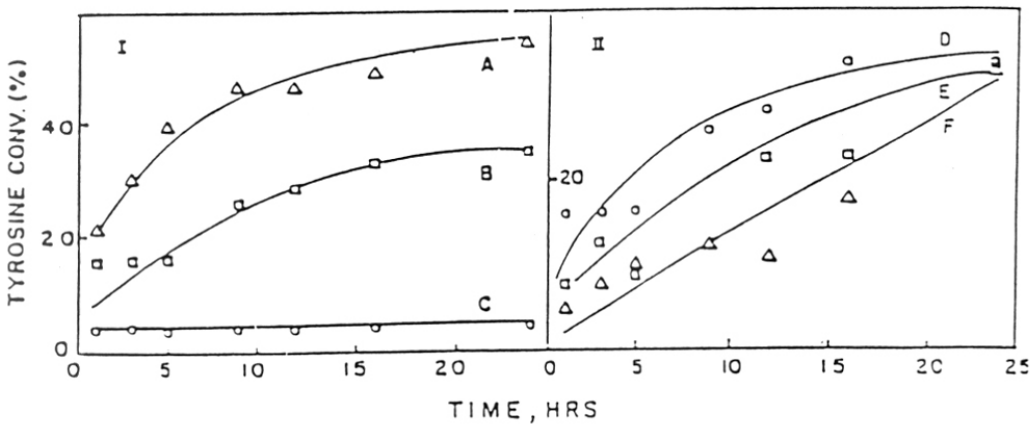

Fig. 2 Kinetic plots for L-tyrosine conversion : Curves A-C represent the influence of catalyst (copper acetate) weight (0.3, 0.2 0.1 g, respectively) at 298 K. Curves D-F illustrate the influence of temperature (298, 313 and 333 K, respectively) with a constant catalyst weight of 0.2 g.

The product with 0.2 g of copper acetate contained relatively more L-DOPA than o-quinones. The quinones were more predominant with larger quantities (0.4 g) of the

catalyst. The product at 298 K (after removal of the catalyst) was colourless. At 313 and 333 K the filtrate was light blue in colour, perhaps, due to the increased solubility of copper acetate in the buffer at these temperatures. In the range of pH = 4.0 to 8.2, L-DOPA production was observed only at pH = 6.5. At this pH, copper acetate is insoluble at 298 K in the buffer (at lower pH values copper acetate dissolves in the reaction mixture) and remains a solid throughout the oxidation reaction. At the start of the reaction, the solid is pale blue in colour which turns pale green on formation of L-DOPA. Cu-Na-Y, Cu-MCM-22 and Cu-VPI-5 also behaved in a similar manner. The pH specificity (as well as the influence of temperature) of the reaction suggests that the copper acetate complex is active only in the solid state where it is present in the dimeric form. When the dimeric structure is absent {as in the dissolved state (lower pH or higher temperatures)}, the complex is inactive.

As in the case of tyrosinase, the presence of ascorbic acid, in addition to averting the initial inhibition period and enhancing tyrosine conversion, reduced the o-quinone formed to L-DOPA (Fig.3) over all the four solid catalysts. In the case of tyrosinase, addition of ancillary reductants like ascorbic acid is known to suppress the induction period and reduce the o-quinones to L-DOPA[18]. The higher conversions obtained in the presence of ascorbic acid under otherwise identical conditions may be understood if the o-quinones were one of the primary products whose further conversion by ascorbic acid (to L-DOPA) *drives* the primary reaction (tyrosine conversion) to a greater extent. It may be mentioned here that there is a controversy in the recent literature[17] whether in the case of the enzyme, tyrosinase-catalyzed oxidations, o-quinones are formed from L-tyrosine in a consecutive manner (via L-DOPA) or are also formed directly as primary products. For a

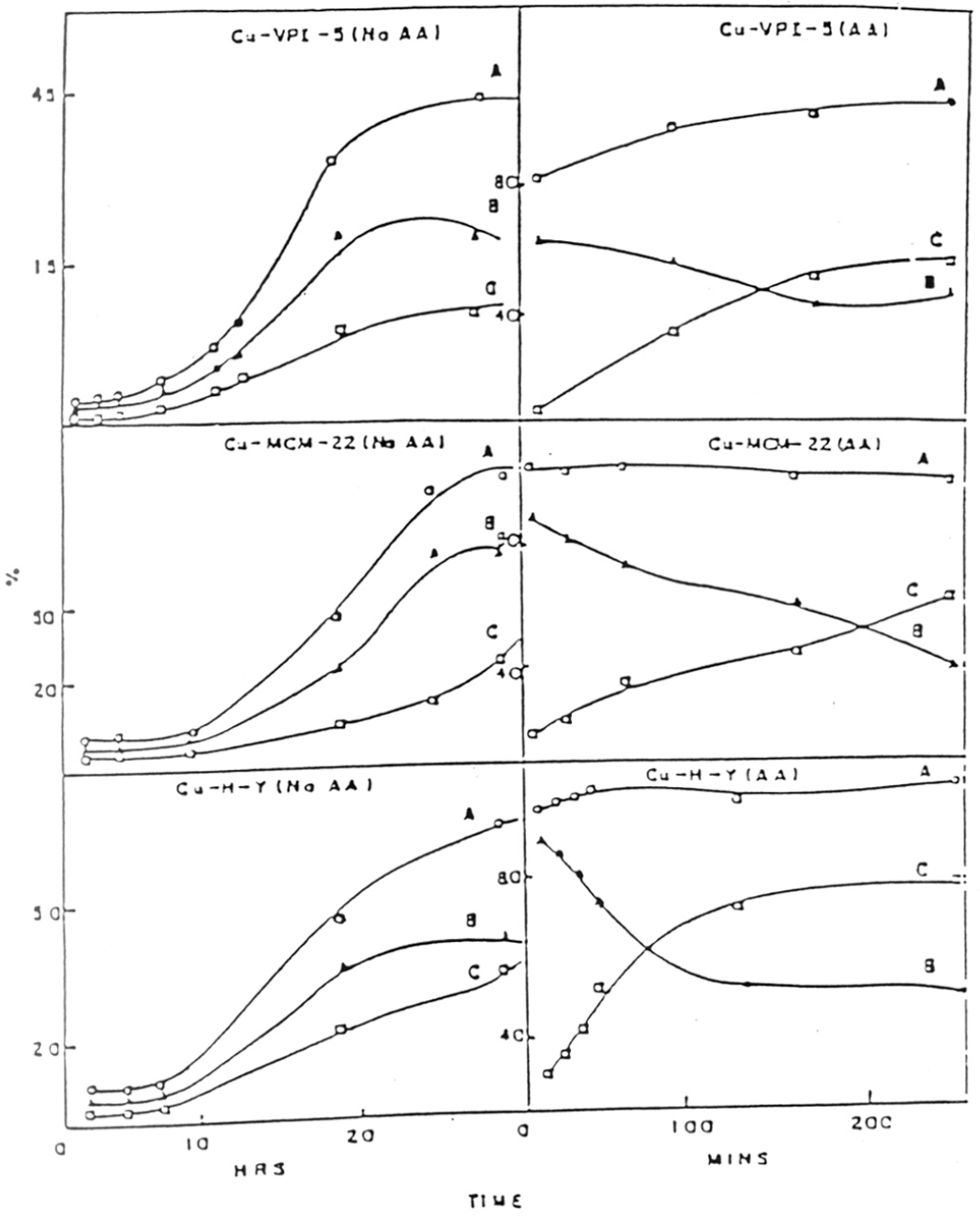

Fig. 3. Influence of ascorbic acid (AA) (0.6 mM) on tyrosine conversion, o-quinone and L-DOPA formation (curves A-C, respectively) at 298 K and 0.4 g of catalyst.

given amount of catalyst, the concentration (in the range 1-4 dM) of L-tyrosine did not affect significantly the rate of hydroxylation.

6.1.3.3 Oxidation of phenols

The specific catalytic activities of the various catalysts are compared in Table 1 for the oxidation of phenol, ortho and meta cresols. In all cases, there is a very significant increase in catalytic efficiency (turnover numbers) on incorporation of the complexes in the microcavities of the molecular sieve. For example, in the oxidation of tyrosine or meta cresol over Cu-MCM-22 (columns A and D, respectively) there is a tenfold increase in the TON when the copper acetate complex is incorporated in the molecular sieve. This increase exemplifies the catalytic advantages arising due to the location of the transition metal complexes in an isolated state inside the cavities of the molecular sieves[24].

The molecular sieve-based catalyst also exhibited a high substrate and regio-specificity; only mono and ortho dihydroxy aromatic compounds (like phenol, catechol and cresols) underwent oxidation though at varying rates.

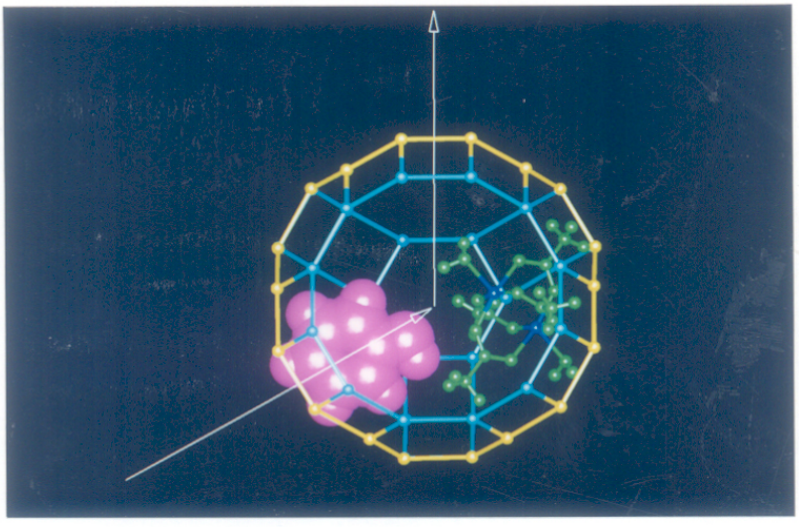

Fig.4 Molecular modeling of phenol in the supercage of faujasite containing the Cu-Ac complex

Aromatic substrates without a phenolic -OH group were not oxidized. Moreover, the monophenols were oxidized always in the ortho position. Oxidation of phenol, for example, yielded only catechol/ o-benzoquinone; hydroquinone/ p-benzoquinone were not observed.

6.1.4 Active Sites

In an effort to identify the nature of the active sites responsible for the ortho oxidation reaction, we have tried to correlate the conversion of the monophenol (from kinetic experiments) with the concentration of the dimeric copper species obtained from the integrated intensity of the seven-line ESR spectra of the dimers. The results (Fig. 5) show that there is, indeed, a linear correlation suggesting the involvement of the copper dimers in the oxidation reaction. It may be mentioned here that these dimers are more

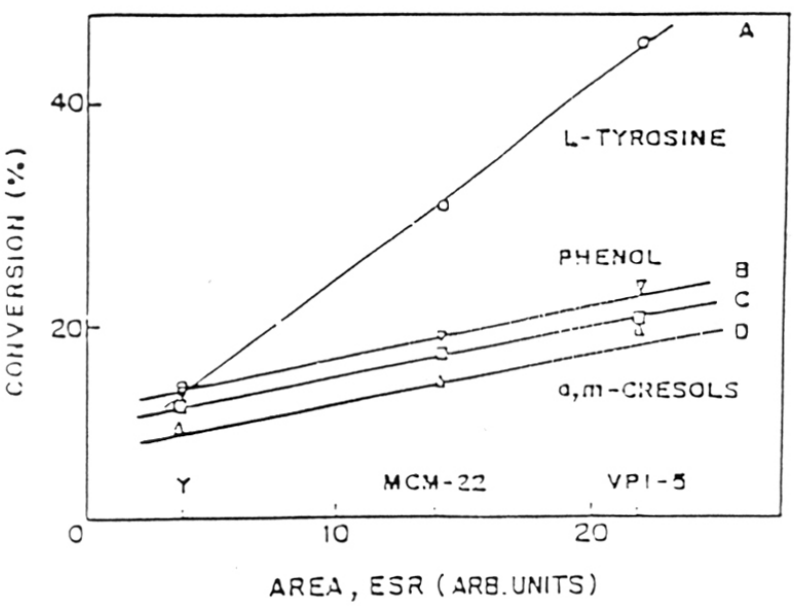

Fig. 5 Correlation between the integrated area of the seven-line ESR spectrum (of Cu-H-Y, Cu-MCM-22 and Cu-VPI-5) and conversion of L-tyrosine, phenol, o-cresol and m-cresol (curves A-D, respectively)

isolated from each other in the molecular sieve matrix than in the *neat* solid state. For example, in Cu-Na-Y, only one in twelve of the unit cells of the Y zeolite contain a dimer of copper acetate. Similarly, in Cu-VPI-5 and Cu-MCM-22 only one in 100 and 30 unit cells, respectively, are occupied by the copper dimer. This physical isolation and dispersion in the molecular sieve matrix is, perhaps, the reason for the higher catalytic efficiency (higher TON) of the molecular sieve-based catalysts compared to the "neat" copper acetate. The similarity of the (1) observed dimeric nature of the copper complex (2) its high substrate specificity (for mono- or diphenols) and (3) high regioselectivity (oxidation of only the position ortho to the phenolic group) to the dimeric copper structure in the enzyme tyrosinase may be noted.

6.2 Oxidation over Copper Phthalocyanine-based Catalysts

6.2.1 Introduction

Selective oxidation of phenols using solid catalysts, preferably at near-ambient conditions and using *clean* oxidants like O_2 or H_2O_2 is a research area of growing importance in recent years. The discovery and commercial utilization of the microporous titanosilicate, TS-1, by Enichem workers[25] for the hydroxylation of phenol with H_2O_2 was a major advance in this area. Hydroquinone and pyrocatechol are obtained with high selectivity. Other efficient catalysts for the hydroxylation of phenols using H_2O_2 as the oxidant, are strong mineral acids or Fenton's reagent producing peroxonium ion and hydroxyl radical, respectively. Metal oxides and carboxylic acids catalyze the reaction of H_2O_2 through the formation of inorganic and organic peracids. Various metal phthalocyanines have been studied as catalysts for the hydroxylation of phenol by H_2O_2[26]. It was found that the metal ion of the catalyst influences both activity and selectivity of the

reaction as well as the distribution of pyrocatechol and hydroquinone. Since H_2O_2 alone is not a hydroxylating agent, catalysts have to be added to make it an oxidizing agent. An active oxidant for the hydroxylation of phenol is an ionic species formed by the activation or reaction of H_2O_2 with metal phthalocyanines. Bimetallic Sn-Mo and Sn-Sb phthalocyanines have also been used to hydroxylate phenols using H_2O_2 as the oxidant[26]. The main products were catechol and hydroquinone, but the rate of hydroxylation with mineral acids is much faster than with metal phthalocyanines. Since very little (2%) of m-dihydroxy benzene (resorcinol) was formed, the authors[26] suggest that the hydroxylation proceeds via an electrophilic substitution mechanism, which is typical for hydroxylation of phenol catalyzed by strong acids or organic peracids. However, metal phthalocyanines facilitate hydrolysis of peroxide bonds[27] and hydroxyl radicals are always produced during the reaction. Amberlite supported Fe and Mn sulfonated phthalocyanines are efficient catalysts for the hydrogen peroxide oxidation of chlorinated phenols.[28] Orita et al[29], have recently reported that copper (II) chloride coupled with amine, hydroxylamine or oxime catalyze the oxidation of 2.3.6, tri methyl phenol to the corresponding p-benzoquinone with dioxygen. Cobalt tetraphenyl porphyrins have also been used for the oxidation of phenols to quinones using molecular oxygen as the oxidant[30]. 2,6 di-tert. butyl phenol was oxidized in water by cobalt phthalocyanine-tetra sulfonate bound to polymer colloids and using dioxygen as the oxidant[31].

In the present section, the catalytic activity of copper phthalocyanines and chloro- or nitro- substituted copper phthalocyanines encapsulated in zeolites X, Y and ZSM-5 in the selective oxidation of phenol to hydroquinone and catechol using H_2O_2 as the oxidant, has been studied.

6.2.2 Experimental

The synthesis of the *neat* copper (II) hexa deca chloro phthalocyanine ($CuCl_{16}Pc$), and copper (II) tetra nitro phthalocyanine {$Cu(NO_2)_4Pc$} and their encapsulation in zeolites X, Y and ZSM-5 is described in detail in Chapter 2 (2.2.1). Copper (II) tetra deca chloro phthalocyanine ($CuCl_{14}Pc$) was obtained from M/s Lona Industries, Bombay. Detailed procedures of the catalytic reaction and product analysis is given in Section 2.2.2.1.

6.2.3 Results and discussion

6.2.3.1 Catalyst Characterization

The physicochemical characteristics of the copper phthalocyanine catalysts used in the oxidation of phenols have been described in Chapter-3

6.2.3.2 Catalytic activity

$CuCl_{14}$ Pc, $CuCl_{16}$ Pc and $Cu(NO_2)_4Pc$ are active catalysts for the oxidation of phenol to hydroquinone and catechol using H_2O_2 as the oxidant. Table 2 illustrates the influence of the copper content (and, hence, the concentration of the copper complex) in the zeolite on the rate of oxidation of phenol as well as the product distribution.

Table-2

Oxidation of phenol with H_2O_2 over phthalocyanines

Catalyst	Cu (% wt)	TON	Products (%)		
			PBQ	CAT	HQ
$CuCl_{14}Pc$		2.1	2.0	59.5	38.5
$CuCl_{16}Pc$		2.1	2.0	49.2	48.8
$Cu(NO_2)_4Pc$		1.21	12.5	0	87.5
$CuCl_{14}Pc$-Na-Y (0.11)	0.11	7.95	0	65.8	34.2

$CuCl_{14}Pc$-Na-Y (0.17)	0.17	8.27	0	63.1	36.9
$CuCl_{14}Pc$-Na-Y (0.26)	0.26	6.77	0	50.9	49.1
$CuCl_{14}Pc$-Na-Y (0.27)	0.27	7.35	6.1	49.1	44.8
$CuCl_{14}Pc$-Na-X (0.14)	0.14	8.25	0	62.8	37.2
$CuCl_{14}Pc$-Na-X (0.28)	0.28	7.36	11.2	46.4	43.4
$CuCl_{16}Pc$-ZSM-5 (0.17) (seeded)	0.17	13.0	35.0	65.0	-
$CuCl_{16}Pc$-ZSM-5 (0.10) (non-seeded)	0.10	9.5	39.2	60.8	-
$Cu(NO_2)_4Pc$-Na-Y (0.09)	0.09	4.70	0	0	100
$Cu(NO_2)_4Pc$-Na-Y (0.16)	0.16	3.95	0	0	100
$Cu(NO_2)_4Pc$-Na-X (0.11)	0.11	4.25	0	0	100
$Cu(NO_2)_4Pc$-Na-X (0.14)	0.14	3.95	0	0	100

Reaction conditions : catalyst wt = 0.75 g; phenol/H_2O_2 = 3 mole; reaction time = 8 h; Temp = 353 K; solvent = acetonitrile = 45g; PBQ = para benzoquinone; CAT = catechol; HQ = hydroquinone; TON = moles of phenol converted per mole of copper in the catalyst.

The following salient features may be noted :

(1). The catalytic efficiency (turnover number) of the copper ions is higher in the encapsulated state than in the *neat* complex;

(2). The chloro complex is more active than the nitro complex;

(3). The turnover number does not vary significantly with copper content suggesting that the copper complexes are well isolated from each other (The conversion of phenol, of course, increases with the concentration of the copper complex in the zeolite);

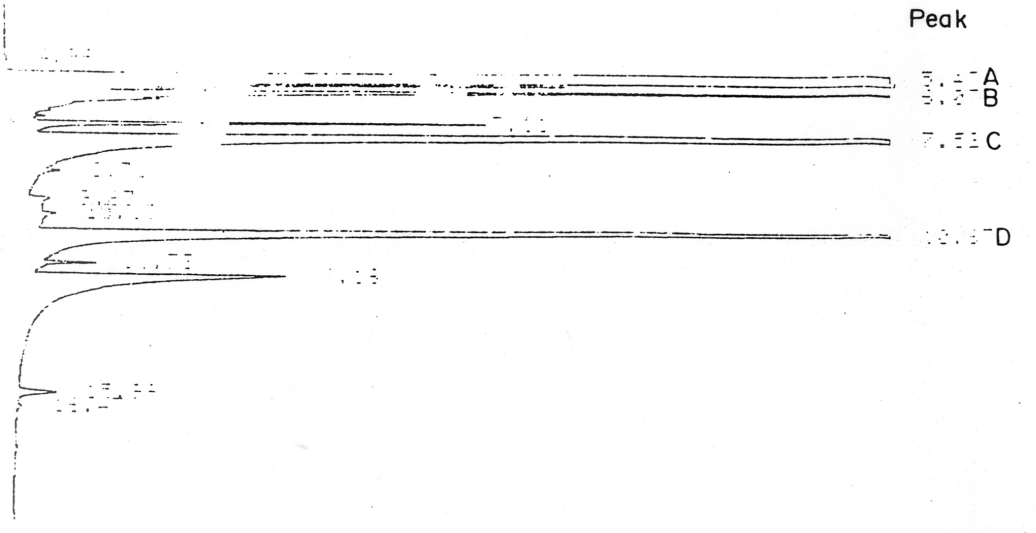

Fig. 6 GC chromatogram of the products of the oxidation of phenol using H_2O_2 as the oxidant; A = phenol; B = PBQ = para-benzoquinone; C = CAT = catechol and D = HQ = hydroquinone.

(4). Catechol (CAT), hydroquinone) and para benzoquinone (PBQ) are the only major products obtained in the ox tion of phenol. The amount of *tar* products was less than 1%. The product was al st colourless (the product distribution in Table 2 is given on a *tar free* basis);

(5). Para benzoquinone is observe mongst the products with zeolites containing relatively larger amounts of encap ated $CuCl_{14}$ Pc complexes (with 0.27 and 0.28% wt. of Cu, respectively).

The catalytic nature of t reaction is confirmed by the data in Fig.7 which illustrates the influence of catalyst weig on the conversion of phenol and product

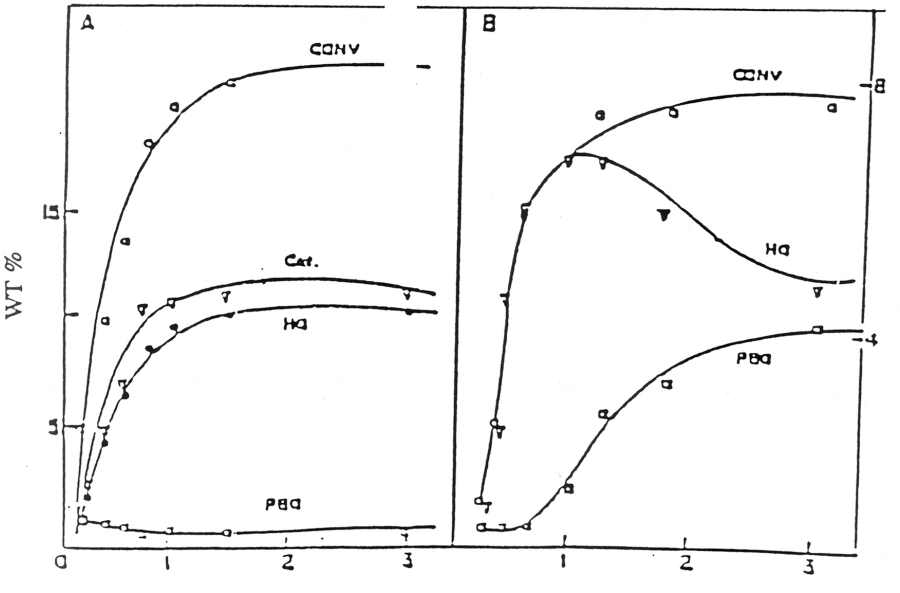

Fig. 7 Influence of catalyst weight on phenol conversion (CONV), and distribution of catechol (Cat), hydroquinone (HQ) and para-benzoquinone (PBQ) over $CuCl_{14}$Pc-Na-Y (0.26) {Fig. A} and $Cu(NO_2)_4$Pc-Na-Y (0.16) {Fig. B}, respectively, at 353 K. See Table-2 for reaction conditions.

distribution. Phenol conversion is negligible in the absence of any catalyst. The conversion increases with catalyst concentration (Fig. 7) and levels off beyond 1 g, probably due to the complete consumption of H_2O_2. In the case of $CuCl_{14}$ Pc-Na-Y (0.26), the concentration of PBQ in the product is almost negligible (Fig.7.A) even at high copper concentration. In the case of $Cu(NO_2)_4$ Pc-Na-Y (0.16), however, PBQ formation is enhanced (Fig.7.B) at higher catalyst concentrations (probably due to the further oxidation of HQ). Surprisingly, there was no formation of CAT under all reaction conditions when $Cu(NO_2)_4$ Pc-Na-Y samples were used as catalysts. The kinetics of oxidation of phenol over $CuCl_{14}$ Pc-Na-Y (0.26) and $Cu(NO_2)_4$ Pc-Na-Y (0.16) are illustrated in Fig.8.A and B,

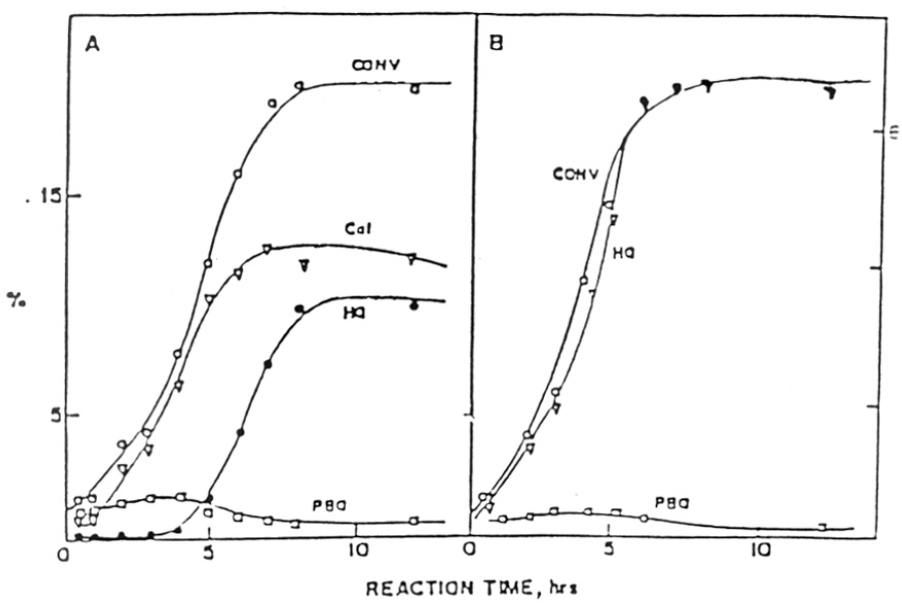

Fig. 8 Kinetic plots for phenol conversion (CONV), and distribution of catechol (Cat), hydroquinone (HQ) and para-benzoquinone (PBQ) over $CuCl_{14}$Pc-Na-Y (0.26) {Fig. A} and $Cu(NO_2)_4$Pc-Na-Y (0.16) {Fig. B}, respectively, at 353 K. See Table-2 for reaction conditions.

respectively. In the case of the former catalyst, the formation of both CAT and PBQ starts from the early stage of the reaction. Significant quantities of HQ are observed in the product only after about 2-3 hrs (Fig. 8.A). Both HQ and PBQ are formed from the beginning in the case of $Cu(NO_2)_4$ Pc-Na-Y (0.16) (Fig. 8.B). The higher activity of the chloro- compared to the nitro- complex may be noted in Fig.8. The influence of temperature on the rate and product distribution (in the oxidation of phenol) for the encapsulated complexes is similar to that of their neat analogs. This is shown in Figures 9 and 10 for the chloro- and nitro complexes, respectively. In general, and, especially, in the case of the chloro complex, slightly lower amounts of PBQ are observed when the copper complexes were encapsulated in zeolites.

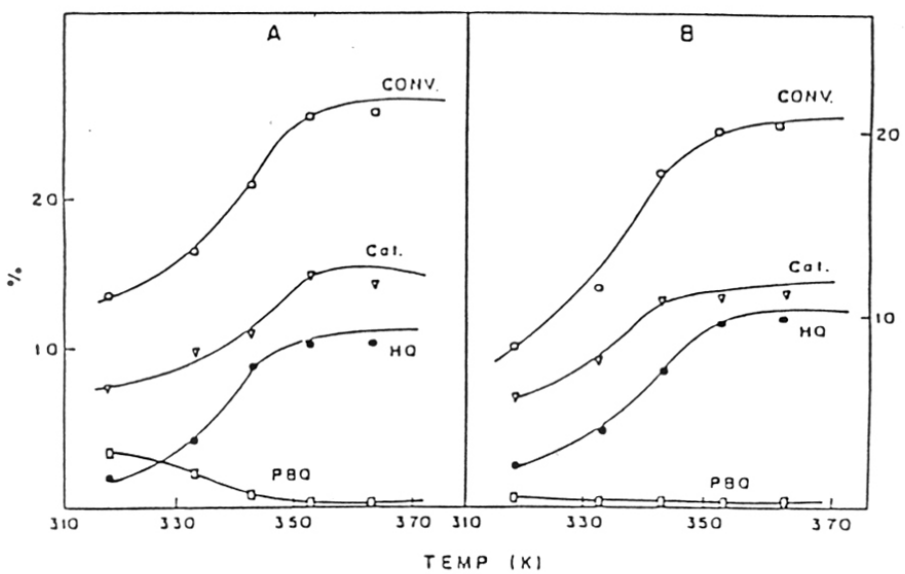

Fig. 9 Influence of temperature on phenol conversion (CONV), and distribution of catechol (Cat), hydroquinone (HQ) and para-benzoquinone (PBQ) over $CuCl_{14}Pc$ {Fig. A} and $CuCl_{14}Pc$-Na-Y (0.26) {Fig. B}, respectively. See Table-2 for reaction conditions.

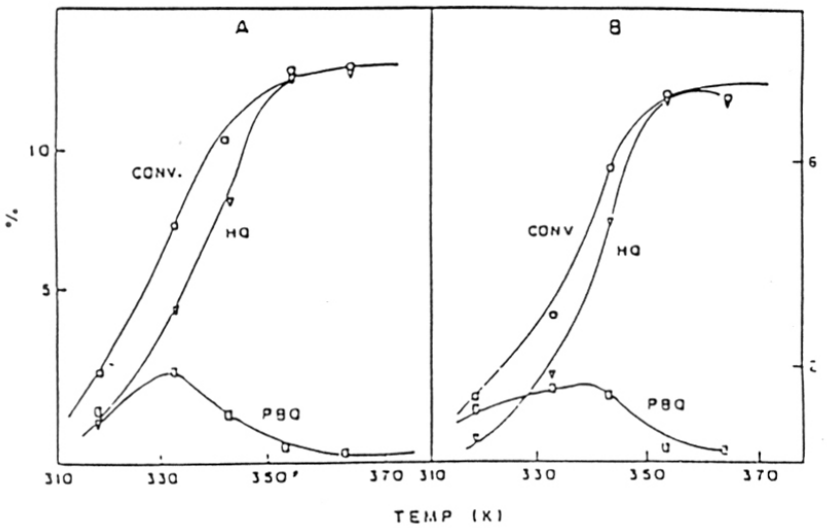

Fig. 10. Influence of temperature on phenol conversion (CONV), and distribution of hydroquinone (HQ) and para-benzoquinone (PBQ) over $Cu(NO_2)_4Pc$ {Fig. A} and $Cu(NO_2)_{14}Pc$-Na-Y (0.16) {Fig. B}, respectively. See Table-2 for reaction conditions.

The influence of the concentration of the oxidant, aqueous H_2O_2, on phenol conversion and product distribution over $CuCl_{14}Pc$-Na-Y (0.26) and $Cu(NO_2)_4Pc$-Na-Y (0.16) are shown in Tables 3 and 4, respectively.

Table-3

Oxidation of phenol over $CuCl_{14}Pc$-Na-Y (0.26)
Influence of H_2O_2 concentration

Phenol : H_2O_2	Phenol	H_2O_2 eff.	Products (%)		
(moles)	conv. (%)	(%)[a]	PBQ	CAT	HQ
1	20.9	20.9	16.4	40.9	42.7
2	21.4	42.8	2.9	48.5	48.6

3	19.7	59.2	0	50.9	49.1
4	17.6	70.4	0	51.2	48.8
5	15.1	75.5	0	53.6	46.4
10	7.9	79.0	0	52.8	47.2

Reaction conditions : catalyst wt = 0.75 g; reaction time = 8 h; Temp = 353 K; solvent = acetonitrile = 45 g; PBQ = para benzoquinone; CAT = catechol; HQ = hydroquinone; [a]H_2O_2 efficiency is defined as the mol percentage fraction of H_2O_2 utilized for the conversion of phenol to (HQ + CAT + PBQ).

The results indicate that, for he maximum utilization of H_2O_2 in the conversion of phenol to (HQ + CAT) and minimum formation of quinones, the phenol: H_2O_2 (mole) ratio must be kept as high as possible. However, lower H_2O_2 concentrations lead to lower phenol conversions. At higher H_2O_2 concentrations, not only more quinones are produced but they also persist in the product for a much longer duration. In addition, part of the H_2O_2 is decomposed noncatalytically to $H_2O + O_2$.

Table-4

Oxidation of phenol over $Cu(NO_2)_4Pc$-Na-Y (0.16)
Influence of H_2O_2 concentration

Phenol : H_2O_2	Phenol	Products (%)		
(moles)	conv. (%)	PBQ	CAT	HQ
1	10.8	39.7	0	60.3
2	7.7	8.6	0	91.4
3	7.0	0	0	100

4	6.4	0	0	100
5	6.2	0	0	100
10	5.9	0	0	100

Reaction conditions : catalyst wt = 0.75 g; reaction time = 8 h; Temp = 353 K; solvent = acetonitrile = 45 g; PBQ = para benzoquinone; CAT = catechol; HQ = hydroquinone;

In the case of $CuCl_{14}$Pc-Na-Y, the ortho-para ratio [catechol/(hydroquinone + PBQ) ratio in Table 3] is lower at very high concentrations of H_2O_2 (phenol : H_2O_2 = 1). This behavior is different from that observed in the case of titanosilicates. Thangaraj et al.[32] had observed that, in the case of oxidation of phenol with H_2O_2 over TS-1 molecular sieves, the relative concentration of catechol was higher at high concentrations of H_2O_2 . For example, at phenol : H_2O_2 mole ratios of 3 and 1, the ratios of catechol to (hydroquinone + PBQ) were 0.94 and 1.56, respectively. The corresponding values for $CuCl_{14}$Pc-Na-Y (Table 3) are 1.03 and 0.69, respectively. The differences in the shape selectivity and relative hydrophobicity/hydrophilicity of TS-1 and Na-Y are probably additional factors that play a role (TS-1, being highly silicic, is more hydrophobic than Na-Y). In addition, the fast conversion of HQ to PBQ at high concentrations of H_2O_2 enhances the formation of the para-substituted product. It may be recalled (Table 2) that the *neat* chloro complex, $CuCl_{14}$Pc, produces 1.5 times more catechol than hydroquinone, a ratio close to the statistical value of 2.0. This (ortho/para) ratio equals unity for $CuCl_{14}$Pc-Na-Y (0.26) and $CuCl_{14}$Pc-Na-Y (0.27), while it is less than unity for $CuCl_{14}$ Pc-Na-X (0.28). The higher, relative concentration of HQ observed over our zeolite-encapsulated chloro complexes (especially at high loadings) is probably due to the geometric constraints imposed by the zeolite matrix.

The influence of solvents on the oxidation of phenol for $CuCl_{14}Pc$-Na-Y (0.26) is

Table-5

Oxidation of phenol over $CuCl_{14}Pc$-Na-Y (0.26)
Influence of solvent

Solvent	Phenol conv. (%)	Products (%)		
		PBQ	CAT	HQ
Acetonitrile	19.7	0	50.9	49.1
Methanol	7.3	0	93.5	6.5
Acetone	1.1	0	100	0
Water	2.3	28.9	32.5	38.6

catalyst wt = 0.75 g; phenol/H_2O_2 = 3 mole; reaction time = 8 h; Temp = 353 K; solvent =15 g; PBQ = para benzoquinone; CAT = catechol; HQ = hydroquinone;

illustrated in Table 5. In acetone and water the conversion is negligible. In the case of $CuCl_{14}Pc$-Na-Y, amongst all the solvents that we had investigated, the conversion of phenol was highest when acetonitrile was used as the solvent. Substantial quantities of tarry products as well as PBQ were formed when water was the solvent. The corresponding results for Cu $(NO_2)_4Pc$-Na-Y are given in Table 6. It may be noted that even though the *neat* complex as well as the zeolite encapsulated analog yield only the para-substituted oxidation product hydroquinone in acetonitrile solvent (Table 2), significant quantities of catechol are formed when the oxidation is carried out in methanol (Table 6). In the oxidation of phenol over titanium and vanadium silicate molecular sieves (like TS-1, TS-2, VS-1 and VS-2) the influence of solvents on the rate and product distribution is quite complex in nature[32]. The identity of the active site for the

Table-6

Oxidation of phenol over $Cu(NO_2)_4Pc$-Na-Y (0.16)
Influence of solvent

Solvent	Phenol conv. (%)	Products (%)		
		PBQ	CAT	HQ
Acetonitrile	7.0	0	0	100
Methanol	11.2	0	24.7	75.3
Acetone	6.1	8.9	0	91.1
Water	3.2	12.5	0	87.5

catalyst wt = 0.75 g; phenol/H_2O_2 = 3 mole; reaction time = 8 h; Temp = 353 K; solvent =15 g; PBQ = para benzoquinone; CAT = catechol; HQ = hydroquinone;

oxidation reaction (Ti or V), temperature, the particle size and hydrophobicity/ hydrophilicity of the zeolite matrix, the comparative diffusion rates (inside the zeolite pores) of the substrate vis-à-vis the solvent molecules under reaction conditions, the bi- or triphasic nature of the reaction mixture, the competition between the substrate and solvent molecules for coordination to the transition metal cation (this factor is especially important in the case of vanadium silicate molecular sieves) were found to be an important parameters that affect the relative catechol to hydroquinone ratio in the product mixture. No simple relationship between any single parameter and the ortho:para ratio could be observed.

6.3 Conclusions

Two novel solid catalytic systems for the selective oxidation of phenol have been discovered. The solid catalysts, known so far to catalyze this oxidation reaction are the amorphous TiO_2-SiO_2 and the crystalline metallosilicates of transition metals like Ti, V and to a lesser extent the Sn, As etc. The activation of dioxygen, at ambient conditions, by dimeric copper acetate complexes incorporated in molecular sieves Y, MCM-22 and VPI-5, in the oxidation of phenols to ortho diphenols and diphenols to o-quinones has been studied. L-tyrosine is oxidized to L-DOPA, phenol to catechol, catechol to ortho benzoquinone and cresols to the corresponding ortho dihydroxy and o-quinone compounds. The incorporated copper acetate complexes have been characterized by IR, UV and ESR spectroscopies. A linear correlation between the concentration of the copper acetate dimer in the molecular sieve (from ESR) and the conversion of L-tyrosine suggests that the dimeric copper atoms are the active sites in the activation of dioxygen. The catalytic efficiency (turnover numbers) of the copper atoms are higher in the incorporated state compared to that in *neat* copper acetate. The above results indicate that copper acetate dimers encapsulated in molecular sieves mimic, in a restricted sense, both the monophenolase and diphenolase catalytic activity of the monooxygenase enzyme tyrosinase.

While unsubstituted copper phthalocyanines are inactive in the hydroxylation of phenol, substitution of the hydrogen atoms on the phthalocyanine nucleus with electron-withdrawing groups like the halogens or the nitro groups converts this catalytically inactive material into an active catalyst for the selective oxidation of phenol with catalytic activity and H_2O_2 efficiency approaching those of TS-1 molecular sieves, especially, when

these complexes are encapsulated in inorganic microporous matrices. The catalytic activity of halogenated and nitro-substituted copper phthalocyanines encapsulated in the zeolites, X, Y and ZSM-5 have been studied in the selective oxidation of phenol to catechol and hydroquinone using H_2O_2 as the oxidant. The catalytic activity increases with the degree of substitution by the electron withdrawing groups. The results on the influence of halogen substituents are similar to those of Lyon et al.[33] who reported recently, that halogenated iron porphyrin complexes are active liquid phase alkane air-oxidation catalysts. Their product profiles (in the alkane oxidation reaction with O_2) were characteristic of radical reactions. The mechanism of aromatic hydroxylation, using H_2O_2 as an oxidant, over the chloro- or nitro- copper phthalocyanines is not clear. However, in view of the complete absence of resorcinol and other meta- substituted products, it is unlikely that the reaction proceeds through a purely radical mechanism. It is more likely that ionic species or ion-radicals are involved as intermediates.

6.4 References

1. J.P. Collman and K.S. Suslick, *Pure Appl. Chem.*, **50** (1978) 951.

2. A.B.P. Lever and H.B. Gray, *Acc. Chem. Res.*, **11** (1978) 348.

3. J.E. Lyons in "*Aspects of homogeneous catalysis*"; R. Ugo (Ed); D. Reidel : Dordrecht, Holland, 1977, Vol. 3 pg. 1.

4. U.K. Patent Appl. 8547/78, 8548/78.

5. J.E. Lyons in "*Fundamental research in homogeneous catalysis*"; M. Tsuitsui, R. Ugo (Eds); Plenum : London, 1977 pg. 1.

6. J.P. Collman, M. Marroco, P. Denisevich, C. Koval and F.C. Anson, *J. Electroanal. Chem.*, **101** (1979) 117.

7. T. Geiger and F.C. Anson, *J. Am. Chem. Soc.*, **103** (1981) 7489.

8. D.R. Corbin and N. Herron, *J. Mol. Catal.*, **86** (1994) 343 and references therein.

9. S.A. Bedell and A.E. Martell, Inorg. Chem., 22 (1983) 364.

10. A. Nishinaga, K. Nishizawa, H. Tomita and T. Matsuura, *J. Am. Chem. Soc.*, 99 (1977) 1287.

11. I.C. Gunsalus and S.G. Sligar, *Adv. Enzymol.*, **47** (1978) 1.

12. H.S. Mason, *Ann. Rev. Biochem.*, **34** (1965) 595.

13. D.A. Robb, in R. Lontie (eds.), *Copper Proteins and Copper Enzymes*, CRC Press, Florida, 1984, p. 207.

14. E.C. Niederhoffer, J.H. Timmons and A.E. Martell, *Chem. Rev.*, (1984) 137.

15. J.H. Dawson, *Science*, 240 (1988) 433.

16. Z. Tyeklar and K.D. Karlin, *Stud. Surf. Sci. Catal.*, 66 (1991) 237.

17. L.M. Sayre and D.V. Nadkarni, *J. Am. Chem. Soc.*, 116 (1994) 3157.

18. E.T. Adman, in C.B. Anfinsen, J.T. Edsall, F.M. Richards and D.S. Eisenberg (eds.), *Advances in Protein Chemistry*, Academic Press, New York, Vol. 42, 1991, p.145.

19. A.S. Ferrer, J.N.R. Lopez, F.G. Canovas and F.G. Carmona, *Biochim. Biophysic. Acta.*, 1247 (1995) 1.

20. N. Kitajima, K. Fujisawa and Y. Moro-oka, *J. Am. Chem. Soc.*, 111 (1989) 8975.

21. E.I. Solomon and M.D. Lowery, *Science,* 259 (1993) 1575.

22. S. Husain, R. Sekar and R.N. Rao, *J. Chromatography A.*, 687 (1994) 351.

23. D.W. Brooks and C.R. Dawson, in J. Peisach, P. Aisen and W.E. Blumberg (eds.), *The Biochemisty of Copper,* Academic Press, New York, 1966 p. 348

24. R. Parton, D. De Vos and P.A. Jacobs, in E.G. Derouane, F. Lemos, C. Naccache and F.R. Ribeiro (eds.), *Zeolite Microporous Solids : Synthesis, Structure and Reactivity,* Khumer Academic Publishers, London, 1991, p. 555.

25. B. Notari, *Stud. Surf. Sci. Catal.*, **37** (1988) 413.

26. Y. Masri and M. Hronec, *Stud. Surf. Sci. Catal.*, **66** (1991) 455.

27. M. Hronec, G. Kiss, J. Sitek, *J. Chem. Soc. Faraday Trans. 1.,* **79** (1983) 1091.

28. S. Alexander and B. Meunier, *J. Chem. Soc. Chem. Commun.*, **15** (1994) 1799.

29. K. Takehira, M. Shimizu, Y. Watanabe, T. Hayakawa and H. Orita, *Stud. Surf. Sci. Catal.,* **66** (1991) 279.

30. Y. Omura, M. Nakamura, M. Oka, Y. Fujiwara, *Japanese Patent*, J.P. 74,127,937.

31. T. Hayrettin and W.T. Ford, *J. Org. Chem.,* **53 (2)** (1988) 460.

32. A. Thangaraj, R. Kumar and P. Ratnasamy, *J. Catal.,* **131** (1991) 294.

33. J.E. Lyons, P.E. Ellis Jr., and H.K. Myers Jr., *J. Catal.*, **155** (1995) 59.

CHAPTER-7

OXYHALOGENATION OF AROMATIC COMPOUNDS

7.0 Oxyhalogenation of aromatic compounds

7.1 Introduction

Marine organisms have developed means to incorporate halogens into their metabolites and many of these halogenated compounds are involved in chemical defense roles. These compounds are also of pharmacological interest, due to their biological activities, which include antifungal, antiviral, antibacterial, anti-inflammatory and other activities. Haloperoxidases are enzymes which catalyze the oxidation of a halide (chloride, bromide or iodide) by hydrogen peroxide, a process which results in the concomitant halogenation of organic substrates :

$$\text{Org-H} + X^- + H_2O_2 + H^+ \rightarrow \text{X-Org} + 2\,H_2O$$

Two types of marine haloperoxidases have been identified : (1). vanadium bromoperoxidase (V-BrPO), a non-heme enzyme and (2). Fe Heme bromoperoxidase (FeHeme-BrPO). Chloroperoxidases can also utilize chloride ion, in addition to the bromide ion, as donors for enzymic halogenation reactions. Many of the spectral and magnetic properties of chloroperoxidases closely resemble those of cytochrome P-450 enzymes[1-3]. In the absence of organic substrates, chloroperoxidases catalyze the peroxidation of chloride and bromide ions to molecular chlorine and bromine. These

molecular species are, however, not formed as intermediates in the enzymic halogenation of organic halogen-acceptor substrates. The rate of oxidation of chloride or bromide to its respective molecular species is considerably slower than the rate of enzymic chlorination or bromination of acceptor substrates.

The oxidative liberation of halogens from hydrogen halides or their salts using H_2O_2 and suitable, homogeneous catalysts, is known for more than 70 years[4].

$$2HX + H_2O_2 \rightarrow X_2 + 2H_2O$$

$$X = Cl, Br, I$$

The halogen generated may be used for halogenating organic substrates[5,6]. Dinesh et al[6], for example, have recently shown that ammonium metavanadate efficiently catalyses the oxyhalogenation of a variety of organic substrates in moderate to good yields, using dilute hydrogen peroxide (30 %) as an oxidizing agent, exhibiting remarkable ortho selectivity with electron-rich aromatics. Similar results had been reported earlier by Conte et al[7] and Rosa et al[8]. In the above studies[6-8] the authors' main goal was the development of functional mimics of the haloperoxidase marine enzymes. These enzymes oxyhalogenate aromatic substrates using H_2O_2 and halide ions present in the marine environment. The biosynthesis of the brominated compounds, for example, is likely to be mediated by vanadium bromoperoxidase through electrophilic bromination by oxidized bromine species. While oxyhalogenation using in-situ generated halogens has many advantages (like fuller utilization of the halogen instead of only half of the available halogen, easier transport and handling of the aqueous hydrogen halides and dilute H_2O_2 compared to halogens, etc.) the major disadvantages of the present day state-of-art processes in the liquid phase are (1). the high cost of H_2O_2 and (2). the disposal of the homogeneous metal catalysts used in the processes. The latter poses additional environmental problems. Very

recently, a two-stage vapour phase process for the conversion of HCl to Cl_2 using solid catalysts has been reported[9]. In the first stage, HCl is reacted over copper oxide at 473 K producing a copper chloride complex. In the second stage, the latter is reacted with O_2 at 633 K oxidizing the copper chloride to copper oxide and Cl_2. A solid-catalyzed, single step process using H_2O_2 or preferably molecular dioxygen as the oxidant for the oxyhalogenation of aromatic substrates at near-ambient conditions using halide ions as the source of halogen will be advantageous. The oxyhalogenation of aromatic substrates using solid catalysts in the liquid phase at low temperature and using O_2 as the oxidizing agent has not been reported so far.

In this chapter the oxychlorination and oxybromination at ambient conditions, of aromatic compounds (like benzene, toluene, phenol, aniline, resorcinol and anisole) using, as catalysts, the phthalocyanines of transition metals (like Fe, Co, Cu) encapsulated in zeolites X, Y and L has been studied. Both H_2O_2 and O_2 have been used as the oxidants. The performance of these novel catalyst systems as solid oxyhalogenation catalysts is quite promising.

7.2 Experimental

7.2.1 *Materials*

The *neat* $CuCl_{16}Pc$, $Cu(NO_2)_4Pc$ and $FeCl_{16}Pc$(where Pc stands for phthalocyanine) complexes were synthesized according to the procedure described in Sections 2.2 (Chapter-2). CuPc, CoPc and $CoCl_{16}Pc$ complexes were obtained from M/s. Lona Industries, Bombay. The synthesis of $CuCl_{16}$ Pc, $Cu(NO_2)_4Pc$, $FeCl_{16}Pc$ or $CoCl_{14}Pc$ complexes encapsulated in zeolites Na-X, Na-Y and K-L is described in detail in Sections 2.2.1 (Chapter-2). Thus $CuCl_{16}Pc$-Na-X (0.27) designates a Na-X zeolite containing

0.27% wt copper in the form of a hexadeca chloro copper phthalocyanine complex encapsulated, most probably, in the supercage of the faujasite structure.

7.2.2 Procedures

Detailed procedures of the catalytic reactions and product analysis is described in Sections 2.2.2.2 (Chapter-2).

7.2.3 Catalyst Characterization

Chapter-3, Section 3.3 describes in detail, the physicochemical characteristics of the catalysts used in the oxyhalogenation of aromatic compounds.

7.4 Results and discussion

7.4.1 Catalytic activity

Experimental evidence that the oxyhalogenations investigated in the present study are indeed catalyzed by the solid zeolite containing the encapsulated complex is presented in Fig. 1.

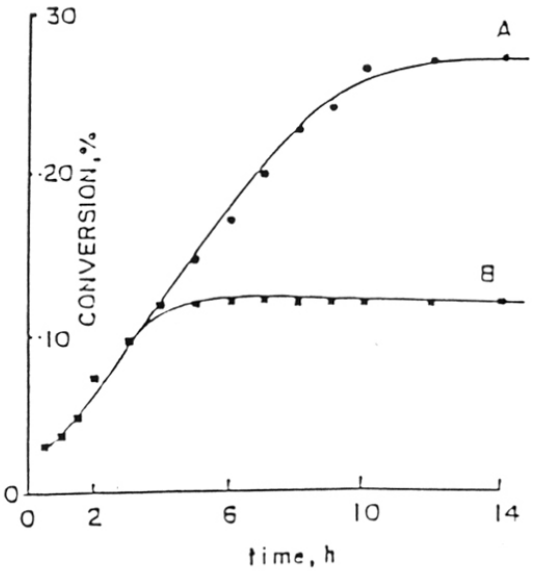

Fig. 1. Kinetics of toluene oxybromination in the presence of the solid catalyst $CuCl_{16}Pc$-Na-X (0.27) (curve A) and when the catalyst is removed from the reaction mixture at 4 hrs reaction time (curve B).

In one of a set of two identical experiments, the solid catalyst was removed by filtration at a reaction time of 4 hrs (Curve B). While conversion of toluene to oxyhalogenated products continued in the presence of the catalyst (curve A), there was no further conversion of toluene when the catalyst was removed from the reaction system (curve B). This indicates that :

(1). The solid catalyst is essential for the oxyhalogenation reaction to occur; this phenomenon was also observed with the other substrates described in this chapter.

(2). Oxyhalogenations of the substrate by dissolved copper complexes leached out from the solid material is negligible. This conclusion was independently confirmed by the absence of copper in the filtrate (atomic absorption spectroscopy) and that;

(3). In the absence of the catalyst, H_2O_2 alone is unable to oxyhalogenate the substrate to any significant extent. In independent experiments carried out in the absence of the catalyst, the conversion of toluene under otherwise experimental conditions of Fig. 1 was about 1.1 % wt. When molecular O_2 with TBHP as the initiator was used as the oxidant under the same reaction conditions, the toluene conversion in the absence of the catalyst was only 2.1 % wt. The zeolites alone were also catalytically inactive in oxyhalogenation. Thus, we may conclude that the oxyhalogenations are indeed catalyzed by the metal complexes encapsulated in the zeolite matrix.

The results of the oxychlorination of toluene, using aqueous HCl as the halogenating agent and H_2O_2 as the oxidant, at 338 K, over the various copper, cobalt and iron phthalocyanine complexes, both in the neat and encapsulated states, are presented in Table 1. The following points may be noted :

(1). The unsubstituted metal phthalocyanines have a low activity; only oxidation reactions by H_2O_2 are observed. Halogenated products are not formed;

Table-1

Oxyhalogenation of toluene
Comparison of catalysts

Catalyst	TON	Products (% wt)					
		A	B	C	D	E	F
CuPc	3.15	-	100	-	-	-	-
CoPc	1.40	-	100	-	-	-	-
$Cu(NO_2)_4Pc$	21.9	21.2	47.0	8.3	5.5	18.0	-
$CuCl_{16}Pc$	89.2	45.0	17.0	15.7	10.7	2.6	9.0
$CoCl_{14}Pc$	69.6	52.0	13.5	11.5	3.3	2.2	17.5
$FeCl_{16}Pc$	73.1	63.5	3.8	5.7	11.0	-	16.0
$Cu(NO_2)_4Pc$-Na-X (0.14)	994	18.0	58.5	5.0	1.5	17.0	-
$CuCl_{16}Pc$-Na-X (0.27)	1613.2	46.5	31.5	14.3	6.3	1.4	-
$CuCl_{16}Pc$-K-L (0.10)	3821	8.5	21.0	18.7	23.5	3.5	24.8
$CoCl_{14}Pc$-Na-X (0.27)	1067	45.0	9.0	18.2	7.5	2.2	18.1
$FeCl_{16}Pc$-Na-X (0.16)	2102.8	49.5	9.5	8.5	15.2	-	17.3

Temp, K = 338; Duration, h = 10; Halide = HCl; Catalyst wt = 0.5 g; Solvent = (CH_3CN : H_2O = 2 : 1, % mole);

Note : (1). A = benzaldehyde

B = benzyl alcohol

C = ortho chloro toluene

D = para chloro toluene

E = benzyl halide

F = di- and tri chloro toluenes

(2). The molar ratio of H_2O_2 : Substrate was 1: 3

(2). The intrinsic catalytic activity (turnover number, TON) of the neat copper, cobalt and iron complexes are of the same order of magnitude. The higher TON value observed for $FeCl_{16}Pc$-Na-X (0.16) may perhaps be due, in part, to the lower loading of the zeolite with the complex. Data on the selective oxidation of aromatic hydrocarbons over these catalysts (Chapter-5, Fig.3) had indicated that the values of TON increase on site isolation of the copper complexes, $CuCl_{16}Pc$ and $Cu(NO_2)_4Pc$ in the faujasite structure. The present data extends this conclusion to oxyhalogenation reactions also; the site isolation is enhanced at lower loadings;

(3). There is a dramatic increase in the turnover number (by more than an order of magnitude) when the halogenated or nitrated complexes are encapsulated in the cavities of zeolites X or L;

(4). Both oxidation (of the side chain) and oxyhalogenation (of both the aromatic nucleus and the side chain) occur. Oxidation of the aromatic ring to cresols, however, does not occur; (5). Oxychlorination was more dominant than oxidation only when the complexes were encapsulated in K-L zeolite. Side-chain oxidation by H_2O_2, was predominant in the case of Na-X. In addition to the above points, it may be mentioned that the central transition metal of the phthalocyanine complex is the seat of catalytic activity. $Cl_{16}Pc$ or phthalocyanines of non-transition metals (like Al) had negligible oxidation or oxyhalogenation activity.

The oxyhalogenation of benzene and toluene over $CuCl_{16}Pc$-Na-X (0.27) using both H_2O_2 and O_2 as oxidants is shown in Tables 2 and 3, respectively. Both hydrogen and alkali halides were used as the sources of halide ions. The absence of di- and tri halogenated products in Table 2 when using O_2 as the oxidant is due to the low levels of

conversion of benzene. The dihalobenzenes were mainly the ortho and para dihaloproducts with the former being predominant. Oxidation products of benzene (like phenol) were not observed under the reaction conditions mentioned in Table 2. Similarly, cresols were absent in the products from the toluene experiments indicating that oxidation / hydroxylation of the aromatic ring (by

Table-2

Oxyhalogenation of benzene over $CuCl_{16}Pc$-Na-X (0.27)

Oxidant	Initiator	Halide	Conv (%)	Halogenated Products (% wt)		
				Mono-	Di-	Tri-
H_2O_2	-	KCl	9.7	47.5	37	15.5
H_2O_2	-	KBr	11.5	58	34	8
O_2	-	KCl	3.2	100	-	-
O_2	-	KBr	4.1	100	-	-
O_2	TBHP	KCl	5.5	100	-	-
O_2	TBHP	KBr	6.2	100	-	-

Temp, K = 338; Duration, h = 10; Catalyst wt = 0.5 g; Solvent = (CH_3CN : H_2O = 2 : 1, % mole);

Note : (1). Oxidations with O_2 (air) were carried out at 400 psig.
Tertiary butyl hydroperoxide (70 % in H_2O) was used as the initiator. The concentration of TBHP was 2 % of the substrate.

(2). The dihalo benzenes were mainly ortho-/para dihalo products.

(3). The molar ratio of H_2O_2 : Substrate was 1: 3

H_2O_2) was negligible. On the other hand, the oxidation of the methyl side chain leading to benzyl alcohol and benzaldehyde was significant. Benzoic acid was not observed at these conversion levels. The absence of nuclear hydroxylation products (like phenols and

cresols) is interesting since, in the absence of the halide ions, they are formed in significant quantities.[10] Apparently the nucleophilic halide ions, when present, coordinate with the copper ions and suppress the formation of intermediates (like dioxygen complexes) that lead to nuclear hydroxylation. As was to be expected from the large pore character of zeolite X, there was no pronounced shape selectivity favouring para halo toluenes.

Table-3

Oxyhalogenation of toluene over $CuCl_{16}Pc$-Na-X (0.27)

Oxidant	Initiator	Halide	Conv (%)	Halogenated Products (% wt)				
				A	B	C	D	E
H_2O_2	-	HCl	31.5	14.5	6.5	-	1.0	78.0
H_2O_2	-	KCl	19.2	20.5	15.0	7.0	6.0	51.5
H_2O_2	-	KBr	26.6	19.0	18.0	15.5	4.5	43.0
O_2	-	HCl	13.5	15.0	27.5	4.5	4.0	49.0
O_2	TBHP	HCl	15.4	9.5	4.5	-	1.5	84.5
O_2	-	KCl	8.2	35.5	20.5	14.5	5.0	24.5
O_2	TBHP	KCl	14.0	30.5	23.0	23.0	4.0	19.5
O_2	-	KBr	11.7	30.5	26.5	9.5	16.0	17.5
O_2	TBHP	KBr	16.8	30.5	26.5	5.5	12.5	25.0

Temp, K = 338; Duration, h = 10; Catalyst wt = 0.5 g; Solvent = (CH_3CN : H_2O = 2 : 1, % mole);

Note : (1) Oxidations with O_2 (air) were carried out at 400 psig.

Tertiary butyl hydroperoxide (70 % in H_2O) was used as the initiator. The concentration of TBHP was 2 % of the substrate.

(2). A = ortho halo toluene
B = para halo toluene

C = di- and tri halo toluenes

D = benzyl halide

E = (Benzyl alcohol + Benzaldehyde)

In order to investigate the oxybromination of toluene in more detail, the kinetics of the reaction was studied (Fig. 2). Oxidation was the predominant reaction in the initial stages (curve 3, Fig. 2A). There is an induction period in the formation of brominated products (curve 2, Fig. 2A). After the significant onset of the oxybromination reaction (about 4 h),

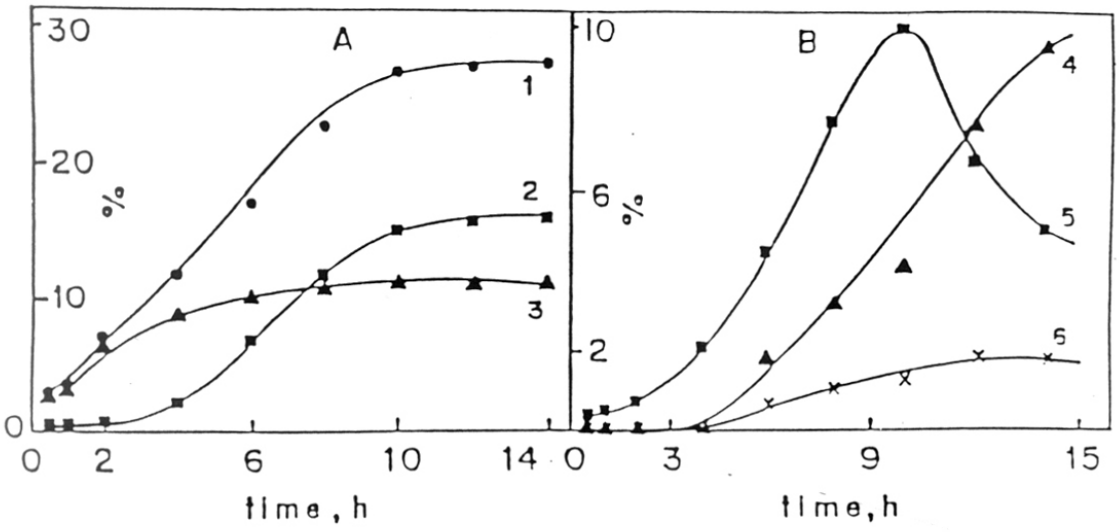

Fig. 2. Kinetic plots for the oxybromination of toluene over $CuCl_{16}Pc$-Na-X (0.27); A : curves 1-3 indicate toluene conversion (1), and formation of halogenated (2) and oxidation (3) products respectively; B : curves 4-6 indicate distribution of mono bromotoluenes (4), di + tri bromo toluenes (5) and benzyl bromide (6), respectively.

the further formation of oxidation products (like benzyl alcohol and benzaldehyde) ceased and toluene was converted mainly to its brominated products. Amongst the brominated products, the bromotoluenes were formed at a much faster rate than benzyl bromide (Fig. 2B) suggesting that the brominating species is not a radical. The latter usually leads to

significant yields of benzyl bromide[11]. Since the liberation of Br_2 from KBr by H_2O_2 in the presence of homogeneous and enzyme catalysts (see **Introduction**) is well known, it was expected that the same situation may prevail in the present case also. If Br_2 is formed from KBr in our system, it can be detected spectrophotometrically through it's complex Br_3^- which has an absorption maximum at 267 nm. The tribromide ion is formed according to the equilibrium :

$$Br_2 + Br^- \rightleftharpoons Br_3^-$$

$$K_e = \frac{[Br_3^-]}{[Br_2]\ [Br^-]}$$

Literature values for K_e vary from 15 to 20 M^{-1} and are dependent on reaction conditions[12]. The analysis for the presence of Br_3^- was done by measuring the absorption at 267 nm spectrophotometrically during the course of oxybromination of toluene (Fig. 3A). In the absence of toluene substantial formation of Br_3^- (and hence Br_2) is detected (curve 1, Fig. 3B). Only a trace amount of Br_3^- is detected in the absence of both catalyst and toluene (curve 2). When toluene is present, the concentration of Br_3^- (and hence Br_2) is suppressed (curves 3 and 4), presumably because the Br_2 formed is immediately consumed in the bromination of toluene and hence no free Br_2 is available to form Br_3^-. Hence, our studies suggest that Br_2, formed by oxidation from Br^- may be the brominating agent. In agreement with this hypothesis, when Br_2 is used to brominate toluene over K-L zeolites, the product pattern (nuclear vs side-chain bromination) was similar[11] to that observed in Fig. 2; products of nuclear halogenation (like chlorotoluenes) predominated over those like benzyl chloride arising from chlorination of the methyl side-chain.

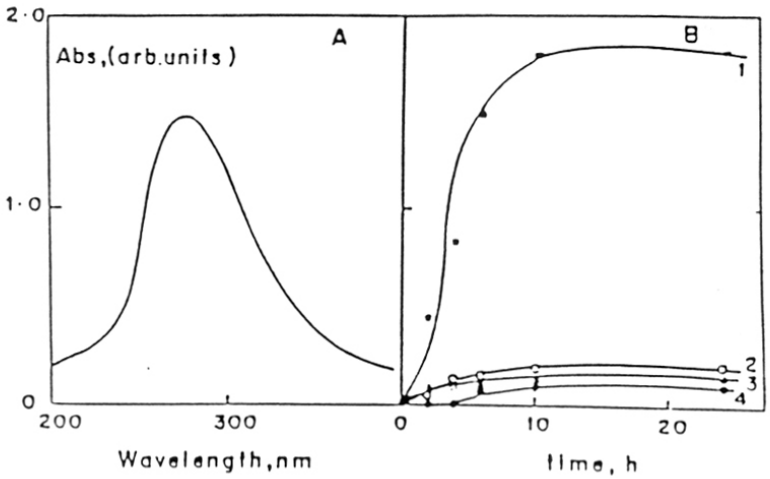

Fig. 3. (A) : UV spectrum of Br_3^- in the reaction mixture during oxybromination of toluene by KBr and H_2O_2 using $CuCl_{16}Pc$-Na-X (0.27) as catalyst; (B) : variation in the intensity of the 267 nm band in the absence of toluene (curve 1); in the absence of both catalyst and toluene (curve 2); in the presence of both catalyst and toluene (curve 3) and in the presence of toluene but absence of catalyst (curve 4).

Table-4

Oxyhalogenation of phenol over $CuCl_{16}Pc$-Na-X (0.27)

Oxidant	Initiator	Halide	Conv (%)	Halogenated Products (% wt)		
				Mono-	Di-	Tri-
H_2O_2	-	KCl	21.2	42.0	32.0	26.0
H_2O_2	-	KBr	24.1	40.0	33.5	26.5
O_2	-	KCl	7.9	64.5	26.5	9.0
O_2	-	KBr	8.8	62.5	33.0	4.5
O_2	TBHP	KBr	18.1	62.0	25.0	13.0

Temp, K = 323; Duration, h = 10; Oxidations with O_2 (air) were carried out at 300 psig. Catalyst wt = 0.5 g; Solvent = (CH_3CN : H_2O = 2 : 1, % mole); TBHP (2 % mole of phenol) was used as the initiator)

The oxyhalogenation of phenol, aniline, anisole and resorcinol are shown in Tables 4-7, respectively. The halogenated derivatives of these aromatics are of significant economic value in the Fine Chemicals industry. The mono halogenated derivatives were ortho/para products with the ortho products in slight excess. Meta halogenated products were not observed. Even though Tables 4-7 present results with KCl and KBr as halogenating agents, similar results were also obtained with NaCl and NaBr, respectively. Dinesh et al[6],

Table-5

Oxyhalogenation of aniline over $CuCl_{16}$Pc-Na-X (0.27)

Halide	Conv (%)	Halogenated Products (% wt)		
		Mono-	Di-	Tri-
KCl	9.7	64.0	30.0	6.0
KBr	10.3	63.0	15.5	21.5

Temp, K = 338; Duration, h = 10; Oxidant = O_2 (Air) = 400 psig. TBHP was used as the initiator. Catalyst wt = 0.5 g; Solvent = (CH_3CN : H_2O = 2 : 1, % mole);
Ortho halo aniline was the major monohalogenated product.

reported the oxybromination of phenol and resorcinol with KBr and H_2O_2 using ammonium metavanadate dissolved in acetonitrile-H_2O as solvent. While phenol could not be brominated by KBr, resorcinol was converted to an extent of about 40 % during 20 h of reaction at room temperature (entries 10 and 8 in Table 1 of ref 6). The major product

obtained by the bromination of resorcinol was the 2-bromo derivative. An advantage in the use of O_2 during oxychlorination of resorcinol is the higher selectivity for the desired monochloro product (Table 7). Conte et al[7] had earlier reported the oxybromination of anisole with H_2O_2 and KBr using dissolved NH_4VO_3 as catalyst. Para bromo anisole was the major monohalogenated product. The results with the solid catalyst $CuCl_{16}$Pc-Na-X (0.27) (Table 6) are different; both the ortho- and para derivatives are formed in significant quantities. Perhaps, as suggested by the authors themselves[7], the two phase, $H_2O/CHCl_3$ solvent system, facilitates the selective formation of the para derivative. The use of solid catalysts in conjunction with O_2 as the oxidizing agent at low temperatures is a significant advance in the technology of oxyhalogenation of aromatic compounds.

Table-6

Oxyhalogenation of anisole over $CuCl_{16}$Pc-Na-X (0.27)

Oxidant	Halide	Conv (%)	Halogenated Products (% wt)			
			Monohalo		2.4. di	2.4.6. tri
			ortho	para		
H_2O_2	KBr	13.8	27.0	21.0	13.0	39.0
O_2	KBr	6.7	18.0	7.5	55.0	19.5
O_2	KCl	4.8	18.5	6.5	60.5	14.5

Temp, K = 338; Duration, h = 10; Catalyst wt = 0.5 g; Solvent = (CH_3CN : H_2O = 2 : 1, % mole);

Note : (1). TBHP was used as an initiator in oxidation with O_2 (air).
For other details see footnote to Table-2.

Table-7

Oxyhalogenation of resorcinol

Catalyst	Oxidant	Halide	Conv (%)	Halogenated Products (% wt)		
				Mono-	Di-	Tri-
$CuCl_{16}Pc$-Na-X	H_2O_2	KBr	31.6	54.5	26.5	19.0
$CuCl_{16}Pc$-Na-X	H_2O_2	KCl	28.5	59.0	30.5	10.5
$CuCl_{16}Pc$-Na-X	O_2	KCl	16.5	85.5	14.5	-
$CuCl_{16}Pc$-Na-X	O_2	KBr	18.2	100	-	-
$CuCl_{16}Pc$-K-L	O_2	KBr	14.9	90.0	10.0	-
$Cu(NO_2)_4Pc$-Na-Y	O_2	KBr	7.5	100	-	-

Temp, K = 323; Duration, h = 10; Catalyst wt = 0.5 g; Solvent = (CH_3CN : H_2O = 2 : 1, % mole); H_2O_2 : resorcinol = 1 : 3 mole;

Note : (1). Oxidations with O_2 (air) were done at 300 psig. No initiator was used.
For other details see footnote to Table-2

The presence of 2-bromo resorcinol and 4-bromo resorcinol in the products was confirmed by GC-MS and is shown in Fig. 4.

The influence of pH on the selectivity for halogenated products in the oxybromination of resorcinol with KBr and H_2O_2 is shown in Fig. 5. The pH was adjusted with a phosphate buffer. The optimal performance of our catalyst system in the pH range 5.0-6.0 is similar to that of the enzyme vanadium bromoperoxidase but differs from dioxovanadium (V) catalysts which require significantly greater acid concentration (≥ 0.001 M H^+).[8] While the reaction mechanism of oxyhalogenation catalyzed by enzymes is not yet clear in all detail, it seems to involve a halogenium ion (X^+) or hypohalous acid (HO^-X^+) as an intermediate of the reaction[13,14].

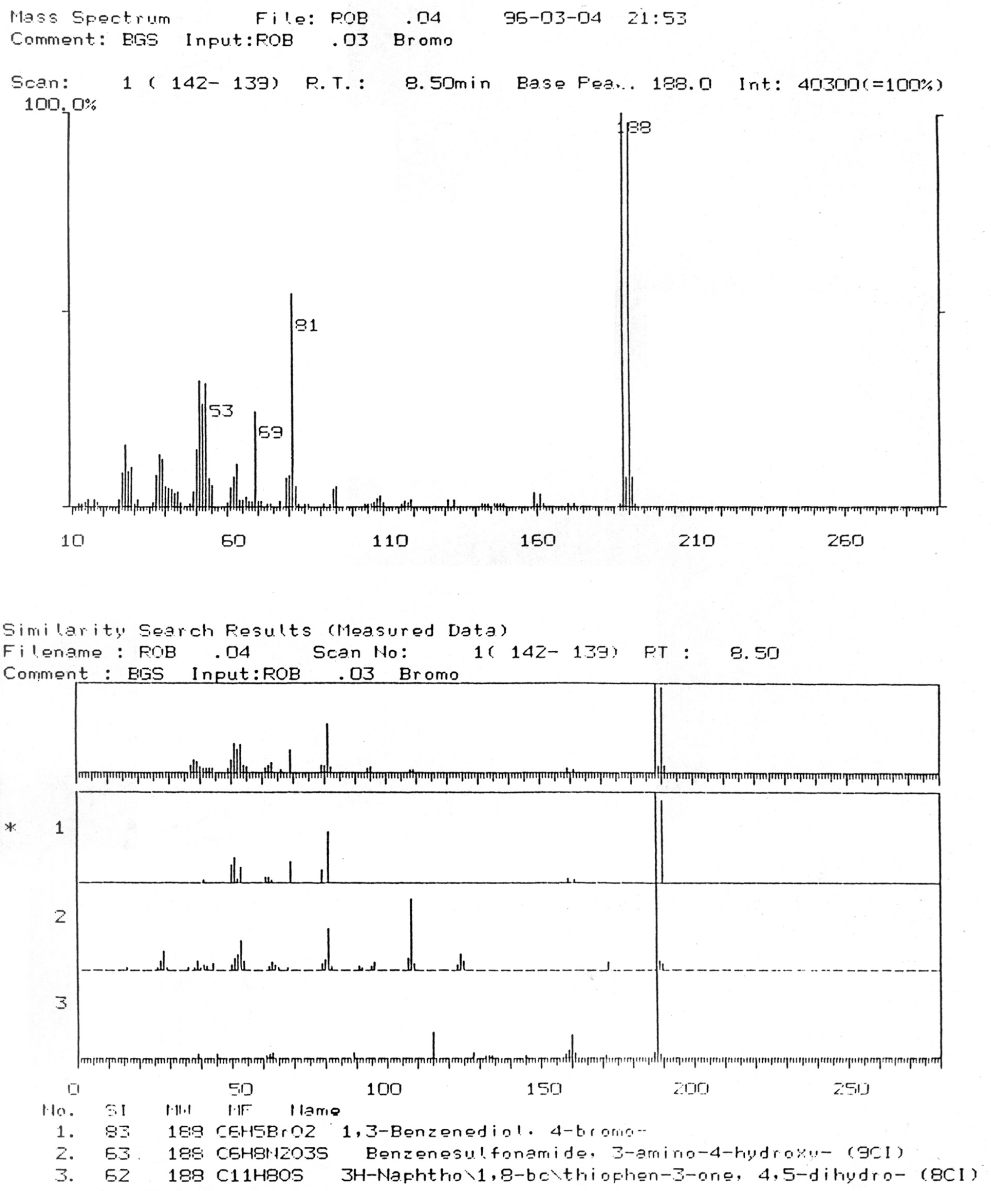

Fig. 4 GC-MS chromatogram and search results of the products of oxyhalogenation of resorcinol

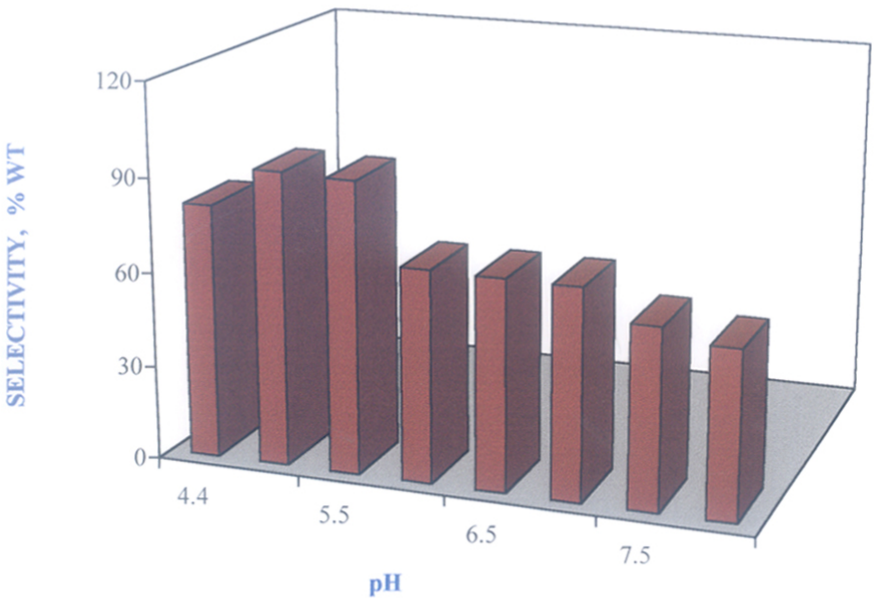

Fig. 5. The influence of pH on the selectivity for brominated products in the in the oxybromination of resorcinol using $CuCl_{16}Pc$-Na-X, KBr and H_2O_2 at 333 K.

Bromine, for example, is known to be in equilibrium with the tribromide ion and hypobromous acid in aqueous systems, the position of the equilibrium being

$$Br_2 \xrightleftharpoons{Br^-,\ H_2O} Br_3^- + HOBr$$

dependent on the pH of the medium. The observation of Br_2 in our system (Fig. 3A), the ortho-para orientation among the nuclear halogenated products (Table 3, for example) and the pH dependence of the conversion (Fig. 5) suggest that the halogenating agent is an electrophilic species.

4. Conclusions

The oxychlorination and oxybromination, at near-ambient conditions, of benzene, toluene, phenol, aniline, anisole and resorcinol, using as catalysts, the phthalocyanines of Cu, Fe and Co encapsulated in zeolites X, Y and L have been carried out. Both H_2O_2 and O_2 have been used as the oxidants. HCl and alkali chlorides/bromides have been used as the sources of halogens. The metal phthalocyanines wherein the aromatic rings are substituted by -Cl or $-NO_2$ groups are more active. There is a dramatic increase in the turnover numbers for substrate conversion when the complexes are encapsulated in the cavities of the zeolites X, Y or L. The oxyhalogenation of both the aromatic nucleus and the alkyl side chains occur. Oxidation of the aromatic ring (to phenols or cresols, for example), does not occur. Alkyl side chains, however, are oxidized by the oxidant H_2O_2 or O_2, to alcohols, ketones and acids. The performance of these novel catalyst systems as solid oxyhalogenation catalysts in utilizing O_2 and halide ions (instead of molecular halogen) in the manufacture of halogenated aromatics holds promise in the organic chemicals industry.

5. References

1. D.R. Morris and L.P. Hager, *J. Biol. Chem.*, **241** (1966) 1763.
2. P.M. Champion, E. Munck, P. Debrunner, P.F. Hollenberg and L.P. Hager, *Biochemistry*, **12** (1973) 426.
3. P.F. Hollenberg, L.P. Hager, W.E. Blumberg and J. Peisach, *J. Biol Chem.*, **255** (1980) 4801.
4. A. Leulier, *Bull. Soc. Chim., France* **35**, 1325 (1924).
5. R. Johnson and K. Reeve, Speciality Chemicals p. 32, October 1992.
6. C.U. Dinesh, R. Kumar, B. Pandey, and P. Kumar, *J. Chem. Soc. Chem. Commun.*, 611 (1995).
7. V. Conte, F.D. Furia, and S. Moro, *Tetr. Lett.*, **35 (40),** 7429 (1994).
8. R.I. de la Rosa, M.J. Clague, and A. Butler, *J. Am. Chem. Soc.*, **114,** 760 (1992).
9. R. Westervelt, in Chemical Week, p. 26, Aug. 14 (1996).
10. Robert Raja and Paul Ratnasamy. *Stud. Surf. Sci. Catal.,* **105** (1997) 1037.
11. P. Ratnasamy, A.P. Singh, and S. Sharma, *Appl. Catal., A* : General **135**, 25 (1996).
12. I.A. Popov, in "Halogen Chemistry", Vol. 1, Academic Press, New York, 225 (1967).
13. H. Yamada, N. Itoh, and Y Izumi, *J. Biol. Chem.*, **260, (22)**, 11962 (1985).
14. N. Itoh, Y. Izumi, and H. Yamada, *Biochem.,* **26,** 282 (1987).

CHAPTER-8

GENERAL DISCUSSION

8.0 GENERAL DISCUSSION

8.1 Introduction

This chapter discusses some of the mechanistic considerations arising out of the catalytic results presented in chapters 4-7. Two novel catalytic systems have been explored in this thesis. They are (1). Dimeric copper acetate complexes encapsulated in zeolites Y, MCM-22 and VPI-5 and (2). Copper phthalocyanines encapsulated in zeolites X, Y, K-L and ZSM-5, wherein some or all of the hydrogen atoms on the phthalocyanine ring have been substituted by electron-withdrawing groups like -Cl or NO_2.

The encapsulated dimeric copper acetate complexes have several interesting features :

- They use dioxygen, O_2, as the oxidant in oxidizing phenols to dihydroxy benzenes and quinones at ambient conditions; They exhibit both mono- and diphenolase activities.
- The reactions are catalytic (turnover numbers = 5-55)
- They show high substrate selectivity; only phenols are oxidized. Aliphatic compounds or other aromatic derivatives are not oxidized significantly.
- They show high pH specificity, performing optimally only at pH = 6.5 $\pm$ 0.5.
- They exhibit a high regiospecificity, oxidation occurring only at the position ortho to the existing phenolic group; eg. L-tyrosine yields only L-DOPA;
- Addition of ascorbic acid suppresses the further oxidation of the diphenol (L-DOPA, for example) to diquinones.

All the above catalytic features are also characteristic of the enzyme, tyrosinase (EC 1.14.18.1) whose prosthetic group also contains a pair of copper ions as the active site. Since the nuclearity of copper and functional characteristics of the enzyme tyrosinase and the encapsulated dimeric copper acetate complex are similar, we will seek inspiration from the known mechanism of oxidation of L-tyrosine to L-DOPA by tyrosinase, in our speculation of the mechanism of oxidation of phenols to diphenols over dimeric copper acetate complexes.

Our second catalytic system, namely substituted copper phthalocyanines are monomeric and there is no evidence of dimer formation. In fact, formation of the dimer is sterically impossible inside the faujasite supercages. The mechanism of activation of oxygen and oxidation of organic substrates is, hence, likely to be different from that of the copper acetate system. Crucial to the action of both these systems is the binding, activation and reduction of O_2 that precedes its incorporation in the organic substrates.

Due to the above considerations, following a general description of binding, activation and reduction of O_2, the mechanism of oxidation over copper acetate dimers and monomeric phthalocyanines encapsulated in zeolites are presented in separate, subsequent sections.

8.2 The binding and activation of O_2

The O-O bond in O_2 has a dissociation energy of 118 Kcal mol^{-1}. In contrast, the dissociation energy of the O-O bond in H_2O_2 is only 35 Kcal mol^{-1}. The stepwise reduction of O_2 may be formulated schematically as shown below. The formation of two potential hydroxylating particles, namely, the perhydroxyl radical ($O_2H^{\cdot}$) and hydroxyl radical ($OH^{\cdot}$) may be noted. These radicals play important roles in oxidation reactions. The hydroxyl radical can also be formed by the reduction of H_2O_2.

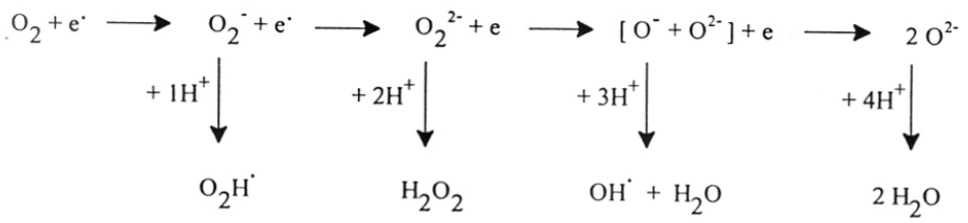

The molecular orbital energy diagram of O_2 in the ground state is given in Fig. 1.[1]

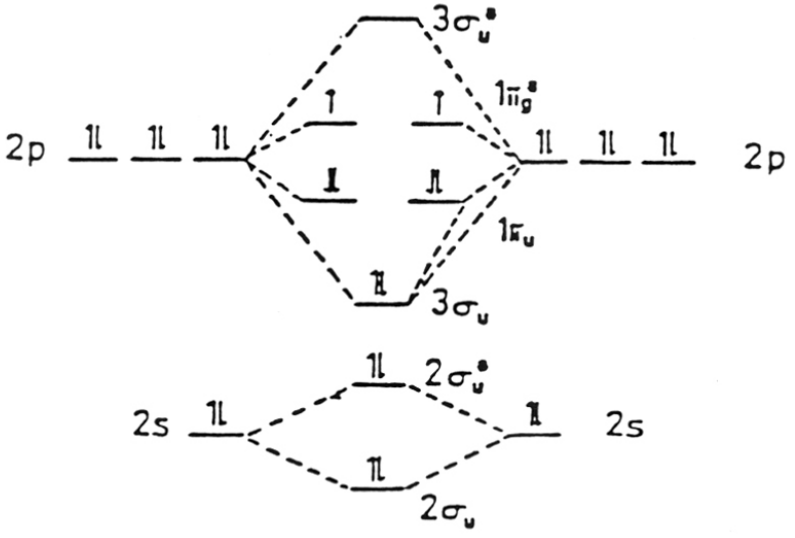

Fig. 1 Molecular orbital energy diagram of oxygen in the ground state.

The ground state is a triplet state and possesses two unpaired electrons located in a doubly degenerate $\prod^*$ antibonding orbital. The bond order is two. The electrons added during the reduction of O_2 occupy the antibonding orbitals thereby weakening the O-O bond. There is, however, a restriction on the reduction of O_2 by H_2 or organic molecules arising from the spin conservation principle. According to the latter, when O_2 in its ground triplet state

interacts with a singlet molecule (like H_2 or organic molecules), the resultant will be a triplet molecule. The spin restriction can be overcome upon coordination of the O_2 molecule to a metal centre. The plausible 1 : 1 and 2 : 1 metal-dioxygen complex structures are illustrated below[1] :

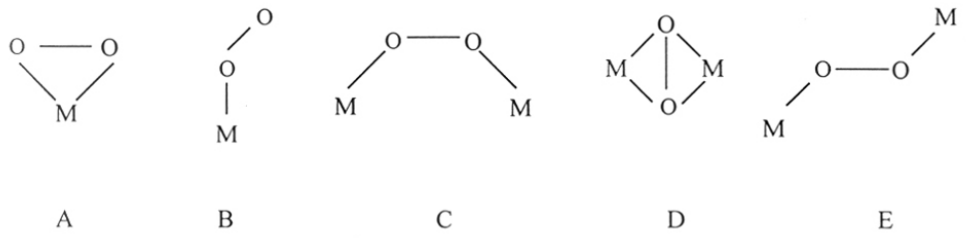

Fig. 2 Possible configuration of O_2 interaction with a metal in a complex

Configuration A involves a side-on interaction of O_2 with the metal. The bonding arises from a σ-type of bond formed by the overlap between a mainly ∏ orbital of oxygen and a d_{z^2} (and s) on the metal and a ∏ backbonded interaction between the metal d ∏ orbitals and the partially occupied ∏* antibonding orbital on O_2. In configuration B (end-on interaction of O_2 with the metal), a δ-rich orbital of O_2 donates electron density to an acceptor orbital d_{z^2} on the metal, forming a σ-type of bond. A ∏ type interaction is also produced between the metal d ∏ (d_{xz} and d_{yz}) orbitals and ∏* on O_2 with charge transfer from the metal to the O_2. Both configurations A and B are relevant in mono metal nuclear complexes like those of copper phthalocyanines encapsulated in zeolites. The main difference between the geometries of A and B are steric factors and the nature of the σ bond formed.[1] This interaction is influenced by the electron density on the metal, which, in turn will be influenced by the nature and the field strength of the ligands. It may be noted that configurations like C to E involving dimeric phthalocyanine complexes are

unlikely due to steric constraints inside the zeolite cavities. However, the copper acetate dimer can be accommodated in the supercages of the faujasite. Configuration D (a μ-η^2 : η^2 complex) is present in the coupled binuclear copper sites in oxygenated hemocyanins[2] and tyrosinase. A more detailed discussion of this system and its relevance to the catalytic activity of copper acetate dimers is presented in the next section. The trans configuration (E) is likely to occur with some cobalt phthalocyanines which form adducts with O_2 in solution.[1] The factors that affect the metal complex-O_2 bonding also influence the catalytic activity of the complex towards O_2 reduction. Another important factor is the particular symmetry of the ligand field which can alter the relative position and energy of the metal d levels and thus affect the overlap of these orbitals with the right orbitals of O_2. For example, the tetragonal distortion of the square planar complex, $CuCl_{16}Pc$ inside the supercages of the Y zeolite (see chapter-3) is expected to facilitate the reduction of Cu (II) to Cu (I) ions; the latter is known to prefer tetrahedral coordination . Similarly, it is known that the presence of Π donors as a fifth ligand on the phthalocyanines increases their catalytic activity towards O_2 reduction.[1] In view of these varied effects of substituents, it is not surprising that replacing the H atoms on the phthalocyanine ligand by electron-withdrawing bulky groups leads to a drastic change in the electronic and catalytic properties of the copper ions. These aspects will be discussed in more detail below.

8.3 Oxidation using dimeric copper acetate complexes

The catalytic functional similarity between the encapsulated dimeric copper acetate and tyrosinase enzyme in the hydroxylation of L-tyrosine to L-DOPA had been noted earlier. The mechanism of hydroxylation by tyrosinase is known in some detail.[2] The active site contains a pair of coupled binuclear Cu ions. The oxygenated form of the

coupled binuclear Cu site involves peroxide bonds to two Cu (II) ions in a μ-η^2 : η^2 structure (structure D in Section 8.2) as shown below :

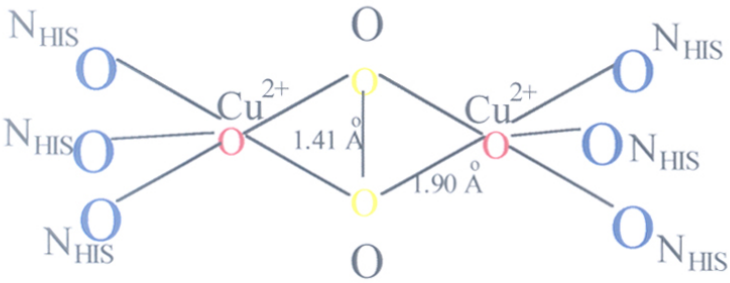

It has been postulated[2] that during the hydroxylation reaction, a tyrosine phenolate group coordinates directly to the Cu. This would lead to the donation of electron density from the substrate tyrosine into the LUMO which is antibonding with respect to both the O-O and Cu-O bonds. This electron transfer in turn, initiates oxygen transfer (of one of the two peroxide oxygens) to the position ortho to the -OH group in the tyrosine molecule. The resultant coordinated catecholate will transfer two electrons to the binuclear cupric site, leading to the dissociative elimination of the product and the formation of the deoxy site for further turnover.

An analogous mechanism for the ortho hydroxylation of phenols over dimeric copper acetate (see structure in section 3.2.5, Chapter-3) is proposed in Fig. 8.3.

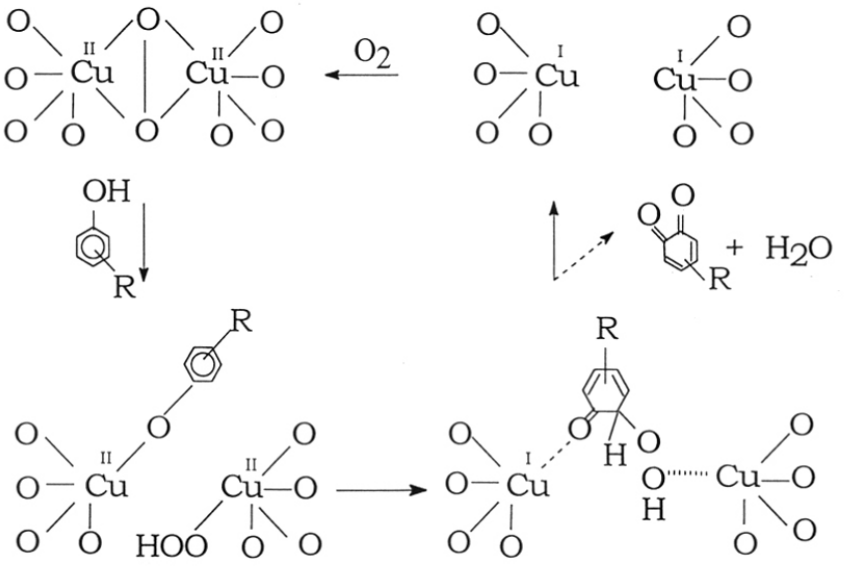

Fig.3 Mechanism for the ortho hydroxylation of phenols over dimeric copper acetate complexes.

8.4 Oxidation using copper phthalocyanine complexes

The redox properties of metal phthalocyanines have been reviewed.[1] Oxidation and reduction processes can take place either on the metal or the phthalocyanine ring. The results on the oxidation properties of encapsulated copper phthalocyanines carrying electron-withdrawing substituents on the phthalocyanine ring are similar those of Lyons et al.[3] They found that halogenated iron porphyrins are highly active catalysts for the direct reaction of alkanes with oxygen to give alcohols and/or carboxyl compounds at mild conditions. They also found, like us, that no coreductants or stoichiometric oxidants are required. The product profile, while characteristic of radical reactions, was sensitive to the nature of the metal centre. Iron porphyrins were more active than those of cobalt,

manganese or chromium. The activity of the iron complex was directly correlated to the Fe(III) / Fe(II) reduction potential of the porphyrin complex.

The oxidation of organic compounds with metalloporphyrin complexes is well documented. Less is known about the catalytic activity of phthalocyanines. Balkus et al[4] have reported on the oxidation properties of fluorinated copper phthalocyanines in catalytic reactions. Our results indicate that the catalytic activity of unsubstituted copper phthalocyanines is generally poor (see Chapter-5, Table-1). One reason for the greater catalytic activity of chloro- and nitro substituted copper phthalocyanines is the greater oxidative and thermal stability of the complex. Replacing the hydrogens with -Cl or NO_2 substituents, reduces the number of C-H bonds that can undergo oxidative attack.[3] $CuCl_{16}Pc$, for example, has no C-H bond that can undergo oxidative attack and consequent cleavage. Moreover, when electron-withdrawing -Cl or $-NO_2$ are introduced in the aromatic ring the phthalocyanine ligand becomes more stable to reduction by the copper ion. In the case of iron, for example, it is known that the porphyrinato iron oxo complex exists as the radical cation, due to electron transfer from the ligand to the iron centre.[5] There was a definite tendency of the active catalyst to behave as an oxocentred radical (P) Fe-O$^{\cdot}$ than a ferryl species ($P^{-\cdot}$) Fe=O with increased electron withdrawal from the ring.[5] In our case, the enhanced catalytic activity of the chloro- and nitro substituted copper phthalocyanines can be attributed to (1). increased Cu (II) / Cu (I) reduction potential due to the electron withdrawal from the copper atom by the -Cl and $-NO_2$ groups and (2). The tetragonal distortion of the square planar complex leading towards a tetrahedral symmetry wherein the Cu (II) $\rightarrow$ Cu (I) transition is more favourable. It may be recalled that while Cu (II) complexes prefer square planarity, the tetrahedral symmetry is favoured by Cu (I).

This tetragonal distortion of the complex due to encapsulation will further increase the Cu (II) / Cu (I) reduction potential leading to a further enhancement of the oxidation reaction.

Keeping the above factors in mind , we may formulate the radical mechanism of oxidation of hydrocarbons by our copper complexes as shown below :

A. $R\text{-}H + [CuPc]^{2+} \longrightarrow R^{\cdot} + [(CuPc)^{2+} H^{\cdot} \longleftrightarrow (CuPc)^{+} H^{+}]$

B. $R^{\cdot} + O_2 \longrightarrow R\text{-}O\text{-}O^{\cdot}$

C. $R\text{-}O\text{-}O^{\cdot} + [(CuPc)^{2+} H^{\cdot} \longleftrightarrow (CuPc)^{+} H^{+}] \longrightarrow R\text{-}O\text{-}O\text{-}H + [CuPc]^{2+}$

D. $R\text{-}O\text{-}O\text{-}H \longrightarrow R\text{-}O^{\cdot} + {}^{\cdot}OH$

E. $R^{\cdot} + {}^{\cdot}OH \longrightarrow R\text{-}OH$

F. $RO^{\cdot} + O_2 \longrightarrow R\text{-}O\text{-}O\text{-}O^{\cdot}$

G. $R\text{-}O\text{-}O\text{-}O^{\cdot} + [(CuPc)^{2+} H^{\cdot} \longleftrightarrow (CuPc)^{+} H^{+}] \longrightarrow R\text{-}O\text{-}O\text{-}O\text{-}H + [CuPc]^{2+}$

H. $R\text{-}O\text{-}O\text{-}O\text{-}H \longrightarrow R\text{-}O\text{-}O^{\cdot} + {}^{\cdot}OH$

When an initiator like tert. butyl hydroperoxide is added to the reaction medium, the reaction rate is enhanced due to the higher availability of the hydroxyl radicals by step D, which is usually the rate determining step. Lyons et al[3] had also established a direct correlation between the reduction potential of the iron porphyrin and the hydroperoxide decomposition activity. If step D (the decomposition of the hydroperoxide) is the rate determining step in our oxidations also, then, the enhancement of the oxidation rate by electron-withdrawing substituents or encapsulation in zeolites is understandable since the latter factors are also known to increase the reduction potential of the complex.

When H_2O_2 is used as the oxidant, instead of O_2, we may still have a hydroxyl radical mechanism by the following process :

$$Cu^{2+} + H_2O_2 \longrightarrow Cu^{+1} + O_2H^{\cdot} + H^{+}$$

$$O_2H^{\cdot} + H_2O_2 \longrightarrow O_2 + H_2O + {}^{\cdot}OH$$

As in the case of the Fenton system, the OH radical is formed by the reduction of H_2O_2. The OH radical has electrophilic characteristics. For example, hydroxylation of acetanilide by the Fenton's reagent yields almost exclusively N-acetyl-p-aminophenol and N-acetyl-o-aminophenol. This fact may explain the ortho-para orientation observed in our studies on the oxidation of aromatic substrates. In the ring oxidation of toluene over the copper complexes, for example, only ortho and para cresols were observed. Meta cresols were never observed, either with O_2 or H_2O_2 as oxidants.

8.5 References

1. J.H. Zagal, *Coord. Chem. Revs.*, **119** (1992) 89.

2. E.I. Solomon and M.D. Lowery, *Science*, **259** (1993) 1575.

3. J.E. Lyons, P.E. Ellis, Jr., and H.K. Myers, Jr., *J. Catal.*, **155** (1995) 59.

4. K.J. Balkus, Jr., A.G. Gabrielov, F. Bedioui and J. Devynck, *Inorg. Chem.*, **33** (1994) 67.

5. J.F. Bartoli, O. Brigond, P. Battioni and D. Mansuy, *J. Chem. Soc. Chem. Commun.*, (1991) 440.

CHAPTER-9

SUMMARY AND CONCLUSIONS

9.1 Summary and Conclusions.

The *synthesis, characterization and catalytic applications of Copper acetate and phthalocyanine complexes encapsulated in molecular sieves* are described in this thesis. Dimeric copper-acetate complexes were incorporated in zeolites, Na-Y, MCM-22 and VPI-5. The structural and compositional integrity of the incorporated copper-acetate complexes were verified by XRD, IR and UV-Vis spectroscopic techniques. ESR was used to prove the dinuclearity of the incorporated copper acetate. These solid catalysts have been used for the activation of dioxygen at ambient conditions and were effective catalysts in the oxidation of L-tyrosine, phenol and cresols to the corresponding ortho diphenols. Even though, several homogeneous tyrosinase models have been developed, so far, none of them catalyze the reaction of L-tyrosine to L-DOPA. The copper acetate system catalyses the conversion of L-tyrosine to L-DOPA and further oxidation of L-DOPA to o-quinones. The quinones could be reduced back to L-DOPA using ascorbic acid as the reducing agent. Only monophenols were oxidized (aromatic compounds such as benzene, toluene and naphthalene, for example, were not oxidized) by this system (substrate specificity) and hydroxylation always occurred at the position ortho to the -OH group (regioselectivity). A linear correlation has been obtained between the concentration of the copper acetate dimers in the molecular sieves (estimated from ESR spectroscopy) and monophenol conversion, suggesting that the copper atom dimers are the active sites in the activation of dioxygen. Since the copper-acetate dimers are well isolated from each other when incorporated in the molecular sieves, the catalytic efficiency (turnover numbers) of the copper atoms are higher in the incorporated state compared to that in the neat copper acetate. The high substrate specificity and regioselectivity of the above catalysts indicate that copper acetate dimers encapsulated in molecular sieves, mimic, in a restricted sense, the catalytic function

(both monophenolase and diphenolase activity) of the monooxygenase enzyme, tyrosinase. So far, no heterogeneous solid mimic of tyrosinase has been reported.

Copper phthalocyanine, copper hexadeca chloro phthalocyanine and copper tetra nitro phthalocyanine complexes were synthesized and have been encapsulated in zeolites X, Y, ZSM-5 and K-L by synthesizing the zeolites around the metal complexes. Substitution of the hydrogen atoms in the aromatic nuclei of the phthalocyanine molecule by electron withdrawing (like the halogens and nitro groups, for example) groups increases the reactivity of these copper catalysts. The structural integrity of the above complexes in the molecular sieves was confirmed by a wide variety of physicochemical techniques such as XRD, UV-Vis, ESCA, ESR, SEM, TGA/DTA and N_2 sorption. Computer modeling and molecular strain energy minimization calculations indicate that the geometry around the copper atom is distorted tetragonally from the square planar symmetry (of the free complex) when encapsulated inside the supercages of the faujasite. This distortion leads to a *hydrophobic* environment around the copper atom These catalysts have been used in the oxidation of alkanes, aromatics, phenols and oxyhalogenation of aromatic compounds. Zeolite encapsulated copper hexadeca chloro phthalocyanine complexes exhibited regioselectivity in the oxidation of n-hexane to predominantly 1-hexanol using molecular oxygen as the oxidant. Cyclohexane was oxidized to cyclohexanol, cyclohexanone and adipic acid with high selectivities. This is also the first solid catalyst system to exhibit high activity and selectivity in the direct oxidation of methane to a mixture of methanol and formaldehyde at ambient and sub-ambient temperatures using tert. butyl hydroperoxide as well as molecular oxygen as the oxidants. Aromatic compounds like benzene were oxidized to phenol. Phenol was oxidized to catechol and hydroquinone and naphthalene was oxidized selectively to β naphthol using H_2O_2 as the oxidant. Ring as

well as side-chain oxidations were observed when toluene and ethyl benzene were used as the substrates. The oxychlorination and oxybromination of benzene, toluene, phenol, resorcinol, aniline and anisole were carried out using HCl as well as alkali chlorides/bromides as the halogen source. The catalytic activity of the zeolite encapsulated copper phthalocyanine complexes was also compared with the halogenated iron and cobalt analogues.

In conclusion, two novel solid catalyst systems namely, (1). dimeric copper acetate complexes (2). copper phthalocyanines, wherein the hydrogen atoms on the phthalocyanine rings are substituted by electron-withdrawing groups like the halogens or nitro groups, encapsulated in molecular sieves have been synthesized and their structure characterized. Their catalytic properties in the oxidation and oxyhalogenation of various substrates like alkanes, aromatics and phenols has been studied in detail.

The advantages of these above catalytic systems are (1). The catalyst remains in the solid state during the entire course of the reaction, thereby providing significant processing advantages in their large scale and industrial operations, as compared to homogeneous catalysts; (2). The more expensive H_2O_2 can be replaced by molecular oxygen as the oxidant; (3). Deactivation of the copper complexes via dimerisation reactions or aggregate formation was prevented by their encapsulation in molecular sieves such as zeolites leading to their enhanced stability, reactivity and life. (4). Oxyhalogenation using *in-situ* generated halogens has many advantages; Hydrogen and alkali halides, in addition to being less expensive, are also easier to transport and handle compared to molecular halogen; (5). The performance of these novel catalyst systems, as solid oxidation and oxyhalogenation catalysts, in utilizing O_2 as well as singlet oxygen sources like H_2O_2 holds promise in the chemicals industry.

LIST OF RESEARCH PUBLICATIONS

1. NMR spectroscopic study of the interaction of 1-butene with the titanosilicates TS-1 and ETS-10.
Robert Raja, P.R. Rajamohanan, S.G. Hegde, A.J. Chandwadkar and P. Ratnasamy,
J. Catal., **155** (1995) 345.

2. Activation of dioxygen with copper complexes encapsulated in molecular sieves.
Robert Raja and P. Ratnasamy
J. Mol. Catal., **100** (1995) 93.

3. Selective oxidation of phenols with copper complexes encapsulated in zeolites.
Robert Raja and Paul Ratnasamy
Appl. Catal. A Gen : **143** (1996) 145.

4. Selective oxidation with copper complexes incorporated in molecular sieves.
Robert Raja and Paul Ratnasamy
Stud. Surf. Sci. Catal., **101** (1996) 181.

5. Selective oxidation of aromatic hydrocarbons over copper complexes encapsulated in molecular sieves.
Robert Raja and Paul Ratnasamy
Stud. Surf. Sci. Catal., **105** (1997) 1037.

6. Direct conversion of methane to methanol.
Robert Raja and Paul Ratnasamy
Appl. Catal., (In Press).

7. Oxyhalogenation of aromatics compounds over copper phthalocyanines encapsulated in molecular sieves.
Robert Raja and Paul Ratnasamy
J. Catal., (Communicated).

8. Copper (II) phthalocyanines occluded in zeolites of MFI topology : Synthesis and Characterization
S. Shevade, **R. Raja** and A.N. Kotasthane
J. Chem. Soc., Chem. Commun., (Communicated).

9. Copper phthalocyanines in Zeolite-Y : An efficient catalyst for the Bayer Villiger oxidation of ketones to lactones.
Robert Raja and M. Sasidharan
Catal. Lett., (To be submitted).

10. One-step oxidation of cyclohexane to adipic acid over zeolite encapsulated copper phthalocyanines.
Robert Raja and Paul Ratnasamy
J. Catal., (To be submitted).

11. Selective oxidation of propane with zeolite encapsulated metal phthalocyanines.
Robert Raja and Paul Ratnasamy
(In preparation)

LIST OF INDIAN/FOREIGN PATENTS

S. No.	Pat. Appl. No.	Date of filing	Title
1.	1218/DEL/95	26-6-1995	Process for the ortho hydroxylation of monohydroxy aromatic compounds.
2.	1796/DEL/95	29-9-1995	Process for the preparation of L-DOPA from L-Tyrosine.
3.	1688/DEL/95	15-9-1995	An improved process for the preparation of adipic acid by the oxidation of cyclohexane **(US, EP)**.
4.	NF-158/95	15-9-1995	Process for the preparation of adipic acid by the oxidation of cyclohexanone.
5.	1791/DEL/95	29-9-1995	An improved process for the oxidation of cyclohexane to a mixture of cyclohexanol and cyclohexanone.
6.	2479/DEL/95	29-12-1995	A process for the manufacture of catechol and hydroquinone **(US, EP)**.
7.	395/DEL/95	22-2-1996	An improved process for the preparation of naphthols by hydroxylation of naphthalene **(US)**.
8.	2056/DEL/95	10-11-1995	An improved process for the preparation of cumene hydroperoxide.
9.	385/DEL/95	23-2-1996	An improved process for the hydroxylation of Ethylbenzene.
10.	2470/DEL/95	29-12-1995	An improved process for the preparation of guaiacol and p-methoxy phenol **(US, EP)**
11.	659/DEL/95	27-3-1996	A process for the oxidation of paraffins to primary alcohols **(US, EP)**
12.	2466/DEL/95	27-12-1995	An improved process for the oxidation of benzene **(US, EP)**
13.	2469/DEL/95	29-12-1995	An improved process for the preparation of cresols **(US)**
14.	661/DEL/96	27-3-1996	An improved process for the manufacture of epichlorohydrin **(US, EP)**
15.	662/DEL/96	25-3-1996	An improved process for the preparation of linear alkylbenzene **(US)**.

16.	696/DEL/96	29-3-1996	A process for the manufacture of cyclohexanoneoxime.
17.	NF-124/96	27-12-96	An improved process for the oxidative halogenation of aromatic compounds **(US)**
18.	NF-282/96	-	An improved process for direct conversion of methane to methanol **(US, EP)**
19.	(Submitted)		Process for the preparation of encapsulated metal phthalocyanine silicates, designated as Encilite-En.